TURUN
YLIOPISTO
UNIVERSITY
OF TURKU

SENSITIVE AND QUANTITATIVE LATERAL FLOW TESTS

with upconverting nanoparticle reporter technology

Iida Martiskainen

TURUN YLIOPISTON JULKAISUJA – ANNALES UNIVERSITATIS TURKUENSIS
SARJA – SER. AI OSA – TOM. 645 | ASTRONOMICA – CHEMICA – PHYSICA – MATHEMATICA | TURKU 2021

TURUN
YLIOPISTO
UNIVERSITY
OF TURKU

SENSITIVE AND QUANTITATIVE LATERAL FLOW TESTS

with upconverting nanoparticle reporter technology

Iida Martiskainen

TURUN YLIOPISTON JULKAISUJA – ANNALES UNIVERSITATIS TURKUENSIS
SARJA – SER. AI OSA – TOM. 645 | ASTRONOMICA – CHEMICA – PHYSICA – MATHEMATICA | TURKU 2021

University of Turku

Faculty of Technology
Department of Life Technologies
Biotechnology
Doctoral programme in Molecular Life Sciences, DPMLS

Supervised by

Docent Sheikh M. Talha, PhD
Department of Life Technologies
Biotechnology
University of Turku
Turku, Finland

Reviewed by

Jussi Hepojoki, PhD, Docent
University of Helsinki/University of Zurich
Medicum/Vetsuisse Faculty
Dept. of Virol./Inst. of Vet. Path.
Helsinki, Finland / Zürich, Switzerland

Leena Hakalahti, PhD
VTT Technical Research Centre of Finland
Oulu, Finland

Opponent

Associate Professor Paul Corstjens, PhD
Leiden University Medical Center
Department of Cell and Chemical Biology
Leiden, the Netherlands

The originality of this publication has been checked in accordance with the University of Turku quality assurance system using the Turnitin OriginalityCheck service.

ISBN 978-951-29-8438-1 (PRINT)
ISBN 978-951-29-8439-8 (PDF)
ISSN 0082-7002 (Print)
ISSN 2343-3175 (Online)
Painosalama, Turku, Finland 2021

Isn't life exciting!
Everything can change all of a sudden,
and for no reason at all!

Moomintroll
from the book Moominpappa at Sea

UNIVERSITY OF TURKU
Faculty of Technology
Department of Life Technologies
Biotechnology
IIDA MARTISKAINEN: Sensitive and Quantitative Lateral Flow Tests – with Upconverting Nanoparticle Reporter Technology
Doctoral Dissertation, 158 pp.
Doctoral programme in Molecular Life Sciences, DPMLS
May 2021

ABSTRACT

Rapid diagnostic tests (RDTs) can be used in settings where access to a central laboratory is limited. These settings include point-of-care (POC) diagnostics performed near a patient during a physician's appointment or in an ambulance. Also, POC testing is used in many resource-limited community healthcare stations, especially in low- and middle-income countries (LMIC). Lateral flow assay (LFA) is one of the dominant formats for RDT. Conventional lateral flow (LF) tests use visually detectable colored reporter technology, which is prone to limited sensitivity and subjective interpretation of the test read-out. Recently, there has been a growing interest towards applying luminescent label technologies in LFA. The use of such technology in combination with miniaturized reader device preserves most of the typical advantages of LF tests. It may also increase sensitivity and analyte quantification and rule out subjective interpretation of the result.

The aim of this thesis was to develop LFAs employing upconverting nanoparticles (UCNPs) for improved detection of viral analytes and cardiac troponin I (cTnI). In LMIC there is a need for rapid diagnostics with performance equal to that of central laboratory diagnostics. Infections by viruses such as Hepatitis B and human immunodeficiency virus (HIV) represent major health problems in many areas. LFAs for Hepatis B virus surface antigen and anti-HIV antibodies were developed in this thesis and evaluated with clinical specimens. In addition to infectious diseases, non-communicable diseases pose an emerging threat to human health with number of cases increasing as the standards of living improve globally. Cardiovascular diseases for instance have become a leading cause of premature mortality. Particularly in the case of myocardial infarction, rapid and accurate diagnosis affects the clinical outcome of the patient. Quantitative determination of cTnI can provide information on the status of the patient experiencing acute chest pain. In this thesis, an LFA for cTnI was developed evaluated in terms of quantitative determination of cTnI concentration in patient samples.

The results obtained show that the use of UCNPs in the LF platform improves sensitivity and enables quantitative analyte detection. UCNP-LF technology has the potential for use in simple and cost-efficient POC tests, and it offers improved performance in contrast to traditional visual LF technology.

TURUN YLIOPISTO
Teknillinen tiedekunta
Bioteknologian laitos
Biotekniikka
IIDA MARTISKAINEN: Herkkien ja kvantitatiivisten lateraalivirtaustestien kehitys käänteisvirritteisten nanopartikkelileimojen avulla
Väitöskirja, 158 s.
Molekulaaristen biotieteiden tohtoriohjelma
Toukokuu 2020

TIIVISTELMÄ

Diagnostisia pikatestejä käytetään sellaisissa olosuhteissa, joissa mahdollisuudet keskuslaboratoriodiagnostiikan hyödyntämiseen ovat rajatut – kuten esimerkiksi tyypillisessä vieritestaustilanteessa, jossa diagnostisen testin tulokset tulisi saada nopeasti lääkärikäynnin aikana oikean hoitopäätöksen mahdollistamiseksi. Tämän lisäksi pikatestejä käytetään matalan tulotason maissa olosuhteissa, joissa resurssit laboratoriodiagnostiikan käyttöön ovat rajalliset. Lateraalivirtaustesti on yksi tyypillisimmistä pikatestialustoista. Useimmat lateraalivirtaustestit perustuvat visuaaliseen tulosten lukuun testilastulta. Visuaalisten määritysten heikkoutena on rajallinen herkkyys sekä tulosten subjektiivinen tulkinta. Kiinnostus korvata visuaalisesti havaittavat värilliset nanopartikkelileimat erilaisilla luminoivilla leimoilla on kasvanut viime vuosina. Luminoivilla leimoilla ja helppokäyttöisellä lukijalaitteella voidaan parantaa sekä määrityksen herkkyyttä, että kvantitatiivisuutta, mutta myös vähentää tulosten tulkinnan subjektiivisuutta.

Väitöstyössä kehitettiin lateraalivirtausmäärityksiä virusanalyyttien havaitsemiseen ja parannettiin määritysten herkkyyttä ja kvantitatiivisuutta käyttämällä käänteisvirritteisiä nanopartikkelileimoja. Monilla resurssiköyhillä alueilla on tarve pikadiagnostiikalle, joka kuitenkin suorituskyvyltään vastaisi keskuslaboratoriodiagnostiikkaa. Hepatiitti B ja HI-virus ovat edelleen suurimpia taudinaiheuttajia näillä alueilla. Väitöskirjatyössä kehitettiin määritykset Hepatiitti B viruksen pinta-antigeenin ja HI-virusvasta-aineiden havaitsemiseen. Kehitettyjen määritysten suorituskykyä arvioitiin potilasnäytteillä. Myös tarttumattomat taudit, kuten sydänsairaudet, ovat maailmanlaajuisesti kasvussa elintason noustessa ja ovat suurin syy eliniänodotteen alenemaan. Sydänkohtauksen sattuessa, nopea ja oikea diagnoosi vaikuttaa oleellisesti potilaan hoitoennusteeseen. Väitöskirjatyössä arvioitiin kehitetyn sydänperäistä troponiini I:tä havaitsevan lateraalivirtausmäärityksen suorituskykyä mitata kvantitatiivisesti sydänperäistä troponiini I:tä potilasnäytteissä.

Tutkimuksen tulokset osoittavat, että hyödyntämällä käänteisvirritteisiä nanopartikkelileimoja voidaan kehittää herkempiä ja kvantitatiivisia lateraalivirtaustestejä. Teknologia mahdollistaisi helppojen ja kustannustehokkaiden testien valmistamisen samalla parantaen testien suorituskykyä suhteessa perinteiseen visuaaliseen lateraalivirtaustekniikkaan.

Table of Contents

Abbreviations

ACS	acute coronary syndrome
AIDS	acquired immunodeficiency syndrome
ALT	alanine aminotransferase
Anti-HBc	anti-Hepatits B core antigen antibodies
Anti-HBe	anti-Hepatits B envelope antigen antibodies
Anti-HBs	anti-Hepatits B surface antigen antibodies
ASSURED	affordable, sensitive, specific, user-friendly, rapid and robust, equipment-free, deliverable
AuNP	gold nanoparticle
C	control line
cccDNA	covalently closed circular DNA
CDC	Centers for Disease Control and Prevention
CE	Conformité Européenne, CE-marking
CLSI	The Clinical Laboratory & Standards Institute
CPDA	citrate-phosphate-dextrose-adenine
CRP	C-reactive protein
cTn I, T and C	cardiac troponins I, T and C
CV	coefficient of variation
CVD	cardiovascular disease
DALY	disability-adjusted life year
ECG	electrocardiography
EIA	enzyme-immunoassay
FDA	Food and Drug Administration (US)
HBcrAg	Hepatitis B virus core-related antigen
HBeAg	Hepatitis B virus envelope antigen
HBsAg	Hepatitis B virus surface antigen
HBV	Hepatitis B virus
HCV	Hepatitis C virus
HICs	high-income countries
HIV	human immunodeficiency virus
HIV-1	human immunodeficiency virus type 1

HIV-2	human immunodeficiency virus type 2
IgG	immunoglobulin G
IgM	immunoglobulin M
IU	international unit
LF	lateral flow
LFA	lateral flow assay
LFIA	lateral flow immunoassay
LiH	lithium heparin
LMICs	low- and middle-income countries
LoB	Limit of Blank
LOC	lab-on-a-chip
LoD	Limit of Detection
MI	myocardial infarction
NA	nucleic acid
NAT	nucleic acid testing
NC	nitrocellulose
NCD	non-communicable disease
PCR	polymerase chain reaction
POC	point-of-care
POCT	point-of-care testing
RDT	rapid diagnostic test
RLS	resource-limited setting
RT	room temperature
SIV	simian immunodeficiency virus
T	test line
UCNP	upconverting nanoparticle
WHO	The World Health Organization
YLL	years of life lost

List of Original Publications

This thesis is based on the following peer-reviewed articles, referred to in the text by their Roman numerals (**I–III**).

I Martiskainen I, Talha SM, Vuorenpää K, Salminen T, Juntunen E, Chattopadhyay S, Kumar D, Vuorinen T, Pettersson K, Khanna N, Batra G. Upconverting nanoparticle reporter–based highly sensitive rapid lateral flow immunoassay for hepatitis B virus surface antigen. *Anal Bioanal Chem* **413**:967–978. (2021)

II Martiskainen I, Juntunen E, Salminen T, Vuorenpää K, Bayoumy S, Vuorinen T, Khanna N, Pettersson K, Batra G, Talha SM. Double-Antigen Lateral Flow Immunoassay for the Detection of Anti-HIV-1 and -2 Antibodies Using Upconverting Nanoparticle Reporters. *Sensors* **21**:330. (2021)

III Bayoumy S, Martiskainen I, Heikkilä T, Rautanen C, Hyytiä H, Wittfooth S, Pettersson K. Sensitive and quantitative detection of Cardiac Troponin I with upconverting nanoparticle lateral flow test with minimized interference [manuscript]

1 Introduction

Viral infections have an enormous impact on global health. Infectious diseases such as those caused by hepatitis B virus (HBV) and human immunodeficiency virus (HIV) infection continue to be major causes of morbidity and mortality in many low- and middle-income countries (LMICs). However, effective programs for prevention of infectious diseases have been set up[1,2]. In addition to vaccinations, feasible, correct diagnosis and serological surveillance play an important part in controlling the spread of communicable diseases. While the effective vaccination and screening programs have helped to control the spread of infectious diseases, the number of non-communicable disease cases are rising worldwide due to increased standard of living. The data collected in 2017 shows that cardiovascular diseases such as ischemic heart disease have become the leading cause of years of life lost (YLL)[3].

There is an emerging need for simple, rapid, yet sensitive methods for infectious disease diagnostics in emergency departments and triage[4,5]. In addition, there is a need for simple, rapid and cost-efficient diagnostics in LMICs struggling with limited resources and limited access to central laboratory[6]. In general, point-of-care testing (POCT), i.e., testing performed at physician's office is a growing global trend. The use of POCT in emergency settings is constantly increasing and the global point-of-care (POC) diagnostics market is projected to reach 38.13 billion USD by 2022 from 23.71 billion USD in 2017[7].

Lateral flow assays (LFAs) are rapid and easy-to-use diagnostic devices and are therefore suitable for POCT. LFAs are based on analyte detection on an immunochromatographic assay strip. Typically, LFAs use visually detectable labels, which limit the assay sensitivity and make the results dependent on subjective interpretation. Over the past decade, there has been an interest in developing LFAs employing luminescent nanoparticle reporters to improve sensitivity. Furthermore, the use of luminescent reporters may provide a novel approach for determining analyte concentrations quantitatively in LFAs. Such detection technology, however, requires instrumentation for the result read-out. Small, portable, and preferably battery-operated reader devices can be developed and utilized in luminescence measurements of LFAs. LFAs utilizing such readers can be used in both resource-

limited settings (RLS) and in POC setting in the case of high-income countries (HICs).

The thesis discusses the development of improved rapid diagnostics for the detection of HBV and HIV infections and myocardial infarction (MI) marker cardiac troponin I (cTnI). The performance of the assays can be considered improved as the assay sensitivity and quantification were improved in contrast to traditional rapid tests. The literature review discusses the impact of these diseases and issues to society and presents currently available diagnostic tools and special traits in diagnostic detection for each disease. In more detail, the literature review describes the current situation in the field of RLS diagnostics, particularly in terms of HBV and HIV. Even though the emphasis is given on the infectious diseases, global burden of non-communicable diseases, particularly in terms of cardiovascular diseases (CVD) and MI, is briefly discussed to provide an overview what LF POCT has to offer there. The literature review also covers technical details related to LFA development. Since the possibilities of different diagnostic technologies are vast, this thesis mainly discusses immunoassay-based methods.

2 Literature Review

2.1 Global burden of infectious diseases

Even though the global disease profile is slowly changing and the proportion of non-communicable diseases associated with higher living standards is estimated to increase[8], infectious diseases continue to have a major impact on global disease burden. In 2017, HIV infection was the 8th common cause of early death[8]. Other transfusion-transmissible infections such as HBV and hepatitis C virus (HCV) infections are common causes of death and disability[9,10]. The disease burden of the communicable diseases is particularly high in many low or middle-income countries[8–10].

The global impacts of HIV and acute HBV infection and related conditions such as liver cirrhosis and hepatocellular carcinoma are shown in disability-adjusted life years (DALYs) in Figure 1. DALY describes the number of life years lost due to early death or disability with the possible reduction in quality of life because of the condition.

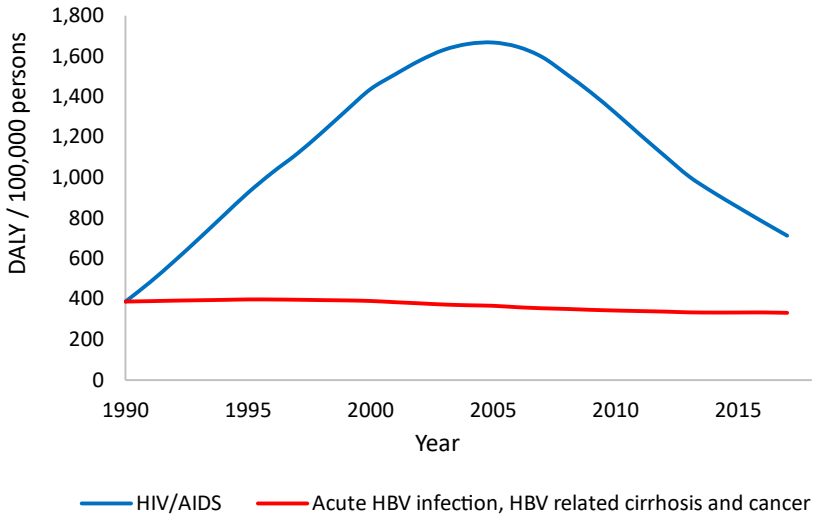

Figure 1. Global disease burden of HIV and HBV infections and HBV-related liver cirrhosis and cancer measured in disability-adjusted life years (DALYs)[11].

HIV infection remains one of the major health problems of our time and it has a significant economic impact. It has been estimated that e.g. in the United States the lifetime cost for one HIV infected patient from total time of infection currently is 379,668 USD[12]. Improved efficiency of HIV diagnosis and treatment would decrease the number patients and associated costs. In 2014, UNAIDS launched an ambitious program, "90-90-90 targets", to increase the access to antiretroviral medication and to decrease HIV prevalence globally[13]. The targets are: 1) to successfully diagnose 90% of all HIV positive people, 2) to deliver antiretroviral therapy to 90% of those diagnosed, and 3) to achieve viral suppression for 90% of those on treatment. If the three-part target is reached, virus suppression would be achieved in at least 73% of people with HIV infection.

Viral hepatitis, particularly caused by HBV and HCV, is one of the leading causes of death and disability worldwide, causing at least as many deaths annually as tuberculosis, AIDS, or malaria[9]. The economic burden of HBV infection is a combination of the acute disease and the related conditions such as liver cirrhosis and hepatocellular carcinoma that may develop over time in patients with chronic HBV infection. World Health Organization (WHO) has published an elimination strategy which aims to eradicate viral hepatitis by 2030[14]. The strategy includes accessible diagnostics, vaccination, and treatment.

2.2 Diagnostic possibilities in low-resource environments

There is a trend for increased centralization in laboratory testing together with increased automation of analytical processes. Centralization enables the analysis of large number of samples with high reliability and low cost. In addition, automation allows shorter turn-around-times and test results to become increasingly integrated with electronic medical records. The test results become faster available for the clinicians and consequently, treatment and outcomes for the patient improve.[15,16]

Advanced centralized diagnostic laboratories require skilled personnel, specialized facilities and expensive equipment that require regular maintenance. Due to these complexities, many standard laboratory tests are inaccessible to most patients and clinicians in remote locations in LMICs. When samples are collected from remote areas and sent for analysis in central laboratories, the delay between the collection and receipt of results become significant.[17]

RLSs often lack laboratory facilities or access to such facilities may be limited due to long distance. Efficient and reliable means of transportation in remote areas may be difficult to arrange, which might delay laboratory results and the subsequent treatment[6]. In general, patients living in rural areas are at risk of receiving delayed diagnosis, treatment, and follow-up[18]. Long distances also put challenges on supply

chains. A lack of proper cold transportation is a common problem, and thus transportation may cause the products to undergo variation e.g., in temperature and humidity[19]. Distance also makes equipment maintenance more difficult and time consuming[6].

In RLS, the conditions may be restrictive as compared to automated central laboratories: there may be poor availability or total lack clean running water and continuous electricity supply or internet access. Dust-free air and surfaces may be unattainable. Lack of safe waste disposal may become a problem, particularly when dealing with chemicals requiring special waste-treatment procedures. Combination of extreme temperatures and lack of electricity prevent the availability of basic refrigeration. Poor basic storage conditions for the necessary reagents may lead to difficulties in maintaining quality of the tests.[6]

2.2.1 Role of point-of-care testing

Alternative technologies such as POC tests and dried blood spots are increasingly being used as diagnostic tools in remote RLS[16]. POC testing (POCT) is defined as testing performed near the patient i.e., outside of centralized laboratories. POC tests are small diagnostic devices rapidly providing qualitative and/or quantitative determination of target analytes.

POCT got started in 1962[20], when a rapid method for measuring blood glucose concentration was introduced, but truly got underway in 1977[21], when a rapid pregnancy test became available. A trend for POCT in clinics and hospitals started developing in the early 1990s when small and portable devices for electrolyte measurement were introduced in emergency departments[22,23]. In the past 20 years, POC tests for diabetes, anemia, pregnancy, HIV and malaria have become useful diagnostic tools in both HICs and LMICs. POC tests can be used in a multitude of patient care related situations such as physicians' offices, outpatient clinics, intensive care units, emergency rooms, medical laboratories, or even patients' homes for self-testing.[16] In LMICs, POC tests are widely used in these settings but also in e.g. blood banks[24,25].

Typically, POC tests are used in resource-replete emergency departments or intensive care units to obtain immediate information to guide emergent interventions. In RLS, POCT provides an applicable alternative for centralized laboratory diagnostics to be used in outpatient clinics or mobile testing units because of the limited access to health care services. POCT aims to accelerate treatment initiation, triage patients appropriately, and improve health outcomes. Furthermore, POCT provides the results during the same visit reducing the need for follow-up visits, improving the rate of patients becoming aware of their status.[15]

Considering infectious diseases, most existing POC tests are immunoassays providing mostly qualitative and, in some cases, quantitative determination of infection markers, typically antigens and antibodies. Non-immunological POC tests detecting and sometimes quantifying pathogen nucleic acids (NAs) are being developed. As all these POC tests are designed to provide the result quickly, they are also referred to as rapid diagnostic tests (RDTs). POC tests can use whole blood, serum or plasma collected by venipuncture yet the use of alternative matrices, such as tiny amounts of fingerstick capillary whole blood or oral fluid, is desired to increase the test usability.[16]

The RDTs are typically considered having the following disadvantages in comparison to the standard laboratory diagnostics: qualitative yes/no result, subjective interpretation that may be inadequate particularly in patients expressing low analyte concentrations, low throughput, and reduced sensitivity in contrast to reference laboratory tests, particularly when oral fluid or fingerstick whole blood are used.[16]

To enable introduction of new diagnostic technologies in RLS, thoroughly conducted studies on the test's diagnostic accuracy, clinical effect and cost are required. When evaluating the accuracy and performance of the RDTs, not only performance comparison between central laboratory test and POCT but also a large-scale evaluation that considers the circumstances of the intended use are recommended.[15] To ensure adequate performance for the RDTs to be used as alternative diagnostic systems, most of the national Ministries of Health call for either a prequalification or assessment by organizations such as the United States Food and Drug Administration (FDA) or the Conformité Européenne (CE-marking) as a prerequisite. In addition to the technical assessment by an international agency, each country has further regulatory requirements that are applied because of different climatic or other conditions under which a test can be used inside the country. These steps are significant for ensuring the quality of diagnostic tests; however, such stringent regulations may delay the access for new POC tests.[6]

2.2.2 Technological solutions

2.2.2.1 Lateral flow immunoassays (LFIAs)

RDTs formats can be divided into LFIAs and microfluidic devices. LFIA is the most common format for RDTs. Technical details of LFIA are described under 2.6 Lateral Flow Immunoassays. The paper-based LFIAs are cost-efficient and easy to use. In addition, they rather easily allow introduction of multiple different analytes on the same platform. Traditionally, the LFIA result is based on visual detection of colored lines on the test strip without instrumentation. Typically, the results are readable

from within minutes to half an hour. LFIAs suffer from some intrinsic technical issues that may reduce the performance in certain applications. Limited sensitivity and subjective interpretation of the result are common problems arising from visual detection. Use of a reader device can improve the sensitivity, measurement accuracy and remove discrepancies arising from subjective "naked-eye" reading.[26]

2.2.2.2 Microfluidics

Microfluidic-based lab-on-chip (LOC) systems are a potential option for resource-limited settings, since they are designed to provide completely integrated and automated 'sample-to-result' outputs[6]. A microfluidics system combines a series of components including reagents and channels designed for conducting individual assay steps[27]. In a microfluidic system, diagnostic procedures are combined into a compact disposable component which can be directly entered into a reader device.[6] Abbott's iSTAT system is an example of a commercial LOC product. It is a handheld device for critical care testing of blood gases, metabolites, electrolytes and coagulation. The system combines self-contained cartridges with microfluidics and implements the required sample processing within the device itself.[26,28]

2.2.2.3 Analyzers

Both LFIA tests and microfluidic devices can be read with POC analyzers, which provide the result in a digital format. POC analyzers intended to be used in RLS should ideally be portable, easy-to-use devices[6,29]. The price of reader-test systems typically consists of the price the reader and after that, cost per test run. For instance, the above-mentioned Abbott's iSTAT analyzer costs approximately 6,000 USD, which may prevent its implementation in some settings. However, the price per test is below 10 USD, which can be considered cost-effective[6].

Miniaturization of light sources (LEDs, laser diodes, etc.) and optical detectors (photodiodes etc.) has enabled the development of low-priced handheld reader devices[6,28]. Recently, smartphones have been applied as reader devices or parts thereof. Smartphone-based applications reduce the need for a power supply and/or separate read-out instruments. Smartphones have enabled time and place independent access to results, thus providing the opportunity for 'on-site' result analysis or remote data transfer to a centralized facility for more detailed analysis.[6,30] However, smartphone-based systems tend to be sensitive to changes in ambient light conditions or interpretation of inconsistent image intensities[6].

2.2.3 Requirements for diagnostic methods in low-resource environments

When RDTs are used in place of standard laboratory diagnostics in RLS, appropriate assessment of test performance is essential. Accuracy and reliability are fundamental characteristics in determining the feasibility of a diagnostic POC test. Typically, test performance evaluation includes studies addressing the sensitivity and specificity, and positive and negative predictive values. Such evaluations are usually addressed in scientific publications, and they estimate the accuracy of a diagnostic POC test by comparing its performance against an accepted gold standard assay or the next best proxy measure.[15]

However, the requirements for RDTs suitability to RLS are not only limited to the performance characteristics such as clinical sensitivity and specificity. The WHO has established ASSURED criteria[31] to describe requirements for performance characteristics for RDTs used for purposes described above. The ASSURED acronym stands for:

Affordable
Test cost should be moderate in order to ensure its availability to those at risk of infection.

Sensitive
Test is highly sensitive aiming at giving very few false-negative results.

Specific
Test is highly specific aiming at giving very few false-positive results.

User-friendly
Test should be simple to perform and require minimal training time.

Rapid and robust
Test should be rapid enough to enable diagnosis and possibly treatment at the first visit. Typically in the context of RLS diagnostics, the term *rapid* test refers to a test that takes no longer than 30 minutes to obtain the result[32,33]. Test should not require refrigerated storage or special transportation conditions.

Equipment-free
Primarily, the test function independently i.e., without requirement for external laboratory or measurement devices. However, minimal equipment fulfilling the other criteria may be acceptable. The requirement for user-friendliness considers the equipment included as well.

Deliverable
Test should be deliverable to those who need it. The test and additional equipment should be transportable to remote rural areas.

WHO runs evaluation-based system known as prequalification and publishes lists of diagnostic tests that have proven adequate quality and performance. The prequalification is a systematic process for evaluating the manufacturer's capacity to produce a product of consistent quality in accordance with international standards and WHO specifications. The prequalification program was set up in 2001 and its purpose has been to facilitate access to medicines, diagnostics and vaccines that meet unified standards of quality, safety and efficacy for widespread diseases in countries with limited access to quality medical products.[34]

2.3 Hepatitis B virus infection

Hepatitis B is a potentially life-threatening liver infection caused by the hepatitis B virus (HBV). HBV specifically infects hepatocytes and causes immune-mediated liver damage[35], and may result in either an acute infection or a chronic disease. Instead of representing a specific clinical condition, HBV infection can lead to a wide range of clinical diseases varying from acute hepatitis and fulminant hepatic failure to inactive asymptomatic carrier state or progressive chronic disease. Over time, the changes caused by chronic hepatitis can lead to cirrhosis or hepatocellular carcinoma.[36]

HBV can be transmitted via percutaneous or mucosal contact with infected blood or body fluids. Such contact includes the transmission through several potential routes: mother-to-child during delivery, household or sexual contact, intravenous drug use and needle-sharing, and occupational or health-care-related situations. In highly endemic regions, HBV transmission most commonly occurs perinatally.[37,38] The likelihood of developing a chronic infection depends greatly on the age at which a person becomes infected. The development of chronic infection is very common among perinatally infected and in children infected before the age of five.[37]

In areas of low endemicity, transmission through sexual contact is common and the risk of infection is higher among people with a high number of sexual partners, among men who have sex with men, and among people suffering from other sexually transmitted infections. The third most common source of HBV infection is unsafe injections related to both healthcare and drug-use, blood transfusions, or dialysis. Even though transfusion-associated HBV infection has been eliminated in most countries due to effective screening of blood products, the risk is still persistent in some developing countries.[38] Furthermore, HBV can survive outside the body on environmental surfaces up to 7 days and can hence be transmitted via contaminated surfaces and objects[37].

Globally, 257 million people have a chronic HBV infection. Annually, HBV-related conditions result in 887 000 deaths, mostly because of HBV-related liver cirrhosis or hepatocellular carcinoma. Hepatitis B prevalence is geographically

unevenly distributed. Western Pacific and African regions, where 6.2% and 6.1% of the adult population are respectively infected represent the regions of highest prevalence. In the Eastern Mediterranean, South-East Asia, Europe, and the Region of Americas respectively 3.3%, 2.0%, 1.6%, and 0.7% of the population are estimated to be infected.[37]

There is no specific treatment for acute HBV infection. Chronic hepatitis B infection can be treated with medicines, including oral antiviral agents. In most cases, the treatment only suppresses the replication of the virus, but does not cure the infection. Correct treatment, however, can slow the progression of cirrhosis, reduce incidence of liver cancer and improve long term survival.[37]

The diagnosis and treatment capabilities of HBV infection are inadequate in RLS. According to WHO, in 2016, only 10.5% (27 million) of people infected with HBV were aware of the infection. Globally the HBV treatment coverage is 16.7% (4.5 million), and often the diagnosis is made as late as at the advanced state of liver disease.[37]

The main prevention strategy for Hepatitis B is through vaccination. In areas of high prevalence, WHO recommends that all infants should receive the HBV vaccine as soon as possible, preferably within 24 hours from birth. In 2019, the worldwide coverage of routine infant vaccination was estimated to be 85%.[37]

WHO has established a strategy for hepatitis elimination by 2030. There is a global aim to reduce new infections by 90% and reduce deaths by 65% by 2030[14]. The program goals include: universal hepatitis B immunization of infants with 90% coverage, birth dose of hepatitis B vaccine and other methods to prevent mother-to-child transmission of HBV with 90% coverage, and injection safety and blood safety with 90% coverage. Overall, 90% of infected people should be diagnosed and 90 % of the diagnosed people should be able to access treatment.[39]

2.3.1 Detection of Hepatitis B infection

2.3.1.1 Genetic variation

As HBV requires an error-prone reverse transcriptase for replication, it constantly evolves resulting in significant genetic variation in the form of genotypes, sub-genotypes, and point mutations[40,41]. HBV is divided into several separate genotypes based on 7.5% or greater intergroup genome divergence[42]. Some genotypes are further divided into subgroups, if they show 4% to 8% genome variation within the genotype[43]. Different genotypes show variation in the rate of disease progression, level of severity, predisposition to chronicity, clinical outcomes, and responses to antiviral therapy or vaccination[40]. Some mutations influence viral latency, viral load, the severity of liver disease, and vaccine as well as diagnostic escape.

Currently, there are 10 known main HBV genotypes. The first four genotypes A, B, C and D were described in 1988 by Okamoto et al.[44], and genotypes E, F[45,46], G[47] and H[48] have been identified later. In addition, genotypes I[49] and J[50] have been identified in rare cases. Global prevalence and geographical distribution of HBV genotypes is presented in Figure 2.

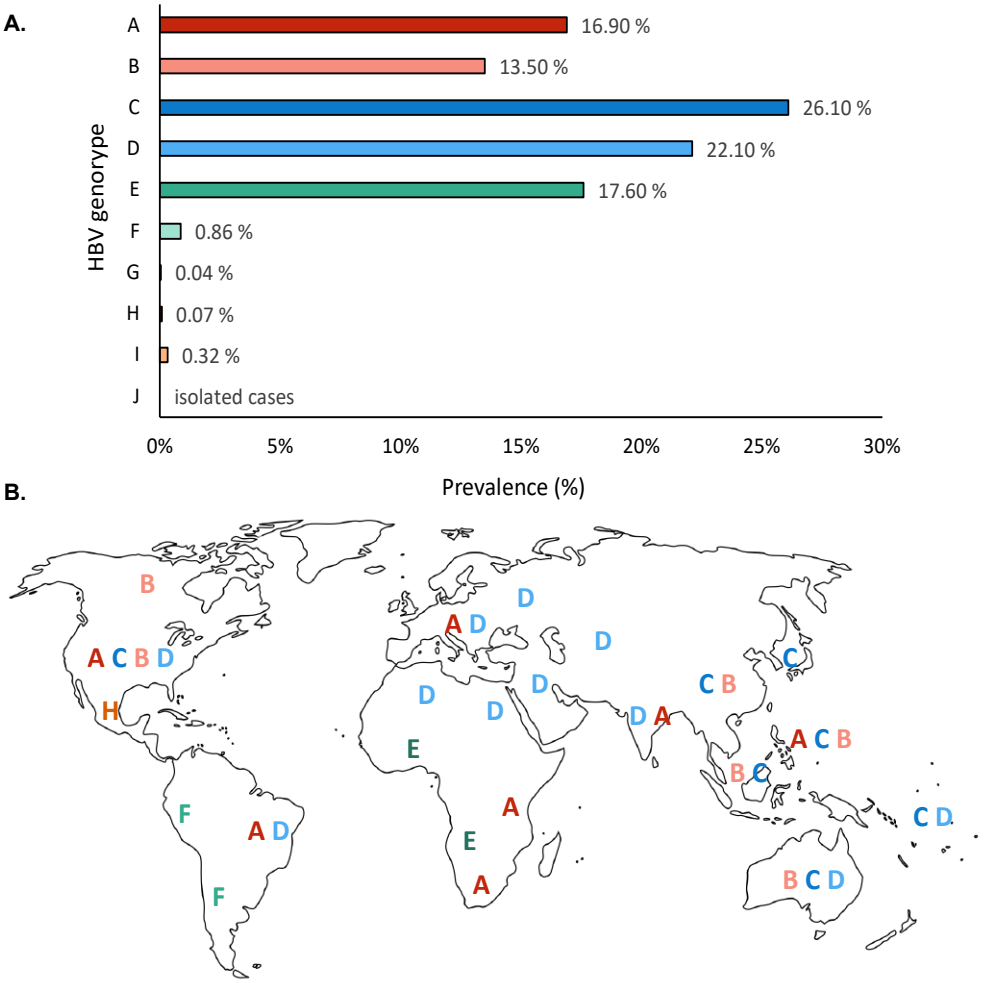

Figure 2. **A.** Global prevalence of HBV genotypes. Approximately 96% of global chronic HBV infections originate from five genotypes: C, D, E, A, and B. Genotypes F to J together cause less than 2% of chronic HBV infections[51]. **B.** Approximate geographical distribution of HBV genotypes. According to a meta-analysis[51], HBV genotypes have a distinct geographical distribution. 99% of both genotype B and C infections occur in Asia, D is distributed to Asia, Africa and Europe, E is highly prevalent in Sub-Saharan Africa, and A is found in Sub-Saharan Africa and in Asia. Figures based on data from[51].

Genetic variation leads to structural changes on HBV surface antigen (HBsAg) which is a widely used marker in HBV diagnostics. HBV genotypes differ with respect to the amount and the composition of intra- and extracellular HBsAg[52]. Therefore, some diagnostic assays detecting HBV infection may not recognize all structural variants of HBV and the sensitivity may suffer[53].

2.3.1.2 Serological profile of HBV infection

The serological markers indicating HBV infection are HBsAg, anti-HBsAg antibodies (anti-HBs), Hepatitis B envelope antigen (HBeAg), anti-Hepatitis B envelope antigen antibodies (anti-HBe), and anti-Hepatitis B core antigen antibodies (anti-HBc). Identification of the different serological markers allows detection of patients with HBV infection, elucidating the course of a chronic infection, assessing the clinical phases of infection, and monitoring the progress of antiviral therapy.

Incubation time of acute HBV infection is on average 10 weeks but can vary from 2 to 12 weeks. Acute HBV infection (Figure 3A) can be detected with serological methods once HBsAg appears in circulation, typically between 1 to 10 weeks after the exposure. Persistence of HBsAg for more than 6 months implies chronic HBV infection.[54,55]

In the acute phase of the HBV infection, anti-HBc can also be detected. In convalescent and recovered patients, clearance of HBsAg happens within 12-20 weeks after the symptom onset when anti-HBs appear in circulation. Anti-HBs are neutralizing and confer long-term immunity. Most recovered individuals stay positive for anti-HBs and anti-HBc. When immunity is acquired through vaccination, anti-HBs is the only serological marker detected in serum.[54,55]

HBsAg levels in circulation remain elevated in a chronic infection (Figure 3B). Anti-HBc IgM antibodies can be used for differentiation between acute and chronic HBV infection. HBV infection is considered chronic if the patient is positive for HBsAg after six months or the patient is HBsAg-positive and negative for anti-HBc IgM antibodies. HBeAg appears somewhat after HBsAg and like HBsAg the HBeAg levels drop in convalescent patients but stay elevated in chronic infection.[54]

Recently, there has been interest towards the detection of hepatitis B core-related antigen (HBcrAg). Chronic hepatitis B infection cannot be completely eradicated since the covalently closed circular DNA (cccDNA) remains in the nuclei of infected hepatocytes. HBcrAg has been shown to correlate with cccDNA levels. HBcrAg could thus serve as a marker for disease monitoring in chronic cases instead of quantification of intrahepatic cccDNA which requires liver biopsy.[56]

Sometimes indirect serum markers serve as an indicator of HBV infection and its prognosis. When hepatocytes are damaged, they may leak enzymes such as alanine aminotransferase (ALT) in circulation[57]. Measurement of HBsAg and ALT

is recommended for diagnosis and therapeutic indications because in many LMIC quantitative detection of HBV DNA is usually unavailable[58].

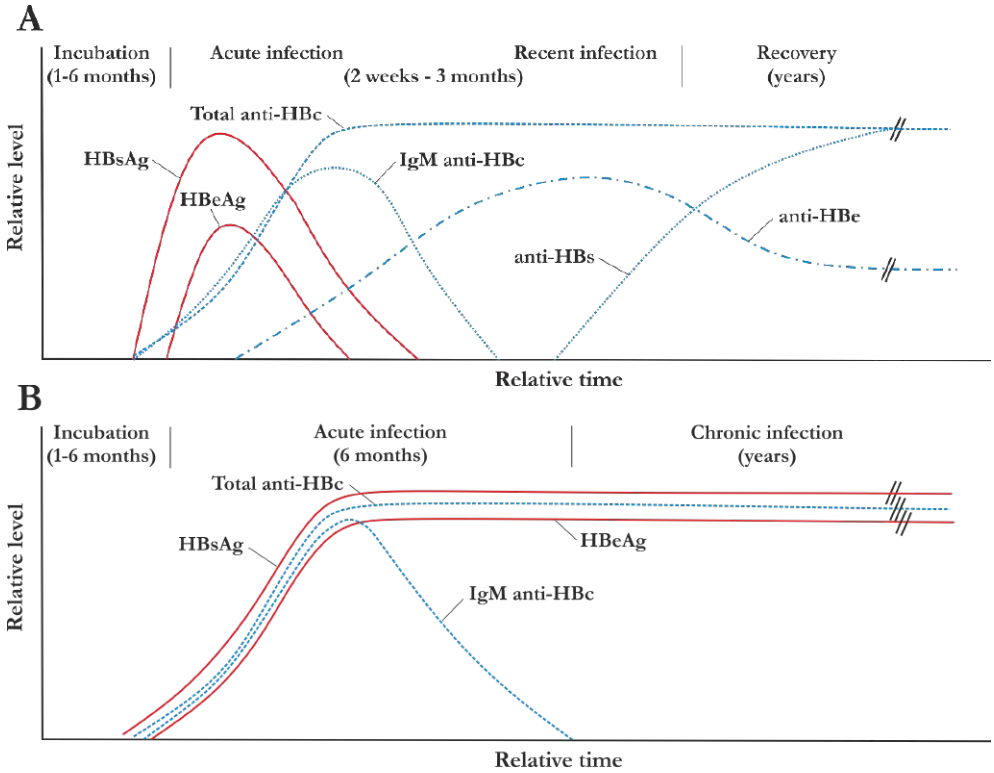

Figure 3. Serological profiles of typical **A.** acute and **B.** chronic HBV infections. In acute Hepatitis B infection HBsAg and anti-HBc IgM antibodies appear after the incubation period. During the recovery, total anti-HBc antibodies and later anti-HBs antibodies appear and HBsAg becomes undetectable. In chronic infection HBsAg level stays elevated but anti-HBc IgM antibodies become undetectable over time. The secretion of HBeAg trails that of HBsAg in both acute and chronic infection. Figures modified from[54].

2.3.1.3 Hepatitis B virus surface antigen – a hallmark of HBV infection

HBsAg is the most used diagnostic marker for the detection of HBV infection. HBsAg detection can be considered as a hallmark of HBV diagnosis – it is present in the early phase of an acute infection and in chronic infection[38].

HBsAg is a structural protein of HBV forming part of the envelope of the intact virions, which have a diameter of 42–45 nm. In addition, HBsAg is secreted to circulation as multimeric filaments and spheres of around 20-22 nm in diameter. It is the first serological marker in circulation after exposure and HBsAg concentrations in blood during acute infection may be 1000 times higher than the concentration of the actual HBV virions[60]. Concentration of HBsAg in circulation

varies during HBV infection and HBsAg levels are also affected by individual factors of the patient and virus genotype[52].

Diagnostic methods detecting HBsAg aim at shortening the diagnostic window period via high sensitivity. The diagnostic window refers to the time when the patient is infected and infectious, but asymptomatic, and antigen and antibody concentrations are undetectable by diagnostic methods. The factors that determine the length of the diagnostic window are the doubling time of viremia and the analytical sensitivity of the screening test. Sensitive serological assays and nucleic acid testing (NAT) can narrow the diagnostic window.[61]

In addition, there has been interest in developing assays for quantitative determination of HBsAg. Initially, the quantitative determination of HBsAg was prospected by Froesner et al. in 1982[62]. However, the diagnostic assays available at that time did not allow routine quantitative testing for HBsAg. Later, in 1992, Zoulim et al. observed a positive correlation between the levels of serum HBV DNA and HBsAg.[63] In 1994, Burczynska et al. suggested the use of HBsAg measurement in the monitoring of chronic HBV infection, and its predictive value on the outcome of interferon therapy[64]. More recently, studies have suggested a potential role for quantitative serum HBsAg measurement in predicting the response to antiviral therapy[65]. It has been shown that HBsAg levels change during the natural course of chronic HBV infection, and a rapid decline in HBsAg levels indicates a strong response to therapy, regardless of the treatment approach[66]. Reduction of serum HBsAg levels correlates well with the reduction of cccDNA and intrahepatic HBV DNA as a response to antiviral treatment[67]. HBsAg quantification is expected to become increasingly important in monitoring and guiding chronic hepatitis B antiviral therapy[68].

2.3.1.4 Diagnostic technologies and requirements

WHO has established the following performance acceptance criteria for analytical sensitivities of commercial in vitro diagnostic HBsAg assays: ≤ 0.13 IU/ml screening for blood donations and ≤ 4.0 IU/ml for the testing of asymptomatic and symptomatic individuals for diagnostic purposes[69]. European Union in its commission decision 2009/886/EC states the same limit of 0.13 IU/ml for analytical sensitivities for diagnostic HBsAg assays, considering both screening assays and rapid tests, in order to entitle CE-marking[70].

Immunoassays for the detection of HBsAg utilize mono- and polyclonal anti-HBsAg antibodies to detect HBsAg in serum or plasma specimens. They are sensitive: the most sensitive assays show analytical sensitivities of less than 0.02 IU/ml[71]. In a large study conducted by Scheiblauer et al. in 2010[72], a total of 70 HBsAg detecting assays were evaluated with samples representing HBV

genotypes A-F and additional clinical specimens. Seventeen of the 70 evaluated HBsAg EIA kits had high analytical sensitivities meeting the requirement of <0.13 IU/ml with 100% clinical sensitivity and recognized the six HBV variants. Six test kits had high sensitivities (<0.13 IU/ml) but showed reduced sensitivity to certain HBV genotypes. Twenty HBsAg EIA kits were in the sensitivity range of 0.13–1 IU/ml. The other eight EIAs and all 19 rapid assays had analytical sensitivities varying from 1 to >4 IU/ml.[72] Current commercially available RDTs for HBV as listed by Global Fund are compiled in Table 1.

NAT is recommended method for the screening of blood products[73] and it is also used in monitoring the effectiveness of antiviral treatment. Moreover, occasionally HBV infection occurs as an occult infection where the patient is HBsAg negative, while the patient is still having 'silent' infection undetectable my HBsAg assays. The occult HBV infection can be detected with NAT methods[74].

Table 1. Rapid tests detecting HBsAg. Information compiled from the Global Fund[75],literature[76,77] and the manufacturers.

Test	Manufacturer	Approved[a]	Sample	Volume required	Assay procedure	Time to result	Antigen detection sensitivity
Determine HBsAg	Abbbott Alere Medical Co. Ltd, Matsudo, Japan	-	Serum/Plasma/ Whole Blood	50 µl	Serum and plasma: Add 50 µl sample. Whole blood: Add 50 µl sample and 50 µl chase buffer.	15–30 min	1–2 IU/ml[76]
Determine HBsAg 2	Abbbott Alere Medical Co. Ltd, Matsudo, Japan	WHO PQ	Serum/Plasma/ Whole Blood	50 µl	Serum and plasma: Add 50 µl sample. Whole blood: Add 50 µl sample and 50 µl chase buffer.	15–30 min	0.1 IU/mL
SD BIOLINE HBsAg WB	Abbott Standard Diagnostics, Inc. (Giheung-gu,Yongin-si, Korea)	WHO PQ	Serum/Plasma/ Whole Blood	100 µl	Add the required volume of specimen to the inlet.	20 min	2.06 IU/ml
VIKIA® HBsAg	bioMérieux SA Marcy L'Etoile, France	WHO PQ, CE	Serum/Plasma/ Whole Blood	75 µl	75 µl WB + 1 drop of buffer/ 3 drops serum or plasma	pos > 15 min, neg 30 min	0.5-1 IU/ml[76]
First Response® HBsAg Card Test	Premier Medical Corporation, Nani Daman, India	CE	Serum/Plasma/ Whole Blood	50–75 µl	Add 2-3 drops (25ul each) of serum or plasma in the sample well.	Interpretation at 5-10 minutes.	NA

[a]WHO PQ: WHO Prequalified, CE: CE-marked

NA=Information not available

2.4 Human immunodeficiency virus (HIV) infection

In the early 1980's, the world faced a devastating epidemic when the first cases of acquired immunodeficiency syndrome (AIDS) emerged[78]. In 1983, the etiological agent of the disease was isolated[79] and later named HIV. HIV is a retrovirus and belongs to the family of *Retroviridae*[80]. As the name implies, the virus causes a deficit in the immune defense mechanisms over time and eventually progresses to AIDS if not treated.

Disease progression

A recent HIV infection is typically asymptomatic or causes vague symptoms, such as fever, eczema, myalgia, pharyngitis and swollen lymph nodes, which can be perceived as symptoms of influenza-like illnesses[81]. These acute phase symptoms have been associated particularly with higher viral loads[82]. Once the acute phase symptoms dissipate, infected patients typically undergo an asymptotic phase which may last many years[80]. The HIV infection stays asymptomatic until an untreated infection progresses to the AIDS phase and symptoms reappear. HIV infects and destroys immune system cells: The main target of HIV are activated CD4 T lymphocytes into which the virus enters via interactions with CD4 and the chemokine co-receptors. Other cells expressing these receptors are also infected, such as resting CD4 T cells, monocytes, macrophages, and dendritic cells.[83] As HIV infection progresses, the loss of CD4 cells leads to a reappearance of unspecific symptoms. The symptoms may include short episodes of fever, diarrhea, malaise, fatigue and loss of weight. As the immunodeficiency progresses and the CD4 cell count drops below 300/µl, the immune response is weakened. This exposes the patient to opportunistic viral and bacterial infections, which eventually turn severe due to lack of immune defense. In addition, the patients are prone to malignant cellular changes which increases the emergence of cancers.[80]

Transmission

HIV can be transmitted by contact with infected body fluids such as blood, plasma or serum, genital secretions and transplanted organs[80]. Typically, HIV transmission occurs via unprotected sexual contact, intravenous drug use, and from mother to child during pregnancy, childbirth and breast feeding. The key populations at risk of HIV infection include particularly men who have sex with men, intravenous drug users, people in prisons and other closed settings, and sex workers and their clients.[84] HIV infection cannot be cured but it can be controlled with antiretroviral therapy. In

the course of antiretroviral treatment, usually within a couple of months, viral load in the circulation decreases to concentrations undetectable by diagnostic assays[83]. Effective antiretroviral therapy can control the virus and help prevent onward transmissions. Overall, antiretroviral treatment has transformed HIV from a progressive fatal illness into a chronic manageable disease. In 2018, 62% of people living with HIV infection were receiving antiretroviral therapy and 53% of those had achieved a suppression level with no risk of further transmission of the virus[84].

Epidemic situation

At the end of 2018, there were approximately 37.9 million people living with HIV worldwide. In 2018, 770 000 people died from HIV-related causes and 1.7 million people were newly infected[84]. HIV prevalence is typically higher in many LMICs, and a major proportion of the world's HIV infected people are living in sub-Saharan Africa[85]. It has been estimated that only 79% of people living with HIV are aware of their status. HIV testing is an important part of AIDS prevention, since it enables the initiation of the antiretroviral therapy and provides awareness for the patient, which helps to prevent further transmissions. Also, by screening blood donations for HIV, transmissions in blood transfusions can be significantly decreased. By utilizing a combination of comprehensive HIV testing and accurate initiation of the antiretroviral therapy, the emergence of new HIV cases can be prevented. It has been shown that between 2000 and 2018, the number of new HIV infections has decreased 37%, and mortality of HIV-related causes decreased 45% resulting in 13.6 million lives saved due to effective screening and antiretroviral treatment.[84]

2.4.1 Detection of HIV infection

2.4.1.1 HIV types and genetic variation

HIV can be divided into two major types, HIV type 1 (HIV-1) and HIV-2, based on the respective sources of initial zoonotic transmission from primates infected with simian immunodeficiency virus (SIV) in Africa. HIV-1 was transmitted to humans from apes and HIV-2 from other primates.[86] When discussing the HIV infection, we often refer to HIV-1. This is because most HIV cases are caused by HIV-1. HIV-2 is morphologically similar but antigenically distinct virus that was found in patients in western Africa a couple of years after HIV-1 was discovered[87]. HIV-2 is significantly less prevalent, and HIV-2 infections are mostly restricted to West Africa with highest prevalence rates recorded in Guinea-Bissau and Senegal[88]. The overall prevalence of HIV-2 is decreasing, and in most West African countries HIV-2 is increasingly being replaced by HIV-1[89]. In fact, HIV-2 infection is estimated to

become extinct in specific regions[90]. However, HIV-2 infections continue to be diagnosed in Europe, India and the United States, mainly because of immigration from endemic regions[91,92].

HIV-2 has lower transmission rate than HIV-1, which associates with lower viral loads in HIV-2 versus HIV-1 infections. The lower viral load might explain why not all HIV-2 individuals develop AIDS.[93] Also, HIV-2 is less likely to transmit via sexual contact or from mother to child[94].

HIV-1 comprises four distinct lineages: subgroups named major (M), outlier (O), non-major non-outlier (N) and new group P. The subgroups have originated from independent cross-species transmission events. During the first AIDS epidemic in 1980's, group M was the first to be discovered and since then it has been the pandemic form of HIV-1. Group M HIV-1 has infected millions of people, and the virus has been found in practically every country worldwide.[86] Subgroup M can be further divided into nine subtypes from A to K.

While subgroup M has been distributed worldwide, infections caused by HI-viruses from the subgroups of N, O and P are mostly restricted to equatorial areas of western Africa. In 1990, group O was discovered[95]. The fraction of global HIV-1 infections caused by group O have been estimated to be less than 1% and it is mainly restricted to areas around Cameroon and Gabon[96]. Group N was identified in 1998[97]. It is limited to Cameroon with an extremely low prevalence of approximately 0.1% [98]. Group P was discovered in 2009[99] and the spread of the strain has been extremely limited yet detectable[100].

The genetic variance of HIV strains results in variation in antigen sequences. This has to be taken into account when designing antigen and antibody binders for HIV immunoassays to ensure comprehensive detection of HIV infections.

2.4.1.2 Biomarkers of HIV infection

HIV is an RNA virus and after exposure to HIV, viral RNA can be detected in the patient's circulation approximately 10 days after exposure (Figure 4). The RNA genome inside the virus particle is protected by a capsid made of p24-protein and the outer shell of the virus is formed by lipids and envelope proteins. In case of HIV-1, the envelope proteins consist of glycoprotein subunits gp120 and gp41[101]. The glycoprotein structure of HIV-2 varies somewhat from that of HIV-1 and it has glycoprotein gp36 instead of gp41[102]. These glycoproteins do not serve as diagnostic markers of HIV infection but they are highly immunogenic[103] and thus can be utilized in antibody detection.

The first detectable serological marker of HIV infection is the p24 antigen, which appears in the circulation within 20 days after infection. The p24 concentration increases over time until the antibody response appears and p24 becomes

undetectable. The immune response induced by HIV leads to seroconversion of anti-HIV IgM and IgG antibodies typically within two to three months after exposure. The IgM response detectable at earlier stage, approximately within 3 weeks after exposure and the IgG response can be detected from 1.5-2 months onwards. The timing of serological markers is shown in Figure 4. The diagnostic window represents the period from exposure until the infection can be diagnosed by detecting the HIV infection biomarkers. By shortening the diagnostic window with earlier detection of serological markers, further HIV transmissions can be prevented. Acute HIV infections are likely to be asymptomatic, yet the virus is more likely to transmit during acute phase rather than in chronic phase.[104]

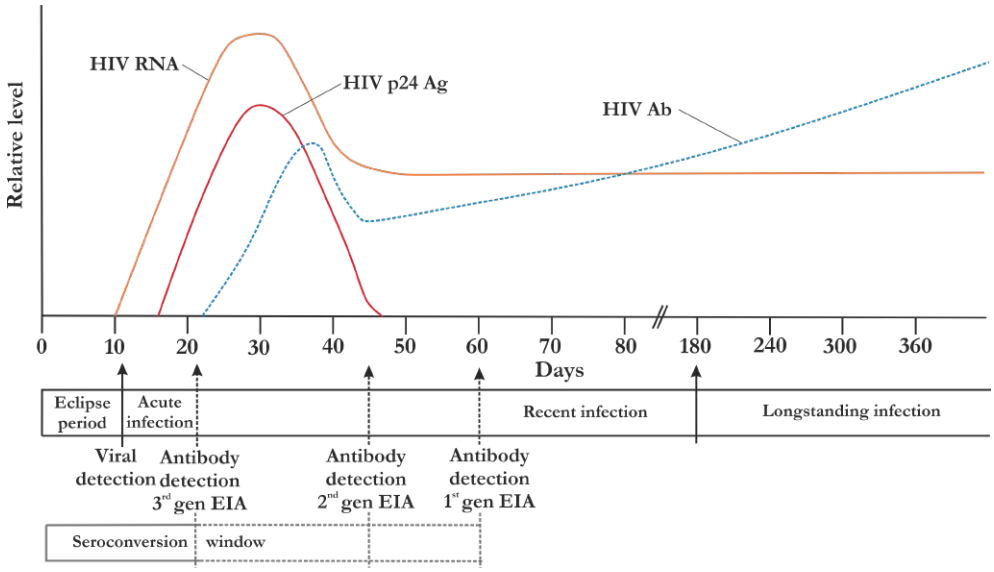

Figure 4. Appearance of biomarkers indicating HIV infection during disease progression and corresponding detection technologies for the markers. Viral RNA becomes detectable in circulation after the incubation period of approximately 10 days. The appearance of the p24 antigen follows within 20 days after exposure and disappears after the seroconversion of anti-HIV antibodies. Total anti-HIV antibody appearance typically occurs within 30 days after infection. IgG antibodies become detectable on average from one to two months after exposure. Figure modified from[104].

2.4.1.3 Diagnostic technologies

The laboratory diagnosis of HIV infection mainly relies on the detection of nucleic acids (NAs) and separate or combined immunoassays for the detection of anti-HIV antibodies and p24 antigen.

In NAT, the target DNA or RNA is detected by amplification[105]. The first diagnostic assays for viral detection were molecular assays based on polymerase

chain reaction (PCR) developed in the late 1980's[106]. The current molecular tools used for HIV detection and/or HIV diagnosis include both quantitative and qualitative NAT. Quantitative NAT can be used for following the progression of HIV infection and evaluation of effectiveness of antiretroviral therapy. HIV RNA loads in plasma are better predictors for disease progress when compared to the CD4+ T cell counts[107,108]. Qualitative NAT is mainly designed to screen for the presence of HIV NAs to confirm the safety of blood products, early diagnosis of acute HIV infections and infections in infants for diagnosing perinatal HIV infection. This is because serological testing cannot be applied in newborns with the age below 18 months of age, due to presence of maternal anti-HIV antibodies.[105]

Immunoassays for HIV detection are usually enzyme-immunoassays (EIAs) and can be divided into five groups classified as generations from 1st to 5th [109]. The 1st and 2nd generation EIAs recognize IgG antibodies against HIV. The 1st generation EIA was developed for detection of HIV infection in 1985. The antibodies were detected by using HIV antigens produced in cell culture with indirect EIA approach. The 1st generation EIAs were sensitive but lacked specificity. The use of cell lysate antigens led to frequent nonspecific reactions. These assays detected only the M-group specific HIV-1 antibodies and were not able detect non-M-subgroup and HIV-2 antibodies.[109,110]

The first 2nd generation EIA was introduced in 1987. In the 2nd generation assays the solid phase cell lysate reagents of the 1st generation EIA were replaced with recombinant HIV proteins. The assays were still performed in the indirect format. The use of recombinant antigens increased the sensitivity and specificity and reduced the window period from 60 days to 33-35 days. The 2nd generation assays also started to utilize recombinant antigens of different groups of HIV; antigens suitable for detection of antibodies against group N and O were introduced in the assays.[109,110]

The 3rd generation EIAs, first developed in 1991, combined the detection of IgG and IgM antibodies. This enabled earlier detection of HIV infection since IgM antibodies appear at an earlier stage of immune response. However, IgM antibodies tend to have lower affinity, and therefore provide only minor improvements to clinical sensitivity in general. Yet, the use of 3rd generation assays reduced the window period to about 22 days. Difference to previous generation assays was that the 3rd generation EIAs were designed in a double-antigen sandwich format i.e., recombinant HIV-1 and HIV-2 proteins were immobilized on the solid phase as well as coupled with the label.[109,110]

The fourth generation EIA format was developed in the year 1997. These combine p24 antigen detection to the 3rd generation assay platform resulting in combined detection of p24 antigen and anti-HIV IgG and IgM antibody response. The 4th generation EIAs shorten the time from infection to diagnosis by enabling antigen detection before the antibody response, but still detect the anti-HIV

antibodies once p24 becomes undetectable. The most sensitive combination assays for anti-HIVs and p24 have been observed to detect HIV infection as early as five days after NA detection[111].

In 2015, the 5th generation EIA was introduced. It detects both anti-HIV IgM and IgG antibodies and HIV-1 p24 antigen but also enables differentiation between for HIV-1 and HIV-2 antibodies[110].

2.4.1.4 Testing algorithms

HIV testing is based on different algorithms, which involve initial testing and, should the first test yield a positive result, confirmatory testing. The algorithms vary depending on the country. However, the algorithm rationale remains the same: a reactive result must be verified with the same or, preferably, with a different assay. The algorithm defines the tests that are used, and in which order they should be performed.[112]

In the United States, Centers for Disease Control and Prevention (CDC) provides recommendations to laboratories on the use of FDA-approved assays for the diagnosis of HIV infection in adults and children older than 24 months. Laboratories should conduct initial testing for HIV infection with an FDA-approved combined immunoassay that detects HIV-1 and HIV-2 antibodies and HIV-1 p24 antigen. No further testing is required if the specimen is non-reactive on the initial immunoassay. Specimens with a reactive result in the assay should be tested with an FDA-approved assay that differentiates HIV-1 antibodies from HIV-2 antibodies. A reactive result in both assays should be interpreted as either positive for HIV-1 antibodies, HIV-2 antibodies or HIV antibodies in general. Specimens with reactive result in the initial combined immunoassay and non-reactive or indeterminate on the HIV-1/HIV-2 antibody differentiation immunoassay should be tested with an FDA-approved HIV-1 NAT. A reactive HIV-1 NAT result and non-reactive or indeterminate HIV-1/HIV-2 antibody differentiation immunoassay result indicates laboratory evidence for presence of HIV-1 infection. A non-reactive HIV-1 NAT result and non-reactive or indeterminate HIV-1/HIV-2 antibody differentiation immunoassay result indicates a false-positive result on the initial immunoassay. Laboratories should use the same testing algorithm to confirm a positive result from any rapid HIV test.[112]

In RLSs, RDTs are often used for laboratory diagnosis of HIV infection. The testing algorithms have been applied for rapid testing in these setting as well. Usually, a reactive result from the first RDT is confirmed by using another RDT. If the results of these two tests are in conflict, the result is resolved with a third RDT.[113] A suitable testing algorithm for RDTs is presented in Figure 5.

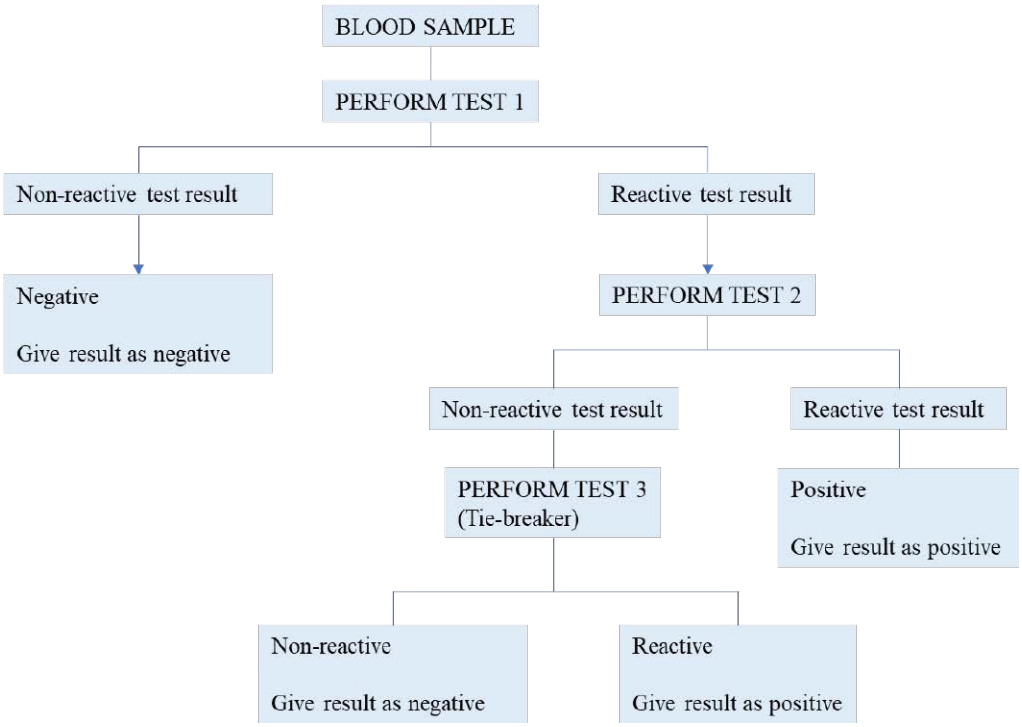

Figure 5. HIV testing algorithm suitable for resource-limited settings where only rapid tests are applicable. Reactive test result will be confirmed with another test and discrepant result from the second test should be confirmed with a third test.

2.4.2 Review of HIV rapid diagnostic tests

Multiple good performance HIV RDTs are available, and they mostly represent tests for the detection of anti-HIV antibodies. According to the listing provided by The Global Fund, in March 2020, there were 30 different HIV RDTs available (self-tests not included) out of which 17 were WHO prequalified products. Out of the 30 tests, 24 tests were suitable for combined detection of anti-HIV-1 and anti-HIV-2 antibodies and 5 tests were able to discriminate between anti-HIV-1 and anti-HIV-2 antibodies. Alere HIV Combo (Abbott Alere Medical Co. Ltd, Matsudo, Japan) combined test was able to discriminate between HIV-1/2 antibodies and to detect HIV-1 p24 antigen, and it was therefore the only test suitable for earlier phase-infection detection. Almost all the tests were LF tests relying on visual detection. Average sensitivity of the tests was 99.7%, varying from 98.9% to 100%. Average specificity was 99.7%, ranging from 98.5% to 100%.[75]

2.5 Point-of-care testing of non-communicable diseases

Access to POC technologies can improve access to better healthcare in settings with limited healthcare infrastructure. POCT of non-communicable diseases (NCDs) such as cancer, cardiovascular diseases (CVDs) and diabetes may facilitate the correct diagnosis and treatment, and widen the repertoire of diagnostic possibilities regardless of geographic and socioeconomic limitations.[6,114]

NCDs, including both CVDs and cancers have increased steadily since 1990 in terms of total number of deaths, driven by ageing and population growth[3]. In 2017, CVDs, including coronary artery disease and stroke, were responsible for an estimated 17.8 million recorded deaths, of which over three quarters were in LMICs[3,115]. It is estimated that by 2030, more than two-thirds of new cancer cases will occur in LMICs[114]. The epidemiological transition with a change from infectious to non-communicable diseases has been recognized in settings such as humanitarian emergencies[116]. To alleviate this overall shift in global disease burden, the development and implementation of appropriately designed affordable technologies for diagnosis and treatment of NCDs is desired and e.g. POCT compatible biosensors for cancer detection are being developed and described in recent research literature[117].

There is a global challenge of providing preventive, personalized and precision medicine -based quality healthcare at an affordable cost. The shift towards personalized medicine requires technological development to enable testing for patients and healthcare providers at POC locations including homes, semi or pre-clinical facilities, and hospitals.[118]

2.5.1 Myocardial infarction and cardiac troponins

Acute coronary syndrome (ACS) is an umbrella term used to describe a range of conditions associated with sudden reduced blood flow to the heart muscle. One such condition is a heart attack (myocardial infarction, MI), which occurs when cell death results in damaged or destroyed heart tissue.[119] Annually approximately 15–20 million patients visit the emergency department (ED) with acute chest pain or other symptoms suggestive of ACS in Europe and the USA[120]. ACS patients represent a substantial proportion of all acute medical admissions, and they account for more than 1 million annual hospital admissions in the United States[121]. The challenge is early identification of ACS among a large heterogeneous patient population, since only one in three patients experiencing chest pain visiting ED ends up with ACS diagnosis[120]. Timely and correct diagnosis to rule-in and rule-out ACS are equally important in terms of cost saving and improving the clinical outcomes of ACS patients.

Cardiac troponin I (cTnI) and T (cTnT) are recommended biomarkers for diagnosis and risk stratification with suspected ACS[122]. In the diagnosis of acute MI, cTn testing is used in combination with electrocardiographic (ECG) and/or imaging evidence of cardiac muscle damage and observed symptoms of acute myocardial ischeamia[123].

Cardiac troponin complex proteins I, T and C are structural proteins specific to cardiac muscle regulating the muscle contraction[124]. Cardiac troponin levels become elevated in damage to cardiac muscle and cTnI release has specificity for cardiac injury[125,126]. After cell membrane disruption the free cytosolic pool of cTnI is released to the circulation within hours after myocardial damage[127]. Measurement of circulating levels of cTnI, particularly observing the rise or fall in cTnI levels, along with the evaluation of patient symptoms and ECG abnormalities are current procedures in the triage of suspected ACS and MI patients[123,128].

In general, low and moderate cTn levels around 50-100 ng/L are suggestive of clinical conditions such as MI, myocarditis, stress cardiomyopathy, pulmonary embolism, heart failure, shock hypertensive crisis and subarachnoid hemorrhage. High to very high cTn levels can be considered ranging from 1000 up to >10 000 ng/L, and are strongly predictive for severe MI.[129,130]

There are five different criteria for the diagnosis of MI and all except one (cardiac death before biomarkers were obtained) include the 99th percentile of cTn or a multiple of it as decision limit[123,128]. The 99th percentile upper reference limit (URL) is defined as the 99th percentile of cTnI distribution in a healthy reference population[131]. The 99th percentile URL is designated as the decision level for the presence of myocardial injury and must be determined for each specific assay[123].

2.5.2 Point-of-care testing of cardiac troponin I

Despite the availability of sensitive central laboratory assays, many physicians decide to use POCT for cTn measurements due to the benefits of a short turn-around time. Furthermore, POCT can be used in e.g., in ambulance to obtain information on the status of the ACS patient prior to admission to hospital. POCT for cTn in the EDs has been shown to reduce the length of stay for patients with suspected ACS.[132] Typically, blood samples for the measurement of cTn are drawn on first assessment and repeated 3–6 h later[123,128]. POCT for cTnI accelerates result availability for the patient follow-up.

Equal performance of cTn-POCT in contrast to central laboratory testing has been demonstrated in some studies[133,134], however, other studies have critically compared the advantages and disadvantages of POCT in contrast to central laboratory testing. It has been pointed out that POCT is not always more cost-effective than central laboratory testing, however, it has the potential to improve the flow of patients through the emergency department to shorten discharge times[135].

Rapid whole blood testing for cTnI by using Abbott i-STAT POCT system has been shown to give generally reliable patient classifications compared with central laboratory testing using plasma samples. However, POCTs tend to end up with a few percent of positive and negative results which may be misclassifications, giving some apparent false positives at low cTnI concentrations. With the studied Abbott i-STAT POCT system, the results of more than 200 ng/L were unlikely to be false-positives, and negative results were unlikely to have more than a minimal elevation in cTnI levels.[136] Nevertheless, the current guideline for MI diagnostics introduced in 2018 for the Universal Definition of Myocardial Infarction, does not distinguish between central laboratory and POC testing, when considering requirements for imprecision of the measurement[123]. There are different POCT systems available for the detection of cTnI. An overview of available options are presented in Table 2[135].

Table 2. Features of available quantitative point-of-care assay systems for measuring cardiac troponin, as reported by assay manufacturers[135,137].

Brand name/company	99th percentile upper reference limit (ng/L)	Technology, reaction detection	Limit of Blank (ng/L)	Sample	Analytic turnaround time (min)
i-Stat Troponin I/Abbott	80	ELISA, ALP	20	16 µl whole blood	10
Triage troponin I/Alere	56	Chromatographic, fluorescence	10	250 µl heparinized whole blood or plasma	15
PATHSFAST troponin I/Mitsubishi	29	Magnetic beads, CL	8	100 µl heparinized whole blood, plasma or serum	17
AQT90 Flex troponin I/Radiometer	23	Sandwich immunoassay, fluorescence	ND	1 mL EDTA or heparinized whole blood, plasma or serum (40 µl for individual tests)	18
RAMP troponin I/Response Biomedical Corp	<100	Chromatographic (LFIA), fluorescence	30	75 µl EDTA whole blood	18
Stratus CS troponin I/Siemens	70	ELISA, ALP	30	3 mL heparinized whole blood (100–200 µl plasma for individual tests)	14
Meritas Troponin I/Trinity	36	Chromatographic (LFIA), fluorescence		200 µl EDTA whole blood or plasma	15
VIDAS/ bioMerieux	10	ELISA, fluorescence		200 µl serum or plasma, heparinized with lithium or centrifuged to eliminate fibrin	20

The data have been obtained from assay inserts and the official home pages of the respective companies. LFIA, lateral flow immunoassay; ELISA, enzyme-linked immunosorbent assay; ALP, Alkaline phosphatase; CL, chemiluminescence; ND, not determined or not available. Manufacturer locations: Abbott, Illinois, USA; Alere, Waltham, MA, USA; Mitsubishi, Düsseldorf, Germany;

Radiometer, Brønshøj, Denmark; Response Biomedical Corp, Vancouver, Canada; Roche, Basel, Switzerland; Siemens, Erlangen, Germany.

2.6 Lateral Flow Immunoassays

The LFA platform is one of the most dominant formats for an RDT due to its ease-of-use and low-cost. LF technology is a well-established mature technology with relatively easy manufacturing processes. In many cases, LFAs can be used as POC tests in clinical environments but also as home-tests. One of the most common applications of LF tests is the at-home pregnancy test, which was first introduced in 1988[138]. In common to all LFAs, the test procedure is based on a few, typically one or two, steps which include the sample addition and possible addition of buffer to the test strip[139].

LFAs are based on immunochromatographic flow of a liquid sample through the test strip by capillary forces. The test strip typically consists of the following functional parts: a sample pad, a conjugate pad, an analytical membrane and an absorbent pad. The strip design is assembled on top of a backing plastic. In commercial applications, the strips are often placed inside of a plastic cassette which serves as protection for the delicate paper-based materials, supports the contact between these materials that is essential for the proper liquid flow and guides the user with correct sample addition and result interpretation. The sample and other possibly required liquid reagents are added directly or via a sample port to the sample pad.

Reporter-conjugates are produced by coating the tracer molecules to the reporter surface. The reporter-conjugates are dried onto a conjugate release pad and are activated and released as the added liquid flows through the pad. The reporter-conjugates have time to react with the analyte present in the sample while the liquid is flowing through the analytical membrane, until the conjugate-analyte complexes reach capture reagents immobilized on a test (T) line zone on the membrane. Excess label conjugates travel further to a control (C) line zone, on which reagent capable of binding the tracer molecule is used to bind the excess conjugates and serve as an internal control.[139,140]

LFAs can be carried out not only in a typical non-competitive (sandwich) format (Figure 6) but also in a competitive format. LFAs are most often immunoassays utilizing mono or polyclonal antibodies as binders, but other non-antibody affinity reagents can also be used. For instance, recombinant affinity proteins e.g. viral surface proteins for the detection of anti-viral antibodies, or antibody derived protein fragments can be applied as binders.[139]

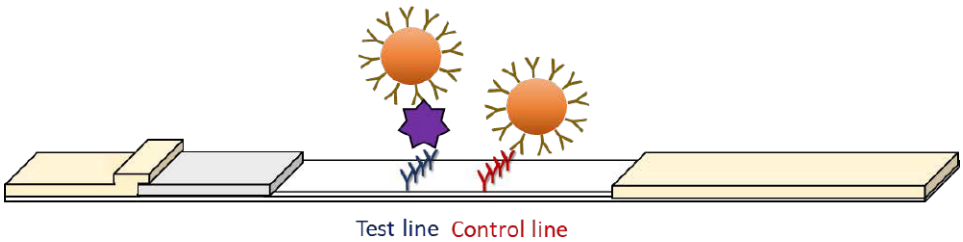

Figure 6. The structure of a typical lateral flow strip for a sandwich LFIA. The sandwich complex is formed in the test line position by immobilized capture antibody, analyte and tracer antibody on the reporter particle surface. Anti-species antibody immobilized on the control line zone captures the tracer antibody-reporter particle conjugates.

LFAs typically require low sample volumes, which serves as an advantage especially when the available sample volume is limited e.g., with a finger prick blood sample. The reverse side of this is that the LF strips typically have a restricted capability to absorb liquid, often around 100 µl in total. This may cause challenges when the analyte concentration in the sample is low. LFAs can utilize a wide range of different sample matrices depending on the target application: serum, plasma, finger prick or venipuncture whole blood, urine and saliva. LF applications are not limited to medical diagnostics. Food and environmental safety, animal health, aqua- and agriculture, forensic science, military and biodefense uses are important market segments for LFAs.[140]

Analyte detection in the LFA is based on signal generation deriving from immunocomplex formation with reporter nanoparticles. Most of the currently available LFAs are based on visual reporters, typically colloidal gold nanoparticles[141]. Alternatively, colored latex particles and other colored nanoparticles can be used. The results provided by visual reporter particles are qualitative or semiquantitative. Trends in current development and research are towards different fluorescent labels in order to achieve quantitative and more sensitive assays. However, the use of fluorescent labels usually increases the cost of the LFA since more sophisticated hardware and software are needed to read the signal.[142] Alternative reporter technologies will be described in detail in chapter 2.6.3.

2.6.1 Strip components

The LF strip is built with a smaller component forming a functional system that enables the liquid flow and the detection reaction to happen. Each component serves as an important part in the functional test and has its own special features and requirements that should be carefully taken into consideration while developing LF based tests.

2.6.1.1 Sample pad

Typically, a sample pad is used to accept the sample and other liquid reagents. The sample pad enables sample flow through with minimal analyte retention and simultaneously it treats the sample in such a way that it is compatible with the assay. Sample treatment may include e.g. filtering out of particulates or red blood cells, changing the sample pH and removing sample matrix components that may interfere with the assay[140]. The pad needs to be pre-treated with selected components. In the pre-treatment procedure, a buffer solution containing the essential reagents required for sample treatments such as salts, detergents and biomolecules, is applied and dried to the pad material prior to use. Also, the viscosity of the pad can be adjusted with additives, and the sample flow rate and thus the total reaction time can be slightly adjusted.[140,143]

To implement sample pre-treatment properties into the sample pad, the pad material must be chosen carefully. The material chosen can have an enormous effect on the assay performance because it affects the pre-treatment solution distribution and thus also to the homogeneity of the produced LF strips. Typical sample pad materials include cellulose, glass fibre, rayon and other filtration capable materials.[140] There are also some proprietary fibre blends developed for certain filtration needs such as filtering red blood cells[143].

The pad material must also be able to accept the needed sample volume applied to it in a controlled manner without leaking. Suitable sample volume depends on the pad material and size of the pad. The materials have different bed volumes which describe the liquid volume required to wet the material.[143]

2.6.1.2 Conjugate release pad

The component following the sample pad on the common LF strip composition is a conjugate release pad. The reporter conjugate is dried onto the conjugate release pad and the primary function of the pad is to preserve the conjugate in stable form during storage. Once the test is run, the pad should release the conjugate with high efficiency and reproducibility.

Conjugate release pad material is typically glass fibre, polyester or rayon. The pad must be hydrophilic to allow rapid flow rates. As many of these materials are hydrophobic by nature, it is often necessary to pre-treat the conjugate pads to obtain optimal release and stability. Pre-treatment is often performed by wetting the pad in aqueous solution containing proteins, surfactants and polymers, followed by drying.[140,143]

The addition of conjugates to the pre-treated pad is crucial for the overall performance of the assay. Variation originating from conjugate deposition and distribution to the pad during drying of the conjugate and the uneven release from

the pad has a major effect on the coefficient of variation (CV) in assay performance. Assay sensitivity can also be adversely affected by poor conjugate release efficiency. Depending on the application, faster or slower release of the conjugate from the conjugate release pad may be preferred, but either way the release must always be consistent.[144]

There are two common methods for conjugate drying. The first method is immersion where the pre-treated conjugate pad is dipped into the conjugate suspension. The second method is conjugate dispensing with quantitative non-contact air spray dispensers.[140] Conjugates are dispensed in a solution containing sugars such as sucrose or trehalose. These serve as preservation and solubilization agents. The sugar molecules form a protective structure around the particles and stabilizes biological structures. When the pad is wetted in the assay run, the sugars dissolve rapidly releasing the particles from the pad into the liquid flow.[143] Conjugate release speed affects the signal generation as only the coincident release of the conjugates with the analyte flowing through the conjugate release pad contributes to the signal generation. Analyte running after the released reporter particles is not capable of generating signal (Figure 7).

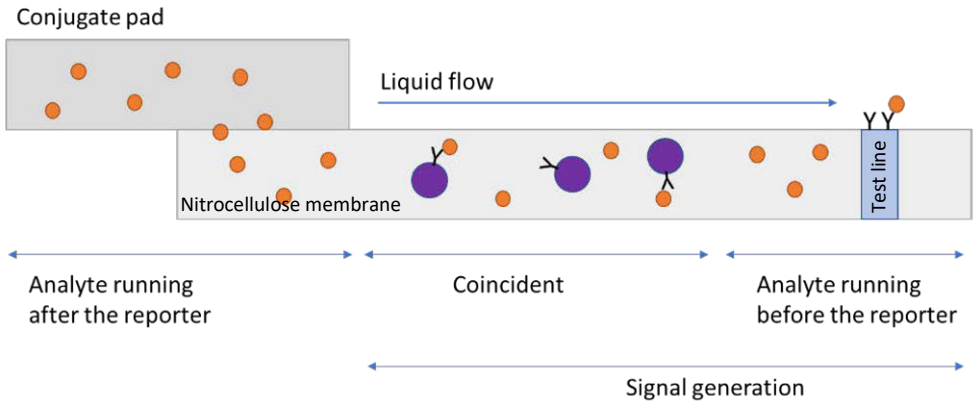

Figure 7. Effect of conjugate release rate on the assay signal generation. Once the dried conjugate (purple particles) has been released, the analyte (orange) running afterwards is not capable of signal generation.

2.6.1.3 Analytical membrane

Analytical membrane serves as a solid phase in LFAs. Its purpose is to bind proteins at the test and control areas and maintain their stability and activity over the shelf-life of the product. Once the test is run, the membrane must take the sample and reporter conjugates from the conjugate pad and allow consistent flow of these

components to the reaction areas and allow the reactions to happen. The excess fluid and reactants should pass the membrane without unspecific binding.

Nitrocellulose (NC) is absolutely the most used material for analytical membrane. Other materials such as polyvinylidene fluoride, nylon, polyether sulfone have their minor uses in some applications.[143] NC provides several advantages such as relatively low cost, suitable capillary flow characteristics and high protein-binding capacity. There is a variety of available products with varying characteristics available for assay development. Drawbacks of NC include particularly the imperfect reproducibility within and between lots and its susceptibility to varying external conditions such as humidity and mechanical stress causing breakage.[140,145]

NC is a polymeric structure that binds proteins by electrostatic, hydrogen, and hydrophobic interactions. Membranes differ in protein binding capacities, which is affected by the polymer surface area available for immobilization. The surface area is dependent on the pore size, porosity, membrane thickness and polymer's surface characteristics.[143] This determines if a given protein is suitable for the membrane[140]. It has been shown that different pH and membrane pore morphologies contribute to different protein adsorption mechanisms. At the isoelectric point of the protein, the repulsion between the protein and the NC membrane is at the lowest and thus, the protein may be more easily attached onto the membrane[146].

It is critical for LFA performance that the membrane binds reactants only at the test and control lines. To avoid unintended binding, an NC membrane can be pre-treated i.e., blocked to prevent the binding of proteins and labeled conjugate to the membrane.[145]

The membrane must be hydrophilic and have consistent flow characteristics. NC is hydrophobic by nature and is made hydrophilic by the addition of rewetting agents i.e., surfactants during the membrane production process. There are differences on how proteins act together with different membranes and pre-treatments. This is another reason for screening multiple membranes during assay development. Also, other membrane performance characteristics can vary remarkably in combination with different proteins. Membrane characteristics affecting the assay performance typically are polymer type used in the membrane, pore size, surfactant type, quantity, and the method of surfactant application.[140]

Flow of the components through the analytical membranes by capillary action can happen only in a porous matrix. Membranes are porous materials with pore sizes ranging from 8 to 15 micrometers. The pore-size of the membrane typically corresponds to the flow rate of the liquid, also called wicking rate or capillary rise time. However, wicking rate is a more appropriate measure for membrane flow characteristics than pore size although they are closely related. As the pore size increases, the flow rate speeds up and vice versa.[143,145] Wicking rate is a manufacturer-defined specification for NC membranes, and it is defined as the time

in seconds required for a fluid front to traverse a 4 cm width of membrane. The wicking rate is an important to factor for the assay kinetics and will thus has effect on assay performance and sensitivity.[140,143]

The flow speed is faster at the initiation of the flow and then decreases proportionally to the square of the distance traversed until the flow achieves a steady rate at the point when the bed volume of the NC becomes saturated[147].

The flow speed of the liquid front in the porous matrix by capillary actions can be modelled by Lucas-Washburn equation (1)[148,149]

$$L = \sqrt{\frac{\gamma r t \cos(\theta)}{2\eta}} \quad (1)$$

where L is the distance the liquid has penetrated the capillary, γ is the surface tension, r is the pore radius, θ is the contact angle between the liquid and the pore wall and η is the viscosity of the liquid.

On the contrary, the flow rate in the fully wetted membrane can be described with the Darcy equation (2)[149,150]

$$Q = -\frac{\kappa w h}{\eta L} \Delta P \quad (2)$$

where Q is the volumetric flow rate, κ is the permeability coefficient that is dependent the on the porous structure of the membrane, *wh* is the membrane area, η is the viscosity, L is the membrane length and ΔP the drop in pressure occurring over the length of the membrane.

2.6.1.4 Absorbent pad

Absorbent pad or wick is typically made from high-density cellulose. It serves as the engine of the strip: it is pulls the fluid added to the strip and supports the flow for the duration of the assay.[140]

2.6.1.5 Covers and support

The LF strip components are held together with adhesive backing material. In some applications, the strip components may be covered with a tape applied on top of the materials. Sometimes strips are placed inside of a plastic housing, which protects the test strip and facilitates strip handling by the test operator. Proper supportive materials can be used to improve the contact between different overlapping strip components and thus maintain consistent liquid flow properties.[145,151]

2.6.2 Lateral flow assay kinetics and binders

Despite the various LF materials, biomolecule binders lie at the heart of LFAs. Commonly, LFAs use IgG antibodies as binders. In a sandwich LFA, immunocomplex formation involves analyte binding to the tracer antibodies on the reporter surface and the analyte-reporter complexes binding to the capture antibody in the T position. Signal generation at the T and C positions is a nonequilibrium process, because the analyte and reporter particles are being actively carried in the liquid stream and can interact with the capture molecules only for the short time when they are adequately close to interact[145]. The interactions occurring in an LFA can be mathematically modelled. The simplest way to describe the reaction kinetics of immunocomplex formation in LFA in T position on NC membrane is shown in Equations 3-5[152].

$$AR + C \rightleftharpoons \mathrm{ARC} \tag{3}$$

$$k_{on}[AR][C] = k_{off}[ARC] \tag{4}$$

$$K_a = \frac{k_{on}}{k_{off}} = \frac{[ARC]}{[AR][C]} \tag{5}$$

where AR is the reporter-analyte complex, C is the capture antibody, K_a stands for the binding constant of the reaction and k_{on} and k_{off} describes the on-rate and off-rate of the reaction, respectively.

However, contrary to immunocomplex formations that are able to reach the equilibrium, the tracer and capture antibody reaction times are merely seconds. In the T position the reaction time for the capture antibody is even shorter than that of tracer antibody coupled to the reporter particle and the analyte. [139,140] In a typical NC membrane it takes approximately 0.16 to 0.66 seconds for the analyte and reporter-conjugate to traverse 1 mm on the membrane, depending on the flow rate of the membrane. Thus, these compounds have approximately from one to six seconds to bind to the capture antibodies while passing the test line zone of 0.5-1.0 mm width[147] This makes the on-rate of T capture antibody a typical limiting factor for LFA detection sensitivity. Therefore, the reaction rate with antibodies can be mainly improved by enhancing the on-rate of the antibodies used. Antibodies used in LFAs should be selected based on a fast on-rate among other properties commonly required for a good antibody[147]. Utilizing other high-affinity binders and linker chemistries such as streptavidin-biotin interaction has also been suggested to improve the reaction rates[152].

Other techniques to adjust the reaction rate in an LFA include selection of a NC membrane with a pore size providing the desired reaction rate as the flow rate is dependent on the pore size[140] and the flow rate has a direct impact on the interaction time at the T position as described above. The reaction rate at the test line can be

altered with physical changes to the strip structure, for instance, by applying narrow wax barriers to alter the reaction surface area[153], laser structuring channels on the membrane[154], spotting wax pillars to reduce the speed of the flow[155] or by using cellulose nanofibers specifically to reduce the pore size at the test line position only and thus reduce the flow rate at the reaction zone[156].

Binders should be immobilized on the NC membrane in a way that the antibody maintains its correct orientation and configuration for the binding reaction. In general, capture antibody immobilization onto NC can result in different target affinities and the antibody behavior on paper can differ significantly from that of in solution. The porosity of the NC membrane enables capillary flow, but porosity also leads to high net surface area which makes the system prone to interface effects. Capture molecules can be trapped inside the pores unreachable for the binding reaction and thus decrease target binding efficiency.[157] Alternative antibody immobilization techniques including covalent attachment through an epoxide-thiol or streptavidin-biotin linkage and use of a NC-binding anchor protein coupled with the capture antibody have been reported to improve the binding efficacy on the membrane[158].

2.6.3 Reporter technologies and assay sensitivity

Visual detection is the most dominant format for result interpretation in LFAs. Commonly, colloidal gold nanoparticles (AuNPs) are used, and they are known for the red-colored lines at the result read-out. However, AuNPs used in LFAs typically provide somewhat limited sensitivity because 20-30 nm AuNPs tend to have relatively low signal-intensity caused by insufficient brightness[159,160]. The sensitivity can be enhanced by using basically three types of nanoparticles (NPs) as alternatives for conventional AuNPs. These include 1) colored labels such as AuNPs, carbon NPs and colloidal selenium NPs in varying diameters, 2) luminescent NPs such as quantum dots (QDs), upconverting NPs (UCNPs) and other dye or lanthanide-ion doped NPs, and 3) magnetic NPs[161]. The main features of colored and luminescent NPs are described below.

2.6.3.1 Colored

AuNP LFAs are widely used because of their simplicity, relatively rapid signal generation and ease of qualitative result interpretation (yes/no). Drawbacks of AuNP LFAs are typically the limited sensitivity and availability of qualitative or semi-quantitative results only. Furthermore, visual result interpretation done by the naked-eye approach is prone to human errors[162]. AuNP use in LFAs is widely investigated and certain methods such as increasing the size of the particles or using particle

clusters have been shown to improve the sensitivity in contrast to traditional AuNP labels[163,164].

Colloidal carbon NPs also called carbon black are also visually detectable label alternative and like AuNPs these provide a qualitative or semi-quantitative read-out. Advantages the carbon NPs provide include ease of preparation and conjugation with the biomolecule, high stability, and non-toxicity. Particularly, carbon NPs possess the property of a high signal-to-background ratio because of the black color in contrast to the white background.[161] The carbon NPs have been reported to provide sensitivities in picomolar range by visual read-out[165,166]. Colloidal selenium nanoparticles are similar to AuNPs and colloidal carbon NPs in terms of qualitativeness/semi-quantitativeness and visual read-out, however, typically selenium NPs tend to have weaker color intensity[167].

Colored NPs in LFAs can be quantitatively detected by using a reader device, which records the optical density of signals. Signal detection is based on the conversion of the color density of T and C lines into optical density units which can then be used to quantify the signal.[168]

2.6.3.2 Luminescent

Luminescent NP labels used in LFAs are typically different lanthanide doped NPs or QDs. QDs are fluorescent semiconductor nanocrystals suitable for LFAs due to their size-dependent emission wavelengths, broad absorption spectrum and narrow emission spectra with strong luminescence intensity[161]. Recently, QDs have been used in LFAs e.g. for the detection of C-reactive protein (CRP) and HIV-DNA[169,170].

Silica NPs can be utilized as luminescent NPs by incorporating luminescent compounds into the silica shell. Lanthanide chelates have been an interesting target for research due to their luminescence properties such as long fluorescence lifetime, wide Stoke's shifts and sharp emission profiles[171]. Lanthanides such as europium (Eu), terbium (Tb), samarium (Sm), and dysprosium (Dy) with different emission spectra can be used. However, conventionally lanthanides have limitations including weaker luminescence and photobleaching. To enhance the fluorescence performance and improve detection sensitivity, silica NPs doped with lanthanide chelates have been developed and used for time resolved immunofluorometric assays[172–176]. Time-resolved fluorescence detection typically exhibits higher detection sensitivity than conventional fluorescence because of lower background autofluorescence. Time-resolved fluorescence techniques separate the emission light from the background through fluorescence lifetime differences.

The sensitivity of fluorescent LFAs is typically limited because of the background interference caused by light scattering and autofluorescence originating from the instrument's optics, the sample matrix, and the test device itself. The

membrane-based LFAs are particularly prone to high background fluorescence in a traditional fluorescence system because of light scattering instigated by the membrane itself[161]. To avoid this phenomenon in LFAs, time-resolved luminescence measurement has been combined also with LFAs[177–179].

Upconverting nanoparticles (UCNPs) are a composition of inorganic host substance (crystal structure) and lanthanide dopant ions. Upconversion takes place when two or more lower energy photons are absorbed sequentially, and a higher energy photon is emitted at a shorter wavelength than the original excitation wavelength i.e. anti-Stokes emission.[180] The UCNPs are often coated with silica or other compounds to achieve better chemical compatibility and ease of surface functionalization by biochemical compounds[181]. In comparison to conventional down-converting fluorescent labels, UCNP technology eliminates measured autofluorescence since the biological matrices do not possess the property of upconversion and thus, the autofluorescence occurs at conventional down-converted wavelengths. In addition, the low absorbance level of biological matrices at the excitation wavelengths is useful for many POC applications, since use of whole blood samples is typically preferred. UCNPs are photochemically stable[182], which enables multiple measurements and long-term storage of UCNP assay systems without loss in light-emitting properties. UCNP-based POC assays can be read by multiple or time-integrated scans and the test can be archived for subsequent verifications. UCNPs have been used in multiple different LFAs in research[183–188]. One of the advantages is improved sensitivity in comparison to other label technologies[189]. Furthermore, LFAs enabling analyte quantification with UCNP reporters have been introduced in limited numbers in research[187,190].

3 Aims of the Study

The overall aim of this study was to develop rapid diagnostic methods for the detection of viral infections and cardiac troponin I (cTnI). The assays were carried out in LF format, which is a suitable for RLS because of its simplicity and cost-efficiency. The main objective of the study was to improve the rapid assay sensitivity and quantification which was achieved by using UNCP reporters.

The aims, described in detail, were:

I: To develop a simple, rapid and highly sensitive LFIA for the detection of HBsAg and to characterize the performance of the developed assay with clinical patient samples, as well as to compare the UCNP-LFIA performance to that of a conventional commercially available LFIA based on visual detection.

II: To develop a rapid double-antigen bridge UCNP-LFA corresponding to the 3rd generation HIV tests for the detection of anti-HIV-1/2 antibodies and to evaluate the assay performance with clinical samples and sample panels, as well as to compare the UCNP-LFA performance with a conventional commercially available LFA.

III: To develop UCNP-LFIA for cTnI and evaluate the detection limits and performance of the developed cTnI-UCNP-LFIA. The aim was to show the quantification capability of the UCNP-LFIA with a set of clinical samples and to establish the determination of Limit of Blank (LoB) and Limit of Detection (LoD) suitable for an LFA in accordance with the The Clinical Laboratory & Standards Institute (CLSI) guidelines.

4 Summary of Materials and Methods

A summary of materials and methods used in this study with some supplemental information are presented here. The complete descriptions of the materials and methods for each individual developed assay can be found in the original publications **I–II** and manuscript **III**.

4.1 Binders and assay configurations

4.1.1 Antibody selection for antigen detection

Available monoclonal antibodies (mAbs) were studied in a competitive binding inhibition assay (**I**) (Figure 8). Eight in-house and two commercial (Medix Biochemica Oy, Finland) mAbs were investigated. Biotinylated anti-HBsAg polyclonal capture antibody was bound to the streptavidin-coated wells. Each anti-HBsAg mAb was labeled with Eu(III)-chelate, and they were tested against each other in labeled and non-labeled format. Eu(III)-chelate-labeled mAb was allowed to compete with an excess of free mAb in the reaction with HBsAg. The amount of competing mAb was optimized prior to competitive binding inhibition assay to ensure an adequate level of inhibition. Affinities of different antibody binders were determined with biolayer interferometry (Octet Red 384, ForteBio, USA).

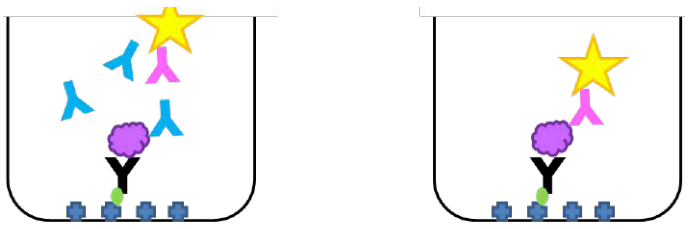

Figure 8. Eu-labeled mAb was allowed to compete against other mAbs in well based assay. Control reaction did not include competing mAb and the Eu-labeled mAb was allowed to react freely with the target analyte.

The inhibition percentage was calculated according to equation 6:

$$Inhibition\ \% = 100 - \frac{specific\ signal}{spesific\ signal\ (control\ reaction)} * 100 \quad (6)$$

A threshold of >80% inhibition previously described in the literature was used[191]. When inhibition of above 80% was observed, it was assumed that the competing antibody binds to an overlapping epitope with the Eu(III)-labeled tracer-mAb, whereas in the case of a lower inhibition percentage it was assumed that the competing antibody binds to non-overlapping epitope.

In publication **I**, the anti-HBsAg mAbs were evaluated for their ability to recognize different HBV genotypes. The mAbs were dispensed on capture lines on LF strips. The strips were tested using Paul Erlich Insitut's 1st WHO HBsAg genotype panel (6100/09). Based on the competitive binding inhibition assay results and evaluation of the genotype detection, the mAbs were divided into groups. Combinations of mAbs from different groups were tested in the LFA and the optimal antibody combination was selected based on analytical sensitivity.

In manuscript **III**, the developed cTnI-LFIA utilized a 3+1 configuration of mAb binders for the detection of cTnI where three antibodies are immobilized on the NC membrane and one mAb is conjugated on the UCNP surface (mAb-625). The 3+1 configuration was selected based on previous research showing reduced cTnI autoantibody effect[192]. More specifically, cTnI-specific mAbs 19C7, 916 and 625, targeting epitopes at aa 41–49, 13-22 and 169–178, respectively (HyTest Ltd, Finland) and anti-h cTnI 9707 SPTN-5 mAb targeting the epitope at residues 190-195 in the C-terminal part of the cTnI molecule (Medix Biochemica Oy) were utilized as binders. The selection of the best binders had been done prior to the thesis study.

4.1.2 Double-antigen bridge assay for antibody detection

Recombinant antigens, r-HIV1-env and r-HIV2-env, were generated[193] and used earlier for the detection of anti-HIV antibodies[194–196]. To use these antigens in the anti-HIV-LFA, the antigens were coupled to the UCNP surface as well as immobilized on the T line of the LF strip. The bridge formation of the double-antigen assay in anti-HIV-1/2 antibody detection is presented in Figure 9.

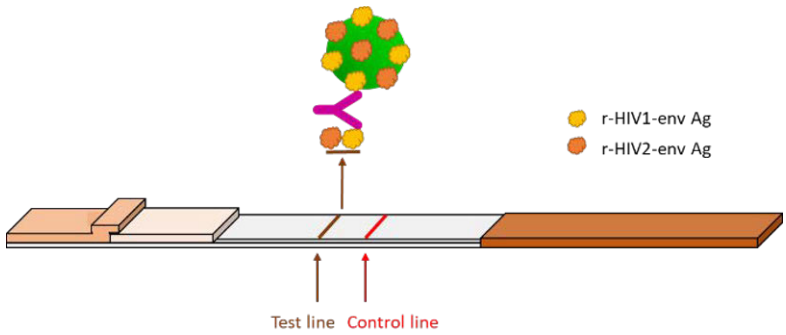

Figure 9. A schematic depiction of double antigen-bridge assay for the detection of anti-HIV-1/2 antibodies utilized in publication **II**. The recombinant HIV-1 and HIV-2 envelope antigens were coupled to the UCNP (green particle) surface as well as immobilized on the test line. Control line (red line) consisted of anti-gp41 immunized rabbit serum for binding r-HIV1-env antigens on UNCP surface.

4.2 Reporter technology

4.2.1 Upconverting nanoparticles

Erbium-doped UCNP particles (RD Upcon®540-L-C1-COOH, product number 46-05RD) with hydrophilic coating (Kaivogen Oy, Finland) were used as reporters in publications **I–III**. The average diameter of the particles was around 70 nm (Figure 10A). The particles were excited with IR laser of wavelength 978 nm. Detection of the Erbium emission peak was done by a band-pass filter approximately at 540–550 nm (Figure 10B). The tracer molecules were covalently coupled to the UCNP surface by using NHS-EDC chemistry.

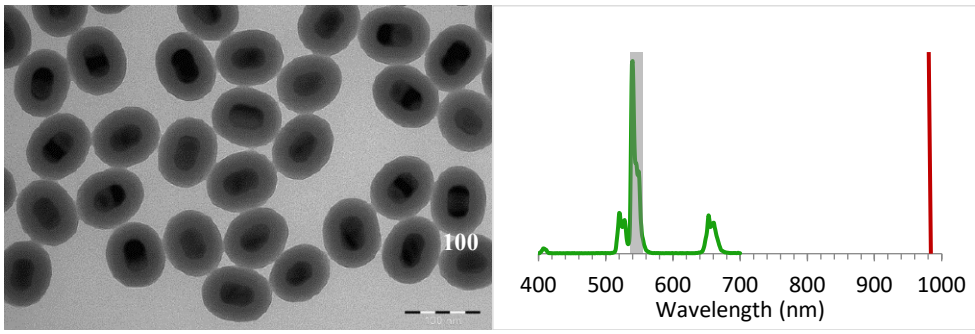

Figure 10. A. Average diameter of UCNPs used was 70-80 nm. TEM-image courtesy of Kaivogen Oy. **B.** Schematic illustration of the emission spectrum of Erbium (green), IR-excitation light at 980 nm (red), and band-pass filtered measurement area (grey).

4.2.2 Bioconjugation of the reporters

The carboxyl groups on the UCNP surface were activated using EDC/sulfo-NHS chemistry. UCNPs were diluted to concentration 8.0 mg/ml in 20 mM MES buffer, pH 6.1. Activation was done by using 20 mM EDC or 2 mM EDC (**III**) and 30 mM sulfo-NHS. The activation reagents were diluted in 20 mM (**I–II**) or 50 mM (**III**) MES, pH 6.1, and added to UCNP solution to a total reaction volume of 260 µl and incubated either for 45 minutes (**I**) or 15 minutes (**II-III**) at room temperature (RT) in rotation. The UCNPs were washed once by centrifuging (10 min, 20 238 x g) and suspending the UCNPs to 20 mM MES, pH 6.1. The UCNPs were centrifuged as previously and resuspended into 20 mM MES, pH 6.1. The tracer molecule content of the reaction was 84 µg of mAb-3D3 (**I**), 65 µg of each antigen (**II**) and 60 µg of mAb-625 supplemented with 100 mM NaCl (**III**) per 1 mg of UCNPs while the total reaction volume was 250 µl. The reactions were incubated for 2.5 hours (**I–II**) or 30 minutes (**III**) at RT in slow shaking. Reaction interception and the surface blocking of activated carboxyl groups was done by adding 50 mM glycine, pH 11, to the reaction. Reactions were further incubated for 30 minutes at RT with shaking. UCNP-conjugates were washed twice to remove unbound compounds by centrifuging (10 min, 20 238 g) and suspending the UCNP-pellet to 250 µl storage buffer. The UCNPs were stored at +4°C until use.

4.3 Lateral flow assay strips

4.3.1 Membranes and materials

Several membranes were used in this study to optimize the assay performance. NC membranes used are presented in Table 3. Conjugate release pad materials used are listed in Table 4 and sample pad materials in Table 5.

Table 3. Nitrocellulose membranes used in the study.

Nitrocellulose membrane	Manufacturer	Wicking rate (s/4 cm)
CNPH-N SS60	Advanced Microdevices (India)	200
CNPH-N SS40	Advanced Microdevices (India)	150
CNPC SS12, 12 µm	Advanced Microdevices (India)	120
CNPC SS12, 10 µm	Advanced Microdevices (India)	140
CNPF SN12, 10 µm	Advanced Microdevices (India)	125
CNPF SN12, 8 µm	Advanced Microdevices (India)	185
LFNC-C-BS023_70	Nupore Filtration Systems (India)	69
LFNC-C-SS22_70	Nupore Filtration Systems (India)	69
LFNC-C-SS22, 15 µm	Nupore Filtration Systems (India)	79
LFNC-C-BS026, 15 µm	Nupore Filtration Systems (India)	79
LFNC-C-BS026, 10 µm	Nupore Filtration Systems (India)	114
HF75	Millipore Corporation (US)	75
HF90	Millipore Corporation (US)	90
HF120	Millipore Corporation (US)	120

Table 4. Conjugate release pad materials used in the study.

Grade	Material	Basis weight (g/m^2)	Caliper (mm)	Wicking rate (s/2 cm)	Water absorption (mg/cm^2)
8950[a]	Chopped glass with binder	50	0.25	12	46
8951[a]	Chopped glass with binder	75	0.38	3	63
8964[a]	Chopped glass with binder	75	0.43	5	79
8980[a]	Borosilicate glass with PVA binder	80	0.42	2.2	56
6613[a]	Polyester fibers	100	0.42	NA	NA
6613H[a]	Treated polyester fibers	100	0.42	30	27
6614[a]	Hydrophilic polyester with binder	75	0.42	5	57
6615[a]	Polyester fibers	35	0.51	NA	NA
PT-R1[b]	Treated polyester	70–120	0.33–0.49	28–48	NA

[a] Manufacturer: Ahlstrom-Munksjö Oy, Finland
[b] Manufacturer: Advanced Microdevices Ltd., India
NA=information not available

Table 5. Sample pad materials used in the study.

Grade	Material	Basis weight (g/m^2)	Caliper (mm)	Wicking rate (s/2 cm)	Water absorption (mg/cm^2)
8950[a]	Chopped glass with binder	50	0.25	12	46
8951[a]	Chopped glass with binder	75	0.38	3	63
8964[a]	Chopped glass with binder	75	0.43	5	79
8980[a]	Borosilicate glass with PVA binder	80	0.42	2.2	56
6613[a]	Polyester fibers	100	0.42	NA	NA
6613H[a]	Treated polyester fibers	100	0.42	30	27
6614[a]	Hydrophilic polyester with binder	75	0.42	5	57
6615[a]	Polyester fibers	35	0.51	NA	NA
Cytosep 1660[a]*	Proprietary fiber blend	73	0.32	74	48
Cytosep 1662[a]*	Proprietary fiber blend	142	0.61	31	76
Cytosep 1663[a]*	Proprietary fiber blend	233	1.04	39	102
Cytosep 1667 HV[a]*	Proprietary fiber blend	70	0.35	62	48
Cytosep 1668 HV+[a]*	Treated proprietary fiber blend	70	0.35	43	48
FR1 0.6[b]*	NA	NA	0.6	NA	NA
FR2 0.7[b]*	NA	NA	0.7	NA	NA
PT-R1[b]	Treated polyester	70–120	0.33–0.49	28–48	NA
PT1-05[c]	NA	NA	NA	NA	NA
GFCP203000 (G041)[d]	Glass fiber	75	0.43	NA	NA

[a] Manufacturer: Ahlstrom-Munksjö Oy, Finland
[b] Manufacturer: Advanced Microdevices Ltd., India
[c] Manufacturer: Nupore Filtration Systems Pvt. Ltd, India
[d] Manufacturer: Millipore Corporation, US
*Red blood cell filtration
NA=information not available

4.3.2 Line dispensing

Line dispensing solutions were prepared in 10 mM Tris buffer, pH 8, for test line analyte-specific antibodies and control line polyclonal rabbit anti-mouse antibody (**I, III**). In **I,** the line antibody-density was 0.3 µg/cm containing equal proportions of capture mAbs 2508, 4G9 and 3G8. In **III,** the test line solution comprised mAbs 19C7, 916 and 9707 and the respective proportions of the mAbs in the dispensing solution were 40%, 40% and 20%. The mAbs were dispensed on the NC membrane with the protein density of 1.2 µg/cm. The lines were dispensed in 10 mM Tris-HCl, pH 8.0 in the presence of 5% EtOH and 1% sucrose on the NC membrane. In **II**, 1:1 mixture of r-HIV-1env and r-HIV-2env antigens were printed to the NC membrane with the density of 0.25 µg/cm of total antigens in 10 mM MES pH 6.1 printing solution. Control line of HIV-1 gp41 rabbit polyclonal serum (ANT-160, ProSpec-Tany TechnoGene Ltd., Israel) was printed to the NC membrane diluted in 1:25 in 10 mM Tris-HCl pH 8.0 printing solution. In **I-II**, the solutions were applied to the NC membranes by using liquid dispenser (Scienion AG, Germany) and in manuscript **III,** the lines were dispensed with BioDot ZX1010 liquid dispenser (Biodot, CA, US). Test line position was at 10 mm distance from the beginning of the NC and the control line was positioned 4-5 mm from the test line. The NC membranes were dried at +37°C for 2 hours minimum and stored at RT in dark until use.

4.3.3 Strip design and assembly

LF strips were prepared by laminating NC membranes of 25 mm width to a backing card (Standard Grade Backing Laminate, Kenosha Tapes, Netherlands). Glass fiber pads of 10 mm width were used as conjugate release pads in I and II. The following materials were used: Grades 8951 (**I**) and and PT-R1 (Advanced Microdevices) (**II**). Pre-treated (10 mM Tris-HCl pH 8.5, 135 mM NaCl, 0.5% Tween-20, 0.1% Triton-X-100, 0.8 mg/ml mouse IgG, 0.2% denatured mouse IgG, 0.24% bovine IgG) 10 mm red blood cell separator mebrane FR1 0.6 (Advanced Microdevices) and 10 mm pre-treated (10 mM Tris-HCl, 0.2% BSA, 0.1% Tween-20, pH 8.5) Cytosep 1662 (Ahlstrom-Munksjö) served as sample pads for **I** and **II**, respectively. In **III**, 16 mm glass fiber sample pad 8950 (Ahlstrom-Munksjö, Finland) was pre-treated with 10 mM Borate buffer solution pH 7.5 containing 0.1% Tween-20, 0.5 % casein and 50 mM EDTA. Cellulose pads of 30-35 mm width (CFSP223000, Merck Millipore, US) were used as absorbent pads in all assays. The pads were laminated to the polystyrene cards overlapping 1 mm of the NC membrane, sample pad if used was overlapping the conjugate release pad by 1 mm. The strips were covered by transparent cover tape (Kenosha Tapes, Netherlands).

4.4 Assay usability

4.4.1 Dry-reagent assays

Sample pads were pre-treated with required buffer components. In **I**, 4x concentration of native and denatured mouse IgG was used to treat the sample pad. The drying of these reagents to the sample pad was intended to reduce the need of refrigerated storage of the strips and allow release of the reagents to the fluid stream coincident with the analyte and reporters.

UCNP conjugates were dried with drying solution containing 5% sucrose to preserve the dried conjugates and to control the release to the fluid stream.

4.4.2 Assay procedures

I: To start the procedure, 50 µl of sample was added into the sample inlet, followed by applying 50 µl of chase buffer (10 mM Tris-HCl pH 8.5, 135 mM NaCl, 0.5% Tween-20, 1% BSA, and 0.1% Triton-X-100). After 30 minutes, the test and control line upconversion photoluminescence signals were measured with Upcon reader device (Labrox Oy, Finland) with excitation at 976 nm and emission at 540-550 nm.

II: First, 10 µl of sample was added into the sample inlet, followed by applying 90 µl of chase buffer (10 mM Tris-HCl pH 8.5, 135 mM NaCl, 0.5% Tween-20, 1% BSA, 0.06% bovine IgG). After 30 minutes, the test and control line signals were measured with Upcon reader device.

III: Pre-incubation of 15 minutes was performed by mixing 25 µl of sample and 25 µl UCNP-conjugate solution (20 ng UCNP diluted in wash buffer solution containing 0.05 M Tris pH 7.5, 0.5 M NaCl, 0.04 % NaN3, 2 mM KF, 1.5 % BSA, 0.06 % bovine IgG, 0.2 mg/ml mouse IgG and 0.05 mg/ml denatured mouse IgG) in microtitration wells in slow shaking at +35°C. First, 50 µl of the mixed sample and the reporter solution was allowed to absorb to the strip followed by immediate addition of 50 µl of wash buffer. The total liquid volume of 100 µl was allowed to absorb to the strip for 30 minutes before measurement. The strips were read with Upcon reader device.

4.4.3 Samples and sample matrices

The developed assays were evaluated with different sample matrices (**I-II**). Model samples with spiked analytes were tested in serum, lithium heparin (LiH) plasma and citrate-phosphate-dextrose-adenine (CPDA) whole blood.

The true performance with clinical specimens was validated with large sample panels. List of samples used in publication **I** are presented in Table 6. Samples used in publication **II** are listed in Table 7.

In manuscript **III**, blood samples (serum and LiH plasma) were collected from apparently healthy individuals at the Department of Biotechnology (University of Turku, Turku, Finland). The samples were stored at -20 °C before use and used for preparation of the sample pools (n=5). The clinical sample panel consisted of LiH-plasma samples (n = 262), which were collected and analyzed at Oulu University Hospital and shipped to the University of Turku (at -20 °C) and stored at -70 °C. The cTnI concentrations in the samples were determined with two methods prior the study: Siemens ADVIA Centaur TnI-Ultra (Siemens Healthcare GmbH, Erlangen, Germany) at Oulu University Hospital and an in-house assay[197] at University of Turku.

Table 6. Clinical specimens used in publication **I**.

Sample/sample panel	Purchased from	Number of Samples	Sample matrix
WHO Third International Standard for HBsAg (12/226)	National Institute for Biological Standards and Control, UK	1	plasma
The 1st WHO International Reference Panel for Hepatitis B Virus (HBV) Genotypes for Hepatitis B Surface Antigen (HBsAg) Assays (6100/09)	Paul-Ehrlich Institut, Germany	15	plasma
AccuSet™ HBsAg Performance Panel (0805-0340)	SeraCare Life Sciences Inc., USA	25	plasma
AccuSet™ HBsAg Mixed Titer Performance Panel Modified PHA207(M) (0805-0217)	SeraCare Life Sciences Inc., USA	12	plasma
AccuSet™ HBV Worldwide Performance Panel (0805-0313)	SeraCare Life Sciences Inc., USA	7	plasma
HBV Seroconversion Panel PHM941 (0606-0060)	SeraCare Life Sciences Inc., USA	9	plasma
HBsAg positive disease state samples	SeraCare Life Sciences Inc., USA	24	plasma
HBsAg positive disease state samples	Biomex GmbH, Germany	49	serum
HBsAg positive disease state samples	Labquality Oy, Finland	18	plasma
Presumed healthy samples	Turku University of Applied Sciences, Finland	100	serum
	Obtained from		
Routine-tested clinical samples negative for HBsAg	Department of Virology, University of Turku, Finland	215	plasma, serum
Routine-tested clinical samples positive for HBsAg	Department of Virology, University of Turku, Finland	16	plasma, serum

Table 7. Clinical specimens used in publication **II**.

Samples/Sample panel	Purchased from	Sample matrix	anti-HIV-1+	anti-HIV-2+	NEG
HIV disease state samples	Labquality Oy, Finland	Plasma	25	6	22
Anti-HIV-1 Mixed Titer (0800-0303) (PRB205)	SeraCare Life Sciences Inc., USA	Plasma	16	0	1
Anti-HIV-1 Low Titer (0800-0301)		Plasma	13	0	2
HIV-1 Early Infection Performance (0800-0297)		Plasma	11	0	12
AccuSet HIV1 p24 perf. Panel (0800-0362)		Plasma	8	0	5
Accuset HIV1/2 perf. Panel (0800-0380)		Plasma	6	6	1
HIV1/2 WW perf. Panel (PRZ206)		Plasma	6	6	1
Seroconversion Panel (PRB955)					
Seroconversion Panel (PRB945)					
Viral Co-infection Panel (PCA201)		Plasma	16	0	7
Anti-HIV positive disease state samples	Biomex GmbH, Germany	Serum	13	5	0
Presumed healthy samples	Turku University of Applied Sciences, Finland	Serum	0	0	100
	Obtained from				
Routine-tested clinical samples negative for anti-HIV	Department of Virology, University of Turku, Finland	Serum/ plasma	0	0	216
Routine-tested clinical samples positive for anti-HIV		Serum	15	0	1

4.5 Determination of the detection limits

In **I**, a two-step approach was used for determining the LoB and LoD, both in serum and in whole blood. In the first step, dilutions of the WHO Third International Standard for HBsAg between 0.01 – 12.8 IU/ml were used for plotting calibration curves. For the calibration curve, 20 replicates were used for each of the three low concentration dilutions (0.05, 0.1, and 0.2 IU/ml) near the pre-estimated detection limit. Four replicate strips were used for the other concentrations.

The cutoff level for the LoB was determined by using 60 replicates of the blank sample and selecting the highest measured signal value from these replicates as the

cutoff value. The LoB (IU/ml) was calculated from the cutoff and the equation obtained with linear regression of the calibration curve.

The LoD was obtained by further analyzing 80 replicates of the three concentrations at the same level and above (0.05, 0.1, and 0.2 IU/ml for serum) as the previously calculated LoB. The sample size of 80 was based on a statistical sampling plan (ISO 2859-1:1999) previously used by Das et al.[198]. Sample size code J was determined by using general inspection level II and was based on a lot size of 501 – 1200. Single sampling plan for normal inspection was used, which resulted in the sample size of 80.

In publication **II**, the aim was qualitatively detecting antibody response to HIV. With the serological detection of antibodies, analytical detection limits are not established. Therefore, the evaluation of the detection limit was not conducted in publication **II**.

In **III**, the limit of blank (LoB) and limit of detection (LoD) were determined according to the Classical Approach of CLSI Guideline EP17-A2 using healthy LiH plasma pool as a zero calibrator and five lithium heparin plasma pools with spiked cTnI concentrations of 1–4×LoB. Initial LoB was determined with 20 replicates of blank pool samples. The blank pools and low concentration samples were run during four days in 5 replicates each. Due to the abnormal distribution of the blank sample results, a non-parametric data analysis approach was used. For low concentration samples, the non-parametric data analysis approach was used because of non-normal distribution of the results from these samples. LoD was selected as a median value of the three highest low concentration samples (total number of the replicates n=60), yielding more than 95% positive scores above LoB.

4.6 Measurement and data-analysis

The interpretation of the results was based on the maximum signal measured at the test line position. The overall baseline signal measured along the strip was subtracted from the test line maximum signal (equation 7). Thus, only the test line peak signal was considered as the outcome of the measurement. The control line signals were interpreted as qualitative control. The data analysis principle is illustrated in Figure 11.

$$S = T - \frac{A+B}{2} \tag{7}$$

S stands for signal read-out from the test line taken into consideration in data analysis, T refers to the total signal measured at the test line position, and A and B refer to the baseline signal measured along the strip before and after test line position (Figure 11).

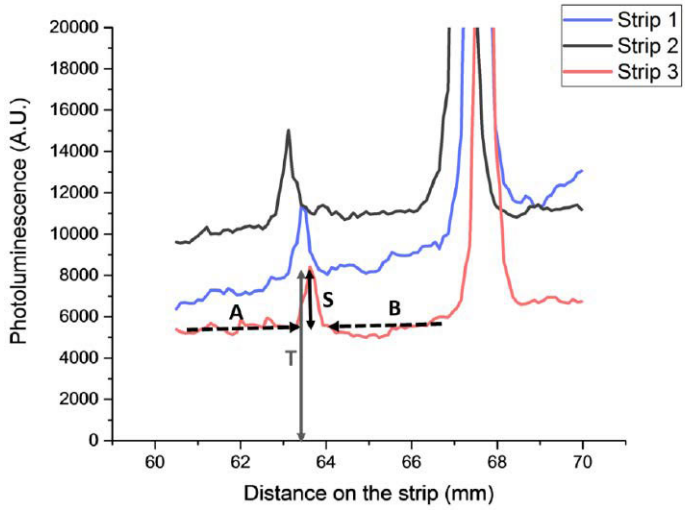

Figure 11. Data analysis principle of the test line peak detection (S): the average baseline signal before (A) and after (B) the test line position was subtracted from the maximum signal value measured from the test line position (T).

5 Results and Discussion

5.1 Binder selection for antigen assays

Available mAbs were characterized with relative epitope mapping to ensure selection of different antibodies capable of recognizing HBV genotype variants. Competitive binding inhibition assay (publication **I**) resulted in two different groups of antibodies: mAb-1H1, mAb-3F10, mAb-3G6, mAb-4G9, mAb-2505 and mAb-2508 (group 1) and mAb-3G8, mAb-1F8, mAb-3E10 and mAb-3D3 (group 2). Inhibition percentages derived from each competing mAb/tracer-mAb combination are shown in Table 8. As tracer, mAb-2505 resulted in high inhibition percentages with itself and with mAb-2508 but was not inhibited by the other group 1 free antibodies. This could be due to weaker affinity of the other mAbs. The mAb-2505 and mAb-2508 may still share the same epitope with group 1 antibodies, but due to the relatively weaker affinity of the other group 1 antibodies, these antibodies were likely not able to compete with the higher affinity mAb-2505 tracer. mAbs 1H1, 3F10, 4G9 and 3G6 had affinity constants (K_D) within the range of 10^{-9} to 10^{-8} M, while K_D values of mAbs 2508 and 2505 were in the range of $<10^{-12}$ M.

Table 8. Inhibition percentages of competing and tracer mAbs used in **I**. Percentages of group 1 are shown in red background and group 2 in blue background.

		Tracer mAb							
Inhibiting mAb[a]	*2505*	*1H1*	*3G8*	*1F8*	*3F10*	*3E10*	*4G9*	*3G6*	*3D3*
2505[b]	97.3	83.9	18.3	6.3	81.5	16.1	81.6	82.4	18.2
2508[b]	96.0	96.7	25.1	16.9	96.5	29.8	96.6	93.7	29.9
1H1	19.9	94.7	0.7	0.0	95.5	8.7	91.6	91.1	0.0
3G8	0.0	20.8	95.1	91.8	8.7	94.8	5.6	37.6	93.0
1F8	3.2	24.3	97.8	96.3	9.0	97.8	2.7	28.2	96.5
3F10	31.3	96.9	5.7	0.0	96.1	12.8	95.7	91.8	0.1
3E10	7.4	13.7	96.9	94.7	5.3	96.6	5.0	37.1	92.4
4G9	17.3	97.1	5.4	0.0	97.7	10.4	97.1	91.7	0.0
3G6	34.6	90.4	34.7	33.8	87.5	31.8	87.3	100.0	26.3
3D3	9.7	22.5	98.3	96.6	15.9	98.4	4.5	29.1	97.7

Group 1 was further divided into two groups based on the results from the evaluation of the 1st WHO reference panel (PEI): mAbs with weak reactivity to genotype D2 (1H1, 4G9, 3F10 and 3G6) and strong reactivity to genotype D2 (2505 and 2508). Results from evaluation of capture antibodies ability to detect different HBV genotypes are shown in Table 9. Capture antibody combinations were selected from different groups to increase the probability of targeting most HBsAg variants. Overall ability to detect multiple genotypes of mAb candidates was considered when mAbs were selected for further studies. The final combination of mAbs was selected based on preliminary determination of analytical sensitivity (data not shown).

Table 9. Signal-to-background ratios obtained by testing different capture antibodies (**I**) against PEI genotype panel samples.

	Capture antibody								
GT*	2505	2508	1H1	3G8	1F8	3 F10	3 E10	4 G9	3G6
A1	35.5	49.2	48.6	40.3	49.3	51.7	48.6	59.2	23.2
A1	39.8	41.7	44.1	40.3	44.6	50.1	49.1	59.4	22.6
A2	44.2	52.4	49.7	40.3	49.2	53.9	48.9	59.4	22.4
B2	20.0	44.2	48.5	39.2	41.2	52.9	47.1	58.7	16.6
B2	27.9	49.0	47.4	40.3	35.6	53.4	47.7	59.4	19.3
C2	40.0	52.5	49.6	40.3	46.7	52.6	48.0	58.0	17.3
C2	34.6	52.5	49.1	40.3	48.3	52.5	41.2	59.4	19.4
C2	38.5	52.5	49.7	40.2	41.7	53.7	45.6	59.4	21.7
D1	26.3	52.5	34.7	39.4	42.4	40.9	19.9	37.7	10.9
D2	25.2	43.1	3.4	36.1	47.2	3.0	18.9	5.6	1.7
D3	24.7	48.7	47.5	40.2	24.0	36.7	25.0	41.4	13.3
E	30.5	51.5	38.9	40.3	47.4	27.5	48.8	39.8	5.6
F2	41.2	52.4	39.5	40.3	49.7	46.3	49.1	53.2	11.3
F2	37.8	52.5	49.7	40.3	49.6	53.9	49.1	59.4	14.1
H	30.7	52.1	49.6	40.3	49.5	53.0	49.1	59.4	23.4

*Darker red shade indicates weaker binding to a certain genotype.

5.2 Reporter technology

5.2.1 Sensitivity

Analytical sensitivity of the HBsAg-LFA (**I**) was evaluated with WHO third international standard. Standard was run in the range of 0.01-12.8 HBsAg IU/mL. The sensitivity calculated from the equation of the curve was 0.05 IU/mL in serum and 0.2 IU/mL in CPDA whole blood, respectively. The fractions of how many

replicates were detected above the cutoff per tested concentration are shown in Table 10.

Table 10. Verification of the limit of detection of the developed LFIA (**I**) by using WHO third international standard for HBsAg (NIBSC 12/226).

	HBsAg-UCNP-LFIA		**Alere Determine HBsAg**
WHO Third International Standard for HBsAg, NIBSC 12/226 (IU/ml)	Diluted in serum Number of replicates detected (%)	Diluted in whole blood Number of replicates detected (%)	Diluted in serum Number of replicates detected (%)
0.01	0/4 (0)	0/4 (0)	
0.05	61/80 (76.3)	3/20 (15.0)	
0.1	79/80 (98.8)	9/20 (45.0)	
0.2	20/20 (100)	70/80 (87.5)	
0.4	4/4 (100)	4/4 (100)	
0.8	4/4 (100)	4/4 (100)	0/4 (0)
1.6	4/4 (100)	4/4 (100)	0/4 (0)
3.2	4/4 (100)	4/4 (100)	4/4 (100)
6.4	4/4 (100)	4/4 (100)	4/4 (100)
12.8	4/4 (100)	4/4 (100)	2/2 (100)

In **I**, the LoD of the developed LFIA was determined in both serum and whole blood with the WHO third international standard for HBsAg. The LoB calculated against the calibration curve generated using serial dilution of international standard was 0.05 IU/ml in serum. Similarly, the LoB in whole blood was 0.2 IU/ml. The LoD was determined by testing additional replicates with HBsAg concentrations close to the LoB. With the HBsAg concentration of 0.05 and 0.1 IU/ml in serum, the assay correctly detected 61 out of 80 (76.3%) and 79 out of 80 (98.8%) replicate strips, respectively (Table 10). Therefore, the LoD in serum for HBsAg-LFIA was 0.1 IU/ml. In the whole blood samples only 70 out of 80 replicates (87.5%) scored positive at a concentration of 0.2 IU/ml (Table 10) indicating the LoD to be approximately 0.4 IU/ml.

The LoD of the HBsAg-UCNP-LFIA was 15 to 100-fold higher than that of the typical RDTs for HBsAg. The UCNP-LFIA showed 32-fold higher analytical sensitivity compared to the conventional LFIA with visual labels that was tested in parallel with the UCNP-LFIA in this study. The developed UCNP-LFIA showed potential to be suitable for diagnostic purposes in terms of the analytical sensitivity requirement of ≤ 4 IU/ml[69]. Moreover, based on the detection limit obtained in serum, the UCNP-LFIA may be suitable for screening of blood products according to the WHO criteria in terms of the analytical sensitivity requirement of ≤ 0.13 IU/ml[69].

In **III**, the obtained LoD was 30 ng/L, and the LoB of the assay was calculated to be 8.4 ng/L. In comparison to these values, low and moderate cTn levels around 50-100 ng/L are suggestive for clinical conditions such as MI, myocarditis, stress cardiomyopathy, pulmonary embolism, heart failure, shock hypertensive crisis and subarachnoid hemorrhage. High to very high cTn levels can be considered ranging from 1000 up to >10 000 ng/L being strongly predictive for large MI. Diagnostic protocols for MI use serial cTn testing at the patient presentation and 3-9 h after admission. Recommended rule-in criteria for MI patients include detection of cTnI concentration above the URL and pre-determined significant change in assay-specific delta value i.e., change in cTnI value during the follow-up period.[129]

5.2.2 Cut-off based result interpretation

One of the main objectives of anti-HIV antibody assay (**II**) development with UCNP reporter technology was to enable clear yes/no cut-off-based result interpretation in case of borderline specimen. The samples giving somewhat equivocal results with anti-HIV UCNP-LFA and Alere Combo rapid tests are compared in Table 11. It was noticed that multiple samples resulting in false negative results with the UCNP-LFA were also giving equivocal results hard to interpret with the visual detection test as well. However, the sensitivity of the UCNP-LFA should be further improved for the correct detection of low titer anti-HIV1/2 samples.

Table 11. Comparison of discrepant results between the UCNP-LFA (**II**) and conventional LFA.

Sample ID	Panel	Status[1]	UCNP-LFA (S/Co)[2]	Alere HIV Combo result[3]
#1	Disease state sample	NEG	0.2	+-
#2	Disease state sample	anti-HIV1+	0.9	+
#3	Disease state sample	anti-HIV1+	3.2	+/-
#4	Disease state sample	anti-HIV1+	1.3	+/-
#5	Disease state sample	anti-HIV1+	0.7	+/-
#6	Disease state sample	anti-HIV1+	0.6	+
#7	Disease state sample	anti-HIV2+	0.5	+
#8	Disease state sample	anti-HIV2+	0.7	+
0800-0301-03	Anti-HIV1 low titer panel	NEG	0.9	+/-
0800-0301-04	Anti-HIV1 low titer panel	anti-HIV1+	0.8	+
0800-0297-16	HIV1 early infection performance panel	anti-HIV1+	0.8	+
0800-0362-02	Accuset HIV1 p24 performance panel	anti-HIV1+	1.2	-
0800-0362-05	Accuset HIV1 p24 performance panel	anti-HIV1+	1.1	-
0800-0362-11	Accuset HIV1 p24 performance panel	anti-HIV1+	0.6	+/-

5.2.3 Quantification

In **I**, the correlation in HBsAg detection expressed in S/Co ratios of the developed UCNP-LFIA and Abbott Architect (automated chemiluminescent immunoassay) were calculated (R^2=0.87) with the results obtained from AccuSetTM HBsAg Performance Panel (SeraCare Life Sciences, Inc.) evaluation (Figure 12A). Quantitative measurement of HBsAg can be used for guiding therapeutic indications[68], particularly in LMICs where methods to detect and quantify HBV DNA are often unavailable[199]. With the UCNP reporter technology, the results of the developed assays could potentially be quantifiable as the assay showed good linearity within the used HBsAg concentration range (Figure 12B). The linearity with higher concentrations and hook effect were not studied. As the HBsAg concentration may be high in chronically infected patients[66,67], sample dilution might be required in order to use the assay for quantification purposes. However, quantitative determination of HBsAg concentrations of clinical specimens was not conducted in this study. Therefore, it should be further investigated before making further claims on the assay's potential for quantitative measurements.

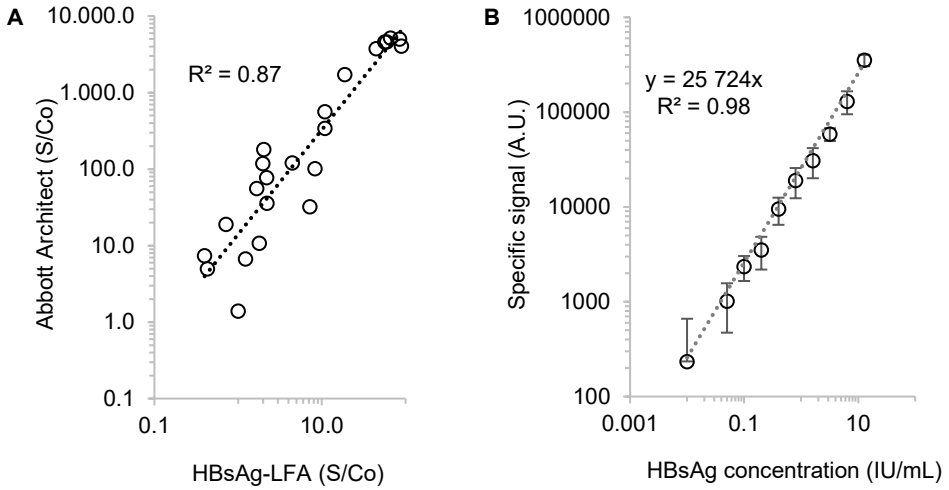

Figure 12. A. Signal-to-cutoff ratio correlation between the developed HBsAg-LFIA (**I**) and Abbott Architect EIA. **B.** Calibration curve for HBsAg in serum determined with WHO third international standard for HBsAg (NIBSC 12/226).

In **III**, the calibration curve for cTnI-UCNP-LFIA (Figure 13) was linear up to 10 000 ng/L (R^2=0.996). Linearity of the UCNP-LFIA was studied with serial dilutions of three patient samples (cTnI concentrations 3 000–10 000 ng/L) diluted from 3 to 81-fold by using blank LiH plasma pool. Linear regression of the observed

cTnI concentration and dilution factor showed linearity R^2=0.969–0.996 over the measured range of 37 ng/L–9 365 ng/L (Figure 14).

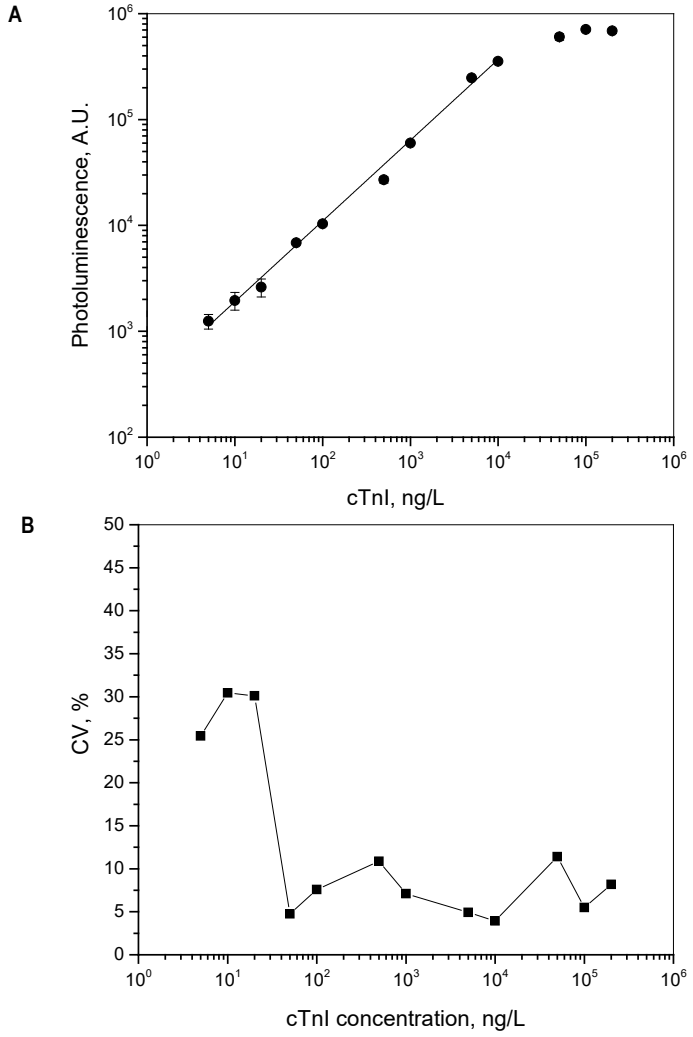

Figure 13. A. Calibration curve for the cTnI-LFIA (**III**). The error bars represent the standard deviation from three replicate strips. Equation of the curve was y=0.76x+2.52, R^2=0.996. **B.** The precision profile obtained from the measurements of the calibration curve.

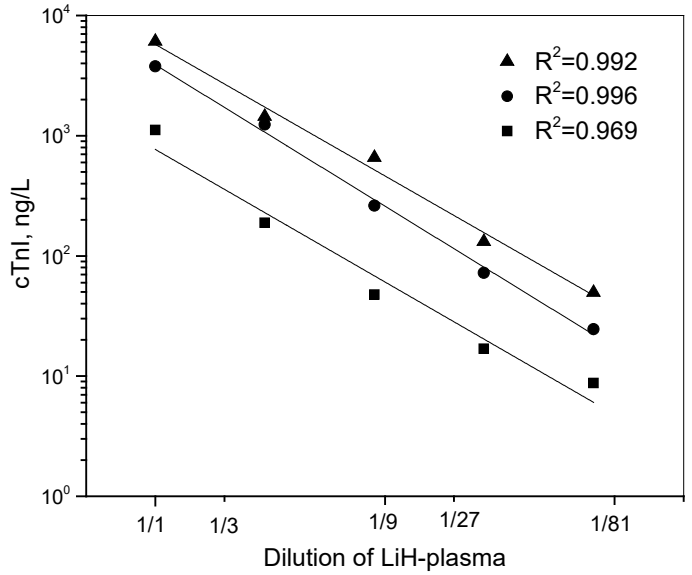

Figure 14. Dilution linearity of the cTnI-LFIA (**III**). Three clinical LiH-plasma samples containing variable amounts of cTnI were serially diluted from 1/1 to 1/81-fold into LiH-plasma pool obtained from healthy individuals without cardiac symptoms.

In **III,** the method comparison was performed with 262 samples. Samples below the LoD of the cTnI-LFIA and the samples above the linear range of cTnI-LFIA were omitted from the quantitative data analysis, i.e., the samples giving result within the linear range 30–10 000 ng/L of the cTnI-LFIA (n=191) were included in the comparison.

Method comparison between the cTnI-LFIA and the in-house well-assay is shown in Figure 15A. Samples above the LoDs of both assays, the cTnI-LFIA and the in-house well assay were included in the comparison (n=188). Three samples yielding values <3.3 ng/L which was below the LoD of the reference assay were excluded from the comparison. Passing and Bablok regression analysis for the cTnI-LFIA and the in-house assay resulted in a slope of 1.11 (95%CI from 1.05 to 1.16) and a y-intercept of -0.08 (95%CI from 0.02 to 0.05). The Spearman correlation coefficient was 0.956 ($p<0.0001$). The mean relative difference between the two methods was 39.4% with the 95% limits of agreement ranging from -55.1% to 134% (Figure 15B).

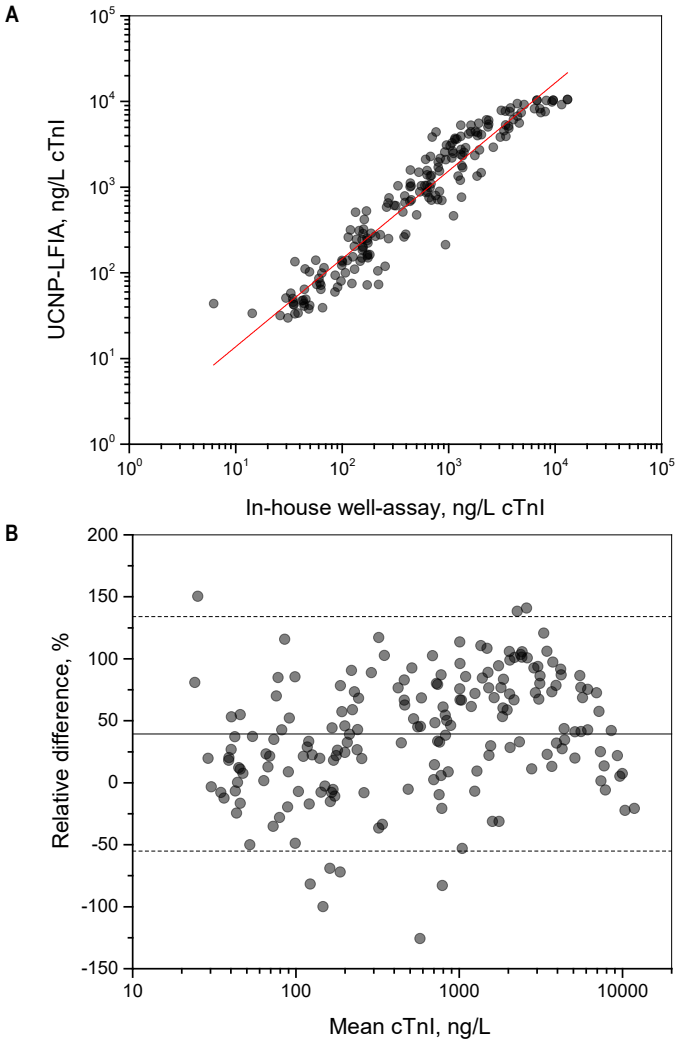

Figure 15. Method comparison. **A.** Correlation between the cTnI-LFIA (**III**) and the in-house well-based reference assay (n=188). **B.** Bland-Altman analysis of agreement. The relative difference is calculated as cTnI-LFIA concentration subtracted by in-house well-based assay concentration divided by mean concentration. The mean difference (39.4%) is presented with a solid line and the 95% limits of agreement (from -55.1% to 134%) are shown with dashed lines.

Method comparison between the cTnI-LFIA and the Siemens Advia Centaur assay is shown in Figure 16A. All samples within the linear range of the cTnI-LFIA (n=191) were above of the LoD of Siemens Advia Centaur (LoD 9 ng/L[200]) and thus included in the comparison. Passing and Bablok regression analysis for the cTnI-LFIA and Siemens Advia Centaur yielded in a slope of 1.07 (95%CI from 1.02 to 1.13) and a y-intercept of -0.79 (95%CI from -0.98 to -0.63). The Spearman

correlation coefficient was 0.949 ($p<0.0001$). The mean relative difference between the two methods was -107.7% with the 95% limits of agreement ranging from -25.1% to -190.4% (Figure 16B).

In contrast to the Siemens Advia Centaur reference assay, the cTnI-LFIA systematically yielded lower cTnI values in patient samples. Antibodies targeting different epitopes may result in differences in cTnI values[201]. This was supported by the observation that the cTnI-LFIA results for cTnI were similar to the in-house well-assay. Both of these assays resulted in lower cTnI values in contrast to the reference assay. The cTnI-LFIA and the in-house well-assay share a very similar 3+1 antibody design. Also, the assays utilized the same calibration material.[197] Medical decision limits must be determined for all assays separately.

Harmonization of cTnI assays and interchangeable medical decision limits for cTnI are still under construction[202]. Cardiac troponin I measurements can show up to 20- to 40-fold differences between assays[203]. The assays have their own reference range and clinical interpretation of the results should be assay-specific. Differences in resulting values may arise from differences in calibration material, different detection technologies and reagents, lack of suitable reference method, the variable antibody immune-reactivity towards different forms of cTnI in circulation and variable antibody specificity[204]. All of these factors contribute to quantitative differences in cTnI assay results. There is an acknowledged need for a traceable reference immunoassay procedure and particularly for a calibration material used as a standard.[202,203,205]

The linear range of the developed cTnI-LFIA reached up to 10 000 ng/L and the assay showed good linearity with dilutions of endogenous samples. The method comparison to the two reference assays showed good correlation and suggests that the cTnI-LFIA could be used for the quantitative determination of cTnI within the range of 30–10 000 ng/L. The cTnI-LFIA could be used for determining the cTnI concentrations in MI patients and monitoring the rise or fall in the cTnI levels of the same patient.

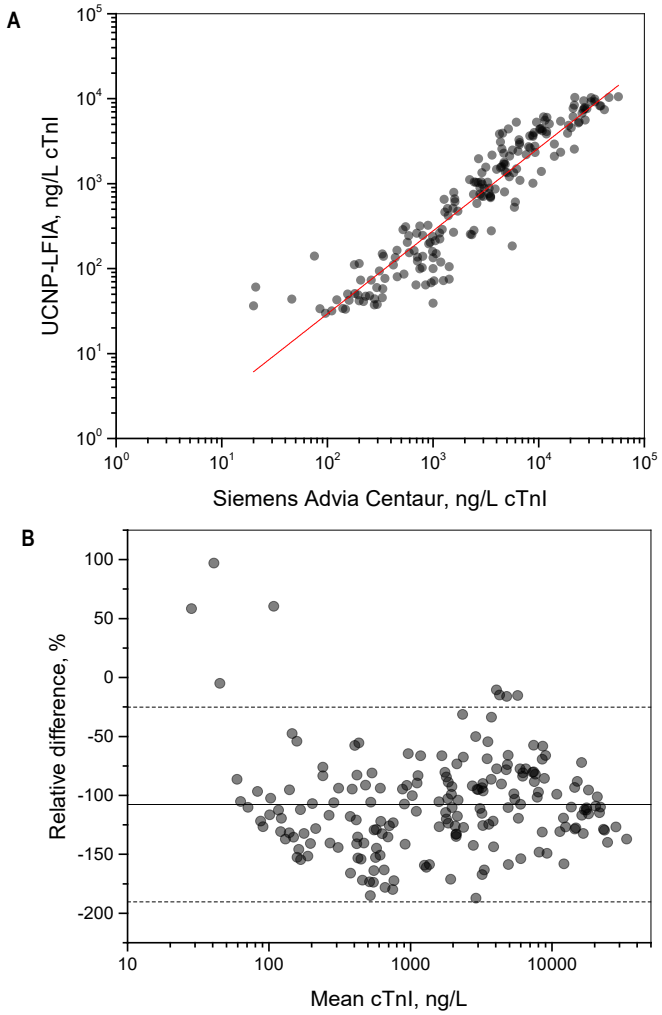

Figure 16. Method comparison. **A.** Correlation between the cTnI-LFIA (**III**) and Siemens Advia Centaur TnI-Ultra reference assay (n=191). **B.** Bland-Altman analysis of agreement. The relative difference is calculated as cTnI-LFIA concentration subtracted by Siemens Advia Centaur TnI-Ultra concentration divided by mean concentration. The mean difference (-107.7%) is presented with a solid line and the 95% limits of agreement (from -25.1% to -190.4%) are shown with dashed lines.

5.3 Lateral flow assay development

5.3.1 Sample matrices

Assay compatibility (**I**) with plasma and serum sample material was investigated with different blood cell separator sample pad materials (Figure 17). It was observed that the use of blood cell separator pad resulted in uniform results between whole blood

and serum sample matrices. Without the blood separator pad signal levels with whole blood samples were somewhat lower (data not shown). The sample volume used in **I** was examined (Figure 18) by using 10 µl, 25 µl or 50 µl of undiluted whole blood. The detection sensitivity of the antigen assay was shown to increase with volume.

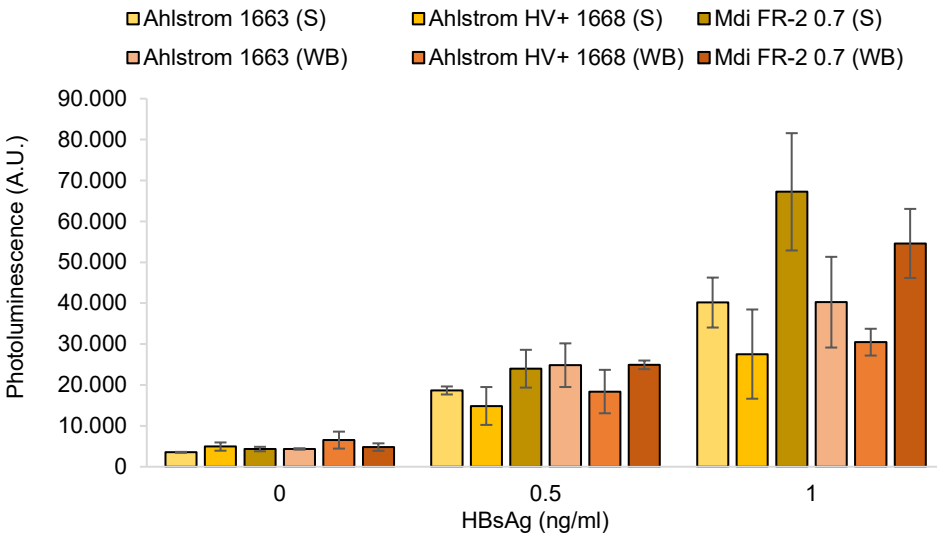

Figure 17. Blood separator sample pads tested in **I** (data not included in the publication) with 10 µl sample volume. S = serum, WB = whole blood.

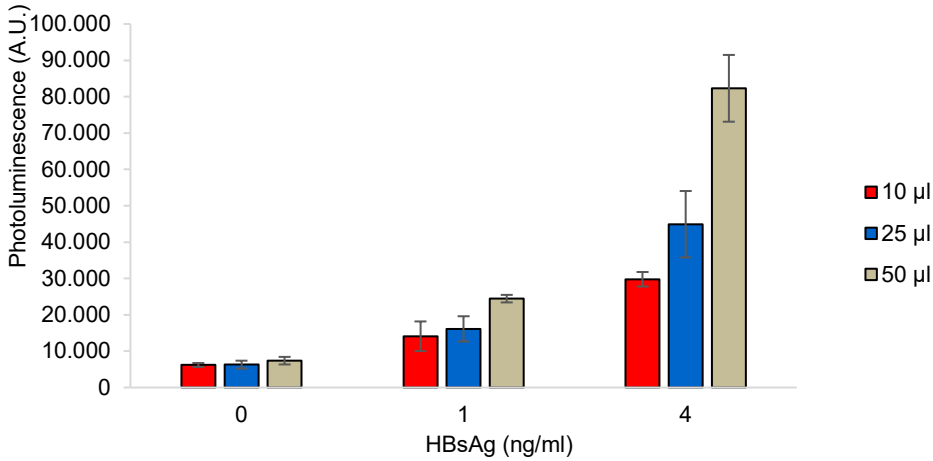

Figure 18. Effect of sample volume on HBsAg-LFIA (**I**) signal response. The sample volume was tested in 10 µl, 25 µl and 50 µl volumes of CPDA whole blood samples spiked with 1 and 4 ng/ml HBsAg (X-axis). The chase buffer was added in volumes 90 µl, 75 µl and 50 µl, respectively. Increase in sample volume led to higher signal responses without significant effect on the background. Error bars represent variation among 3 replicate strips.

5.3.2 Lateral flow strip materials and dry-reagent assays

Sample pad treatment with buffer components was done to enable a simple assay in dry-reagent format. Furthermore, drying buffer components such as proteins on the sample pad enables simplification of the buffer and reduces the need for refrigerated storage. In **I**, the effect of drying buffer components on the sample pad was compared with components dissolved in chase buffer. In dry-reagent format, the reagents including mouse and bovine IgG blocking substances have more time to interact with potential interfering substances in the sample matrix. In buffer these components are added to the test strip while reaction between the analyte and reporter conjugates has already been started. Blocking substance concentration in chase buffer was increased in the same proportion of 5x to the increase in sample volume (from 10 µl to 50 µl), however a lower concentration (2x) was used for the drying process due to viscosity and effect on the sample flow to the strip. The results of the comparison are shown in Figure 19. The drying of the IgG blocking substances showed clear improvement in case of negative samples giving high false positive signal (samples number 4 and 5) and resulted in better differentiation of the signal deriving from the positive sample (sample 1). There was no effect on previously low-signal negative samples.

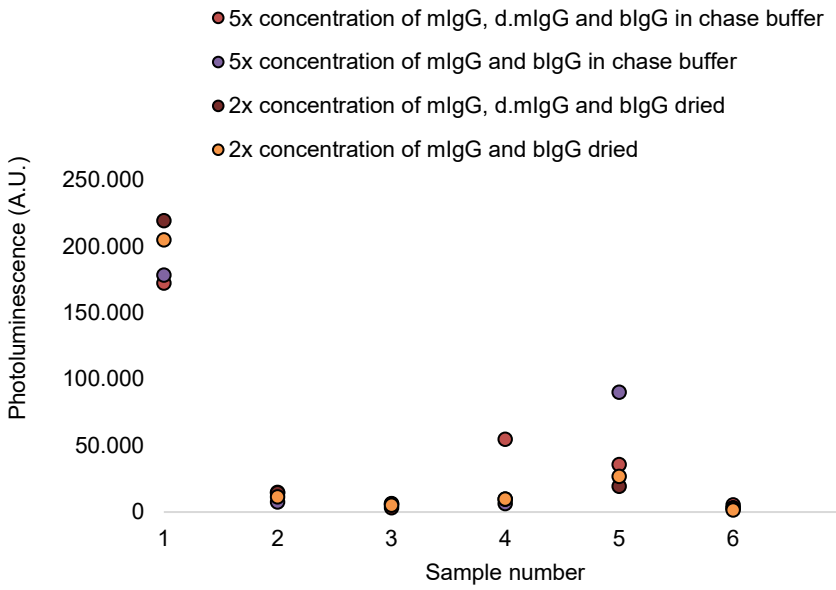

Figure 19. Effect of IgG-blockers in HBsAg-LFIA (**I**) either dried on the sample pad or diluted in the chase buffer. Patient samples: 1. PHA2017-14 (HBsAg positive), 2. PHA207-21 (HBsAg negative), 3–7. HBsAg negative. Abbreviations: mIgG; mouse immunoglobulin G, d.mIgG; denatured mouse immunoglobulin G, bIgG; bovine immunoglobulin G.

In the optimization phase of the assay (**I**), different combinations of conjugate release pad and sample pad materials were compared in dry-UCNP format (Figure 20). It was observed that the same materials in different combinations tend to have different effect on the signal levels and CV percentages. The findings indicate that the materials should be studied in combinations to achieve optimal conditions to ensure efficient conjugate release and minimal sample leakage during sample addition.

Abilities of glass fiber sample pads to absorb the desired volume of liquid in the desired assay turn-around-time were studied (Figure 21). Pads with fast wicking rates and a high water absorption capacities were expectedly able to absorb the liquid volume within 15 minutes. The pads with slow wicking rate and low water absorption capacity required at least 20 minutes to absorb the liquid volume. The results showed the importance of selecting the material based on requirements for assay time and liquid volume. The wicking rates and water absorption capacities of the used materials are presented in Tables 4 and 5.

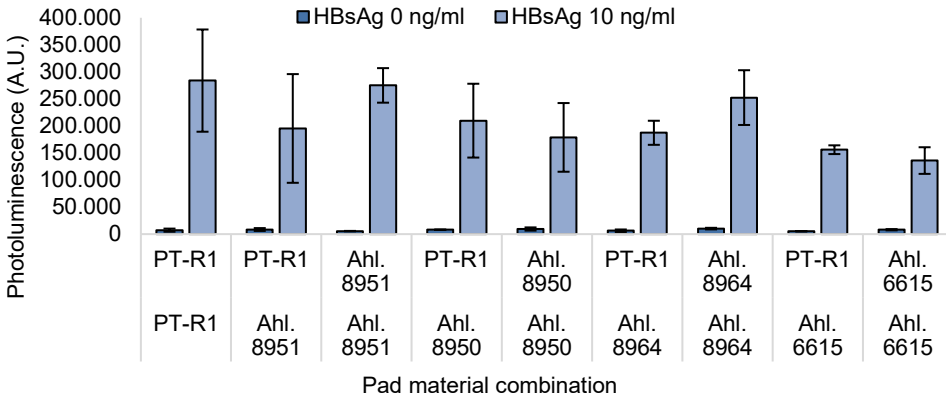

Figure 20. Different glass fiber conjugate release (above) and sample pad (below) combinations (**I**).

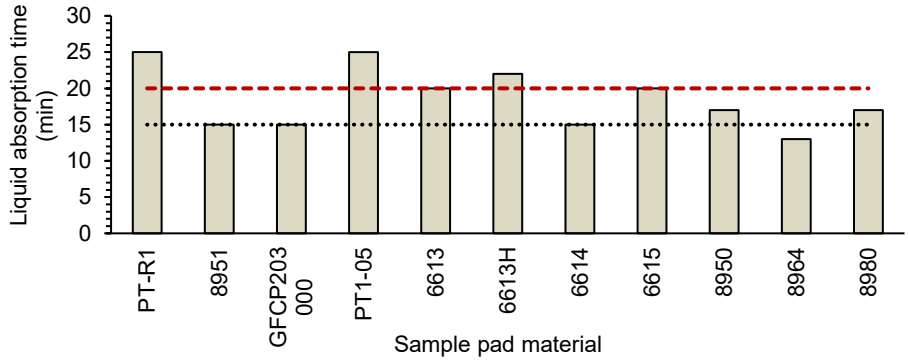

Figure 21. Effect of sample pad material on the liquid absorption to the strip. Black line represents threshold of 15 minutes and red line that of 20 minutes.

5.3.3 Nitrocellulose membranes and binder dispensing

In **II**, the NC comparison was performed in UCNP-LFA. Membrane performance comparison in the UCNP-LFA is shown in Figure 22. Faster membranes showed reduced detection capability of anti-HIV antibodies. Further comparison of the three best performing membranes is shown in Figure 23. One of the membranes (CNPH-N-SS60) was observed to improve anti-HIV antibody detection in contrast to the two other membranes. These three membranes used in the comparison represented relatively slow wicking rates (150–220 s/4 cm). However, the slow wicking rate was not the only parameter affecting the membrane performance in the UCNP-LFA, as the slowest membrane did not outweigh the performance of the second slowest membrane CNPH-N-SS60. For instance, membrane surfactant is known to affect membrane compatibility with the capture protein[140].

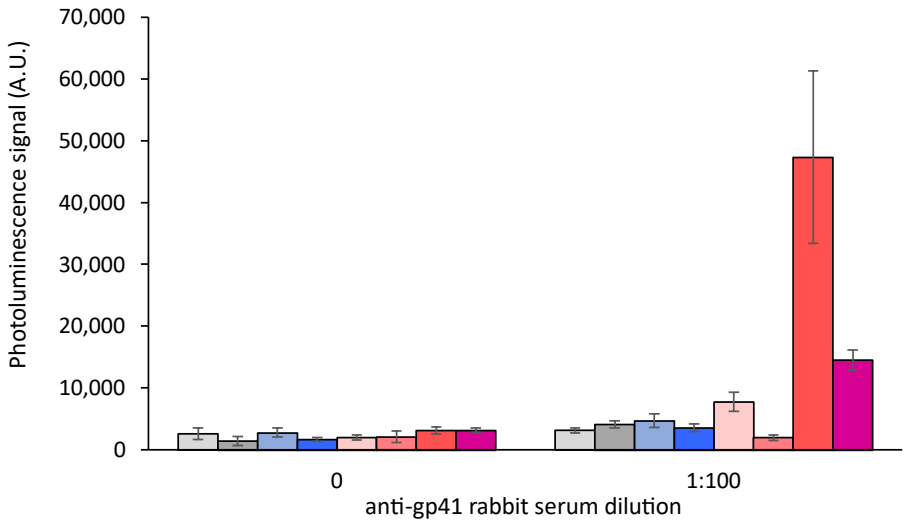

Figure 22. Nitrocellulose membrane comparison in the anti-HIV UCNP-LFA (**II**). Eight different nitrocellulose membranes with wicking rates of 100, 120, 125, 140, 150, 180, 200 and 220 s/4 cm (from left to right, respectively) were compared in the UCNP-LFA with 1:100 dilution of anti-gp41 rabbit serum. The error bars represent the standard deviation among three replicate strips.

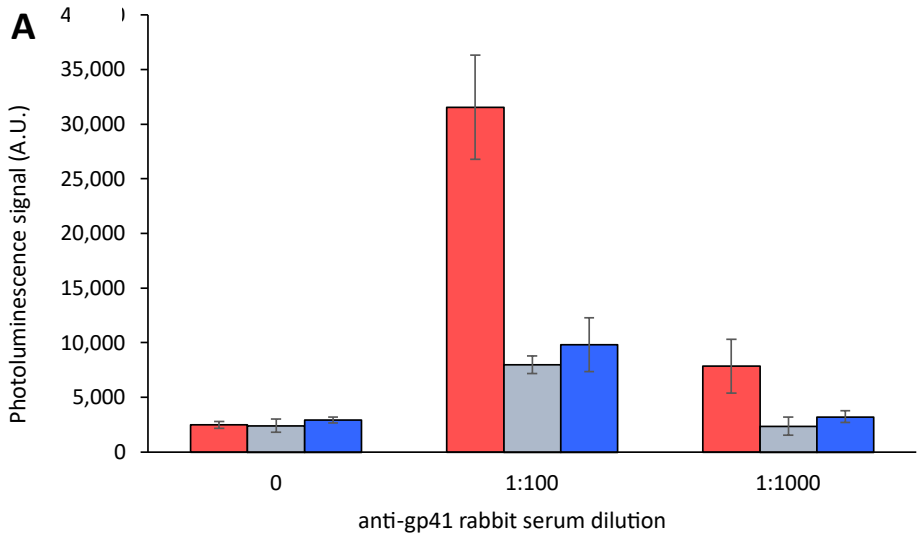

Figure 23. Antigen dispensing on different nitrocellulose membranes (**II**). Antigens were dispensed on the following membranes: CNPH-N-SS60 with wicking rate of 200 s/4 cm (red), CNPH-N SS40 with wicking rate of 150 s/4 cm (grey) and CNPF SN12, 5 µm with wicking rate of 220 s/4 cm (blue). The error bars represent the standard deviation among three replicate strips.

In **III**, the amount of capture antibody dispensed on NC was increased from density of 300 ng/cm up to 1,200 ng/cm. It was observed from specific signal increase that the binding capacity of the test line was improved while the background signal remained low (Figure 24). Typically, high antibody concentration is used at the test line in LFAs. Concentrations even up to 1-3 µg/cm can be used. While considering the dimensions of a typical test line (5 mm width x 0.5 mm depth x 1mm length), the local antibody concentration at the test line becomes very high in comparison to a microtiter well.[147] This may enable efficient binding reaction in an LFA despite of extremely short reaction times. The results showed the positive effect of increasing the capture line density on signal generation in the LFA.

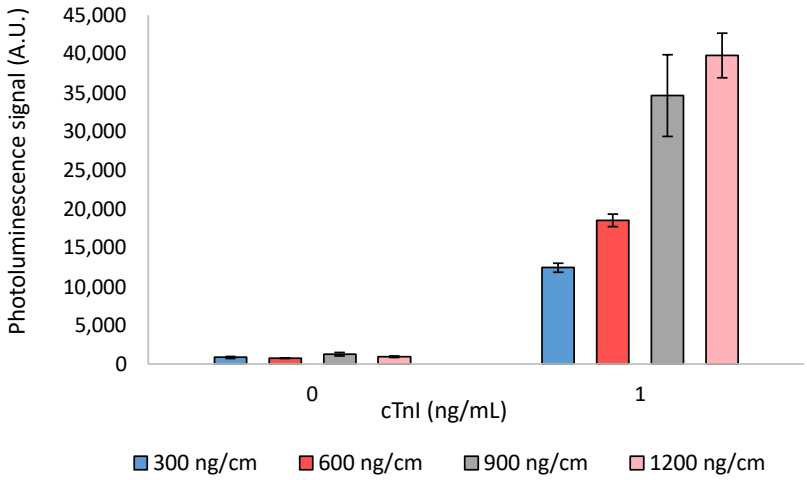

Figure 24. Effect of capture antibody density on nitrocellulose membrane. In **III**, anti-cTnI antibodies were dispensed on nitrocellulose membrane in different densities of 300 ng/cm (blue), 600 ng/cm (red), 900 ng/cm (grey) and 1,200 ng/cm (light red). Error bars represent variation between three replicate strips.

In **II**, two different liquid-dispensing instruments were used to apply the test and control lines on the NC membranes and investigate line width effect on the UCNP-LFA. With the thinner lines, higher signals were detected at the test line in the anti-HIV UCNP-LFA (Figure 25). Traditionally with visual LFAs, wider lines are often desired as visual signal detection may improve by larger colored areas. However, in case of sensitive detection of UCNP labels, a thinner line may provide an advantage since a higher local concentration of the immune complex is achieved at the thin line. Use of measurement instrumentation may not require as wide lines as visual read-out for adequate resolution.

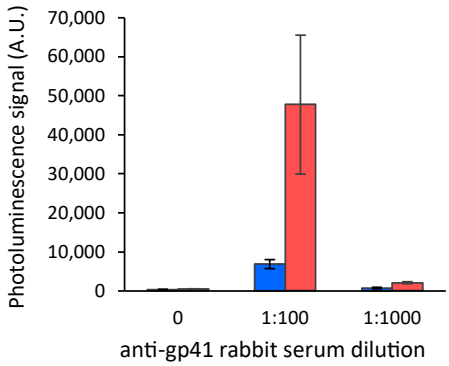

Figure 25. Comparison of line widths for antigen dispensing (**II**). Thinner lines of 0.5 mm width (red) provided higher signal levels in the presence of anti-HIV antibodies in contrast to the wider lines of 1 mm width (blue). Error bars represent the standard deviation among three replicate strips.

5.3.4 Assay measurement and kinetics

Fourteen different NC membranes were tested in HBsAg-LFIA (**I**) with dried UCNP conjugates (Figure 26). The strips were measured at 10-minute intervals and dried overnight. Samples containing HBsAg produced a signal peak at 10 minutes on some NC membranes, however, the signal was lost when UCNP flow continued. Once the UCNP flow had passed the test line, the remaining signal peak was considered reliable. In other words, if the signal levels were constantly increasing over time at different time points, the results were considered valid. NC membrane CNPH-N SS60 was selected to the final assay set up because it showed a consistent signal increase over time and resulted in highest specific signals at 30-minute measurement point.

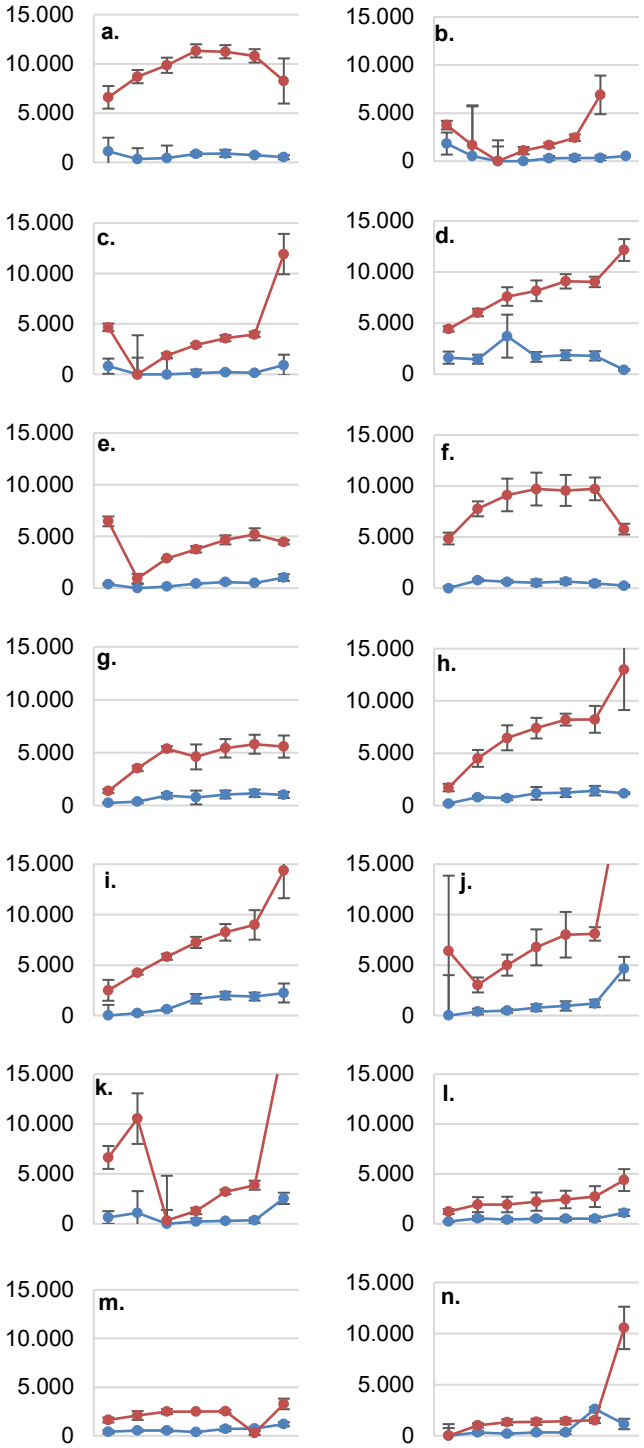
a.
b.
c.
d.
e.
f.
g.
h.
i.
j.
k.
l.
m.
n.
15.000
10.000
5.000
0

5.4 Performance evaluations

The clinical samples and sample panels, used in **I** and **II**, are shown in Tables 6 (**I**) and 7 (**II**). The clinical serum and plasma samples from different individuals presenting natural HBsAg levels within population (i.e., samples not belonging to a commercial sample panel with pre-selected samples) were used for determining the sensitivity and specificity of the assay. Total numbers of samples used for the calculation of the assay performance were 108 HBsAg-positive and 315 HBsAg-negative samples. In **II**, the developed UCNP-LFA was evaluated with 145 anti-HIV antibody positive and 309 anti-HIV antibody negative plasma and serum samples. In both **I** and **II**, the optimal clinical cutoff value was determined based on receiver operating characteristic (ROC) analysis executed by SAS JMP Pro 14 statistics software. To calculate the signal-to-cutoff (S/Co), photoluminescence signal obtained from each sample with peak detection was divided by the cutoff. Samples with S/Co values ≥1 were considered reactive.

In **I**, the sensitivity of UCNP-LFIA was 95.4% [95%CI 89.5–98.5%] based on correct determination of 103/108 HBsAg positive samples and the specificity was 97.1% [95%CI 94.7–98.7%] based on correct determination of 306/315 negative samples. In publication **II**, the UCNP-LFA showed 96.6% (95%CI: 92.1-98.8%) sensitivity and 98.7% (95%CI: 96.7-99.7% specificity. The results obtained from performance evaluations are summarized in Table 12.

The most significant advantage of using UCNP reporters in LFA is the improvement in analytical sensitivity and quantification. These properties are useful particularly when developing f highly sensitive UCNP-LFA tests for sensitivity-demanding antigen markers. For instance in **I**, 15-fold improvement in analytical sensitivity was observed in contrast to visual LFA. However, antibodies typically occur in high titers. Therefore, the direct advantage of high analytical sensitivity is more limited when testing for an antibody response. In **II**, direct improvement in assay performance due to UCNP reporter technology was not observed. However, developing multiple assays on same platform may improve its usability in RLS. Use of the same detection technology in a variety of tests, e.g., a test panel for infectious diseases including antigen and antibody markers, allows the use of a single measurement instrument with automated result interpretation, archiving and transfer of results.

◄ **Figure 26.** Comparison of assay kinetics on different NC membranes (**I**). Membranes were **a.** CNPH-N SS60, **b.** CNPH-N SS40, **c.** CNPC SS12 12 µm, **d.** CNPC SS12 10 µm, **e.** CNPF SN12 10 µm, **f.** CNPF SN12 8 µm, **g.** LFNC-C-BS023_70, **h.** LFNC-C-SS22_70, **i.** LFNC-C-SS22, 15 µ, **j.** LFNC-C-BS026, 15 µ, **k.** LFNC-C-BS026, 10 µ, **l.** HF75, **m.** HF90 and **n.** HF120. Comparison was done with negative (blue series) and positive 4 ng/ml (red series) HBsAg dilutions in whole blood. The x-axis represents measurement points at 10-minute intervals, starting from 10 minutes up to 60 minutes, except the last dot which represents o/n measurement. The y-axis represents the upconversion photoluminescence signal (A.U.). Error bars represent variation between 3 replicates.

Table 12. Performances of the developed UCNP-LFAs.

Assay	% Sensitivity (95% CI)	% Specificity (95% CI)
HBsAg-LFA (**I**)	95.4% (95% CI: 89.5–98.5%)	97.1 % (95% CI: 94.7–98.7%)
anti-HIV-1/2 LFA (**II**)	96.6% (95%CI: 92.1–98.8%)	98.7% (95%CI: 96.7–99.7%)

6 Conclusions

There is a need for POC diagnostics that can be used in remote locations and/or in RLSs, while still providing performance comparable to central laboratory diagnostics. This serves the goal of the WHO to provide access to good-quality diagnostics regardless of the location or socioeconomic status of the patient. Increasing interest towards simple, cost-effective POC diagnostics is driving research and development towards creating new solutions or improving the performance of the existing technologies.

In this thesis, the well-established LF technology was combined with luminescent reporters, and the potential of the UCNP-LF technology in terms of analytical sensitivity and quantification was evaluated.

In contrast to traditional LF tests, UCNP-LF requires reader technology. However, measurement optics required for UCNP reporters can be provided in miniaturized and cost-effective format and POCT compatible UCNP readers have been described in the literature[206,207]. Traditionally in ASSURED criteria, the requirement for a reader device is considered as a drawback. However, the use of a reader is in alignment with the inevitable development of modern societies. Availability of smart phones and other smart devices enable the implementation of these new technologies increasingly also in remote settings. Measurement instrumentation used for UCNP-LF platform possesses ideal next generation POCT features such as connectivity to cloud, smart applications and portal services, and enable access to the POCT results and test history anytime and anywhere[30].

The main conclusions based on the original publications are:

I: UCNP-LFIA technology can be used to produce assays with performance able to fulfill strict requirements set for HBsAg assay sensitivity. The assay described reached LoD below 0.13 IU/ml. This is considered sufficiently stringent for HBsAg assays to be used in situations requiring high level performance and reliability such as in the screening of donated blood. The potential of the UCNP-LFIA for quantitative determination of HBsAg could be further studied.

II: UCNP-LFIA platform is feasible for different kind of analytes such as anti-viral antibodies. Wide range of analytes detected by the same platform provides an advantage in terms of cost savings and patient data analysis processes. For viral infections, a clear cut-off-based result interpretation is not prone to errors caused by the experience-level of the user, or external circumstances such as light.

III: UCNP technology can be used for sensitive and quantitative measurements of cTnI. The UCNP-LFIA platform can reach good dynamic range of 2 orders of magnitude. The developed assay showed good correlation when compared with well-based systems including a central laboratory test.

To conclude, findings in this thesis demonstrate that UCNP-LF technology can be used for qualitative and quantitative analyte detection in complex matrices such as blood specimens. In addition, the technology shows potential for the applications with high sensitivity requirements. However, the UCNP technology still suffers from the main obstacle of LF technology, namely, the variation arising from the membrane materials used and their liquid flow properties. Still, the measurement technology along with fine-tuned strip design provides competitive performance able to even meet the criteria set for EIAs.

UCNP-LF in general has potential to become a future application for POCT testing, meeting requirements of ASSURED and REASSURED[208] criteria (real-time connectivity, ease of specimen collection, affordable, sensitive, specific, user-friendly, rapid and robust, equipment-free or simple and environmentally friendly, and deliverable to end-users). Quantitative measurements open possibilities for development of assays for a wide range of target analytes to support clinical diagnosis in near patient settings.

Acknowledgements

This doctoral research was conducted at the Department of Biotechnology, University of Turku, during 2018-2021. A major part of the research was funded by the Wellcome Trust foundation. This thesis was mostly written during the coronavirus outbreak, which constantly reminded me of the importance of developing convenient diagnostics methods for the detection of viral infections. I have been honored to have a chance to work with *in vitro* diagnostics and with great people whose experience and knowledge is outstanding. This department has been a great place to grow.

It has been a privilege to work in the inspiring and supportive atmosphere we have at the Department of Biotechnology. I want to most sincerely thank Professor Emeritus Kim Pettersson, Professor Tero Soukka, Professor Urpo Lamminmäki and Assistant Professor Saara Wittfooth for giving me the opportunity to carry out this research at the department and for working towards the common good of the department.

I wish to sincerely thank my supervisor Adjunct Professor Sheikh Talha and research director Professor Tero Soukka for their expertise, help and support without which this PhD project could not have been accomplished. I am deeply grateful to Dr. Sheikh Talha for being the main supervisor of this research and sharing his great experience and support for this work. The advisory committee members Professor Tero Soukka and Dr. Terhi Riuttamäki are warmly acknowledged for their advice and encouragement.

I am extremely grateful for my esteemed pre-examiners Associate Professor Jussi Hepojoki and Dr. Leena Hakalahti for reviewing this thesis. I am thankful for all the valuable and constructive comments.

My most heartfelt thanks go to all the co-authors without whose valuable contributions the original publications would not exist: Dr. Sheikh Talha, Karoliina Vuorenpää, Dr. Teppo Salminen, Dr. Etvi Juntunen, Souvick Chattopadhyay, Dinesh Kumar, Dr. Tytti Vuorinen, Dr. Navin Khanna, Dr. Gaurav Batra, Sherif Bayoumy, Taina Heikkilä, Carita Rautanen, Dr. Heidi Hyytiä, Dr. Saara Wittfooth and Professor Kim Pettersson. In particular, I would like to thank Dr. Batra for thorough

input for the HBsAg paper and all the collaboration within the Wellcome Trust project.

I want to thank the 'LF group' Etvi, Talha and Teppo for sharing their enthusiasm for technology development, providing great scientific discussions and creating an atmosphere in which it is fun to work. I want to thank Sherif for collaborating with me in the troponin work - I wish you the best of luck with your PhD project! All those who have collaborated in the Wellcome Trust project during these years are greatly acknowledged. Also, Anttoni Korkiakoski, Liisa Niinistö and Rita Ojaniemi are additionally acknowledged for their valuable input for the lateral flow projects.

I wish to extend my warmest thanks the former and present personnel of the Department of Biotechnology with whom I have had a chance to work with. The atmosphere is always nice and welcoming. Teija Luotohaara, Sanna Laitinen, Paula Holmberg, Jari Vehmas, Pirjo Pietilä and Riikka Lankinen are thanked for keeping the department and laboratory running smoothly.

I am especially grateful to my dear friends for the many happy and unforgettable moments we have shared. Kaisa and Pia thank you for sharing the experience of studying in technology education and *teekkarikulttuuri* in Turku. I am thankful for the long-lasting friendship beyond those study years. Tiia and Johanna, thank you for your friendship originating from even longer in the past, your company has meant a lot to me.

I am deeply grateful for my whole family. Mom and dad, thank you for always encouraging me for doing the thing that feels the most right.

Finally, my deepest gratitude belongs to my dearest husband Teppo. You truly are my best friend, soulmate and partner in LF development. In a very concrete way, which involves some intensive pipetting and lots of brainstorming, I could not have done this without you.

Turku, April 2021

Iida Martiskainen

List of References

1. Chang, M. H. *et al.* Long-term Effects of Hepatitis B Immunization of Infants in Preventing Liver Cancer. *Gastroenterology* **151**, 472-480.e1 (2016).
2. Ward, J. W. & Hinman, A. R. What Is Needed to Eliminate Hepatitis B Virus and Hepatitis C Virus as Global Health Threats. *Gastroenterology* **156**, 297–310 (2019).
3. Roth, G. A. *et al.* Global, regional, and national age-sex-specific mortality for 282 causes of death in 195 countries and territories, 1980–2017: a systematic analysis for the Global Burden of Disease Study 2017. *Lancet* **392**, 1736–1788 (2018).
4. Bouzid, D. *et al.* Rapid diagnostic tests for infectious diseases in the emergency department. *Clinical Microbiology and Infection* **27**, 182–191 (2021).
5. Pulia, M. S., O'Brien, T. P., Hou, P. C., Schuman, A. & Sambursky, R. Multi-tiered screening and diagnosis strategy for COVID-19: a model for sustainable testing capacity in response to pandemic. *Ann. Med.* **52**, 207–214 (2020).
6. Sharma, S., Crawley, A. & O'Kennedy, R. Strategies for overcoming challenges for decentralised diagnostics in resource-limited and catastrophe settings. *Expert Rev. Mol. Diagn.* **17**, 109–118 (2017).
7. Carraro, P. The point-of-care testing in the emergency department. *Emerg. Care J.* **15**, (2019).
8. Institute for Health Metrics and Evaluation. *Findings from the Global Burden of Disease Study 2017*. www.healthdata.org (2018).
9. Stanaway, J. D. *et al.* The global burden of viral hepatitis from 1990 to 2013: findings from the Global Burden of Disease Study 2013. *Lancet* **388**, 1081–1088 (2016).
10. Wang, H. *et al.* Estimates of global, regional, and national incidence, prevalence, and mortality of HIV, 1980–2015: the Global Burden of Disease Study 2015. *Lancet HIV* **3**, e361–e387 (2016).
11. Institute for Health Metrics and Evaluation. Global Burden of Disease Collaborative Network. Global Burden of Disease Study 2017 (GBD 2017) Results. (2018).
12. Centers for Disease control and Prevention. HIV Cost-effectiveness https://www.cdc.gov/hiv/programresources/guidance/costeffectiveness/index.html (2021). Accessed 23.4.2021.
13. UNAIDS. *90-90-90 An ambitious treatment target to help end the AIDS epidemic*. https://www.unaids.org/sites/default/files/media_asset/90-90-90_en_0.pdf (2014). Accessed 15.3.2020.
14. World Health Organization. Global Hepatitis Report. *Global Hepatitis Report* (2017). Accessed 23.4.2021.
15. Drain, P. K. *et al.* Diagnostic point-of-care tests in resource-limited settings. *Lancet Infect. Dis.* **14**, 239–249 (2014).
16. Chevaliez, S. & Pawlotsky, J.-M. New virological tools for screening, diagnosis and monitoring of hepatitis B and C in resource-limited settings. J Hepatol **69**, 916-926 (2018)
17. Drain, P. K. *et al.* Diagnostic point-of-care tests in resource-limited settings. *Lancet Infect. Dis.* **14**, 239–249 (2014).
18. Peeling, R. W. & Mabey, D. Point-of-care tests for diagnosing infections in the developing world. *Clinical Microbiology and Infection* **16**, 1062–1069 (2010).

19. Jorgensen, P., Chanthap, L., Rebueno, A., Tsuyuoka, R. & Bell, D. Malaria rapid diagnostic tests in tropical climates: The need for a cool chain. *Am. J. Trop. Med. Hyg.* **74**, 750–754 (2006).
20. Clark, L. C. & Lyons, C. Electrode Systems for Continuous Monitoring in Cardiovascular Surgery. *Ann. N. Y. Acad. Sci.* **102**, 29–45 (1962).
21. National Institutes of Health. The History of the Pregnancy Test Kit - A Timeline of Pregnancy Testing. https://history.nih.gov/exhibits/thinblueline/timeline.html. Accessed 20.4.2021.
22. Woo, J., McCabe, J. B., Chauncey, D., Schug, T. & Henry, J. B. The evaluation of a portable clinical analyzer in the emergency department. *Am. J. Clin. Pathol.* **100**, 599–605 (1993).
23. Erickson, K. A. & Wilding, P. Evaluation of a novel point-of-care system, the i-STAT Portable Clinical Analyzer. *Clin. Chem.* **39**, 283–287 (1993).
24. Pruett, C. R. *et al.* The Use of Rapid Diagnostic Tests for Transfusion Infectious Screening in Africa: A Literature Review. *Transfus. Med. Rev.* **29**, 35–44 (2015).
25. Prugger, C. *et al.* Screening for transfusion transmissible infections using rapid diagnostic tests in Africa: A potential hazard to blood safety? *Vox Sang.* **110**, 196–198 (2016).
26. Sharma, S., Zapatero-Rodríguez, J., Estrela, P. & O'Kennedy, R. Point-of-Care Diagnostics in Low Resource Settings: Present Status and Future Role of Microfluidics. *Biosensors* **5**, 577 (2015).
27. Pandey, C. M. *et al.* Microfluidics Based Point-of-Care Diagnostics. *Biotechnology Journal* **13** (2018).
28. Myers, F. B. & Lee, L. P. Innovations in optical microfluidic technologies for point-of-care diagnostics. *Lab Chip* **8**, 2015 (2008).
29. Päkkilä, H. & Soukka, T. Simple and inexpensive immunoassay-based diagnostic tests. *Bioanal. Rev.* **3**, 27–40 (2011).
30. Vashist, S. K., Luppa, P. B., Yeo, L. Y., Ozcan, A. & Luong, J. H. T. Emerging Technologies for Next-Generation Point-of-Care Testing. *Trends in Biotechnology*. **33**, 692–705 (2015).
31. Peeling, R. W., Holmes, K. K., Mabey, D. & Ronald, A. Rapid tests for sexually transmitted infections (STIs): The way forward. *Sexually Transmitted Infections*. **82,** v1–v6 (2006).
32. World Health Organization. Rapid HIV tests: Guidelines for use in HIV testing and counselling services in resource-constrained settings. https://apps.who.int/iris/bitstream/handle/10665/42978/9241591811.pdf?sequence=1&isAllowed=y (2004). Accessed 19.11.2020.
33. Allain, J.-P. & Lee, H. Rapid tests for detection of viral markers in blood transfusion. *Expert Rev. Mol. Diagn.* **5**, 31–41 (2005).
34. World Health Organization. WHO Prequalification of Medicines Programme. https://extranet.who.int/prequal/. Accessed 20.4.2020.
35. Cheng, X. *et al.* Hepatitis B virus evades innate immunity of hepatocytes but activates cytokine production by macrophages. *Hepatology* **66**, 1779–1793 (2017).
36. Dény, P. & Zoulim, F. Hepatitis B virus: From diagnosis to treatment. *Pathol. Biol.* **58**, 245–253 (2010).
37. World Health Organization. Hepatitis B Factsheet. https://www.who.int/news-room/fact-sheets/detail/hepatitis-b (2019). Accessed 15.4.2021.
38. Trépo, C., Chan, H. L. Y. & Lok, A. Hepatitis B virus infection. *Lancet* **384**, 2053–2063 (2014).
39. World Health Organization. *Combating Hepatitis B and C to reach elimination by 2030*. https://apps.who.int/iris/bitstream/handle/10665/206453/WHO_HIV_2016.04_eng.pdf?sequence=1&isAllowed=y (2016). Accessed 15.4.2021.
40. Zhang, Z. H. *et al.* Genetic variation of hepatitis B virus and its significance for pathogenesis. *World Journal of Gastroenterology*. **22,** 126–144 (2016).
41. Blum, H. E. Hepatitis B virus: Significance of naturally occurring mutants. *Intervirology* **35**, 40–50 (1993).
42. Kramvis, A. Genotypes and genetic variability of hepatitis B virus. *Intervirology* **57**, 141–150 (2014).
43. Kramvis, A., Kew, M. & François, G. Hepatitis B virus genotypes. *Vaccine*. **23,** 2409–2423 (2005).

44. Okamoto, H. *et al.* Typing hepatitis B virus by homology in nucleotide sequence: Comparison of surface antigen subtypes. *J. Gen. Virol.* **69**, 2575–2583 (1988).
45. Norder, H., Hammas, B., Lofdahl, S., Courouce, A. M. & Magnius, L. O. Comparison of the amino acid sequences of nine different serotypes of hepatitis B surface antigen and genomic classification of the corresponding hepatitis B virus strains. *J. Gen. Virol.* **73**, 1201–1208 (1992).
46. Norder, H., Courouc, A. M. & Magnius, L. O. Complete genomes, phylogenetic relatedness, and structural proteins of six strains of the hepatitis B virus, four of which represent two new genotypes. *Virology* **198**, 489–503 (1994).
47. Stuyver, L. *et al.* A new genotype of hepatitis B virus: Complete genome and phylogenetic relatedness. *J. Gen. Virol.* **81**, 67–74 (2000).
48. Arauz-Ruiz, P., Norder, H., Robertson, B. H. & Magnius, L. O. Genotype H: A new Amerindian genotype of hepatitis B virus revealed in Central America. *Journal of General Virology*. **83**, 2059–2073 (2002).
49. Olinger, C. M. *et al.* Possible new hepatitis B virus genotype, southeast Asia. *Emerg. Infect. Dis.* **14**, 1777–1780 (2008).
50. Tatematsu, K. *et al.* A Genetic Variant of Hepatitis B Virus Divergent from Known Human and Ape Genotypes Isolated from a Japanese Patient and Provisionally Assigned to New Genotype J. *J. Virol.* **83**, 10538–10547 (2009).
51. Velkov, S. *et al.* The Global Hepatitis B Virus Genotype Distribution Approximated from Available Genotyping Data. *Genes (Basel).* **9**, 495 (2018).
52. Hassemer, M. *et al.* Comparative characterization of hepatitis B virus surface antigen derived from different hepatitis B virus genotypes. *Virology* **502**, 1–12 (2017).
53. Harrison, T. J. Current issues in the diagnosis of hepatitis B and C virus infections. *Clin. Diagn. Virol.* **5**, 187–190 (1996).
54. World Health Organization. *Hepatitis B Surface Antigen Assays: Operational Characteristics*. https://www.who.int/diagnostics_laboratory/evaluations/en/hep_B_rep1.pdf (2001). Accessed 23.4.2021.
55. Song, J. E. & Kim, D. Y. Diagnosis of hepatitis B. *Annals of Translational Medicine*. **4** (2016).
56. Mak, L.-Y. *et al.* Review article: hepatitis B core-related antigen (HBcrAg): an emerging marker for chronic hepatitis B virus infection. *Aliment. Pharmacol. Ther.* **47**, 43–54 (2018).
57. Kumar, A., Pant, S. & Narang, S. Significance of alanine aminotransferase testing in diagnosis of acute and chronic HBV infection. *Asian Pac. J. Cancer Prev.* **10**, 1171–2 (2009).
58. Allain, J.-P. & Opare-Sem, O. Screening and diagnosis of HBV in low-income and middle-income countries. *Nat. Rev. Gastroenterol. Hepatol.* **13**, 643–653 (2016).
59. World Health Organization. *Hepatitis B Surface Antigen Assays: Operational Characteristics*. https://www.who.int/diagnostics_laboratory/evaluations/en/hep_B_rep1.pdf (2001). 23.4.2021.
60. Seitz, R. Hepatitis B Virus. *Transfus. Med. Hemotherapy* **27**, 226–234 (2000).
61. Keechilot, C. S. *et al.* Detection of occult hepatitis B and window period infection among blood donors by individual donation nucleic acid testing in a tertiary care center in South India. *Pathog. Glob. Health* **110**, 287–291 (2016).
62. Frösner, G. G. *et al.* Diagnostic significance of quantitative determination of hepatitis B surface antigen in acute and chronic hepatitis B infection. *Eur. J. Clin. Microbiol.* **1**, 52–58 (1982).
63. Zoulim, F. *et al.* New assays for quantitative determination of viral markers in management of chronic hepatitis B virus infection. *J. Clin. Microbiol.* **30**, 1111–9 (1992).
64. Burczynska, B. *et al.* The value of quantitative measurement of HBeAg and HBsAg before interferon-α treatment of chronic hepatitis B in children. *J. Hepatol.* **21**, 1097–1102 (1994).
65. Brunetto, M. R. A new role for an old marker, HBsAg. *J. Hepatol.* **52**, 475–477 (2010).
66. Liaw, Y.-F. Clinical utility of hepatitis B surface antigen quantitation in patients with chronic hepatitis B: A review. *Hepatology* **53**, 2121–2129 (2011).
67. Su, T.-H. *et al.* Serum hepatitis B surface antigen concentration correlates with HBV DNA level in patients with chronic hepatitis B. *Antivir. Ther.* **15**, 1133-1139 (2010).

68. Cornberg, M. *et al.* The role of quantitative hepatitis B surface antigen revisited. *J. Hepatol*. **66**, 398-411 (2017)
69. World Health Organization. *WHO Performance Evaluation Acceptance Criteria for HBsAg In vitro diagnostics in the context of WHO Prequalification*. https://www.nibsc.org/documents/ifu/03-262.pdf (2016). Accessed 18.3.2020.
70. 2009/886/EC. *Commission Decision of 27 November 2009 amending Decision 2002/364/EC on common technical specifications for in vitro diagnostic medical devices*. (2009).
71. Chudy, M. *et al.* Performance of hepatitis B surface antigen tests with the first WHO international hepatitis B virus genotype reference panel. *J. Clin. Virol.* **58**, 47–53 (2013).
72. Scheiblauer, H. *et al.* Performance evaluation of 70 hepatitis B virus (HBV) surface antigen (HBsAg) assays from around the world by a geographically diverse panel with an array of HBV genotypes and HBsAg subtypes. *Vox Sang.* **98**, 403–414 (2010).
73. Hans, R. & Marwaha, N. Nucleic acid testing-benefits and constraints. *Asian Journal of Transfusion Science*. **8**, 2–3 (2014).
74. Makvandi, M. Update on occult hepatitis B virus infection. *World Journal of Gastroenterology*. **22**, 8720–8734 (2016).
75. The Global Fund. *List of HIV Diagnostic test kits and equipments classified according to the Global Fund Quality Assurance Policy*. https://www.theglobalfund.org/media/5878/psm_productshiv-who_list_en.pdf (2020). Accessed 1.4.2020.
76. Servant-Delmas, A., Ly, T. D., Hamon, C., Houdah, A. K. & Laperche, S. Comparative performance of three rapid HBsAg assays for detection of HBs diagnostic escape mutants in clinical samples. *Journal of Clinical Microbiology*. **53,** 3954–3955 (2015).
77. Chevaliez, S. & Pawlotsky, J.-M. New virological tools for screening, diagnosis and monitoring of hepatitis B and C in resource-limited settings. *J. Hepatol.* **69**, 916–926 (2018).
78. Gottlieb, M. S. *et al.* Pneumocystis carinii Pneumonia and Mucosal Candidiasis in Previously Healthy Homosexual Men: Evidence of a New Acquired Cellular Immunodeficiency. *N. Engl. J. Med.* **305**, 1425–1431 (1981).
79. Barré-Sinoussi, F. *et al.* Isolation of a T-lymphotropic retrovirus from a patient at risk for acquired immune deficiency syndrome (AIDS). *Science.* **220**, 868–871 (1983).
80. Seitz, R. Human Immunodeficiency Virus (HIV). *Transfus. Med. Hemotherapy* **43**, 203–222 (2016).
81. Vanhems, P. *et al.* Clinical features of acute retroviral syndrome differ by route of infection but not by gender and age. *J. Acquir. Immune Defic. Syndr.* **31**, 318–321 (2002).
82. Hoenigl, M. *et al.* Signs or symptoms of acute HIV infection in a cohort undergoing community-based screening. *Emerg. Infect. Dis.* **22**, 532–534 (2016).
83. Maartens, G., Celum, C. & Lewin, S. R. HIV infection: epidemiology, pathogenesis, treatment, and prevention. *Lancet* **384**, 258–271 (2014).
84. World Health Organization. HIV/AIDS Fact Sheet. https://www.who.int/news-room/fact-sheets/detail/hiv-aids (2019). Accessed 15.4.2020.
85. UNAIDS. *Global Aids Up Date 2016*. https://www.unaids.org/sites/default/files/media_asset/global-AIDS-update-2016_en.pdf (2016). Accessed 23.4.2021.
86. Sharp, P. M. & Hahn, B. H. Origins of HIV and the AIDS pandemic. *Cold Spring Harb. Perspect. Med.* **1**, (2011).
87. Clavel, F. *et al.* Isolation of a new human retrovirus from West African patients with AIDS. *Science.* **233**, 343–346 (1986).
88. de Silva, T. I., Cotten, M. & Rowland-Jones, S. L. HIV-2: the forgotten AIDS virus. *Trends in Microbiology*. **16,** 588–595 (2008).
89. Olesen, J. S. *et al.* HIV-2 continues to decrease, whereas HIV-1 is stabilizing in Guinea-Bissau. *AIDS* **32**, 1193–1198 (2018).
90. Fryer, H. R. *et al.* Predicting the extinction of HIV-2 in rural Guinea-Bissau. *AIDS* **29**, 2479–2486 (2015).

91. Campbell-Yesufu, O. T. & Gandhi, R. T. Update on human immunodeficiency virus (HIV)-2 infection. *Clin. Infect. Dis.* **52**, 780–7 (2011).
92. De Mendoza, C. *et al.* HIV type 2 epidemic in Spain: Challenges and missing opportunities. *AIDS.* **31**, 1353–1364 (2017).
93. Rowland-Jones, S. L. & Whittle, H. C. Out of Africa: What can we learn from HIV-2 about protective immunity to HIV-1? *Nature Immunology*. **8,** 329–331 (2007).
94. Popper, S. J. *et al.* Low Plasma Human Immunodeficiency Virus Type 2 Viral Load Is Independent of Proviral Load: Low Virus Production In Vivo. *J. Virol.* **74**, 1554–1557 (2000).
95. De Leys, R. *et al.* Isolation and partial characterization of an unusual human immunodeficiency retrovirus from two persons of west-central African origin. *Journal of virology : JVI.* **64**, 1207–1216 (1990).
96. Bush, S. & Tebit, D. M. HIV-1 Group O Origin, Evolution, Pathogenesis, and Treatment: Unraveling the Complexity of an Outlier 25 Years Later. *AIDS Rev*. **17**, 147–158.
97. Simon, F. *et al.* Identification of a new human immunodeficiency virus type 1 distinct from group M and group O. *Nat. Med.* **4**, 1032 (1998).
98. Vallari, A. *et al.* Four new HIV-1 group N isolates from Cameroon: Prevalence continues to be low. *AIDS Res. Hum. Retroviruses* **26**, 109–115 (2010).
99. Plantier, J. C. *et al.* A new human immunodeficiency virus derived from gorillas. *Nat. Med.* **15**, 871–872 (2009).
100. Alessandri-Gradt, E. *et al.* HIV-1 group P infection. *AIDS* **32**, 1317–1322 (2018).
101. Wilen, C. B., Tilton, J. C. & Doms, R. W. HIV: Cell binding and entry. *Cold Spring Harb. Perspect. Med.* **2**, (2012).
102. Chen, Y. H., Christiansen, A., Bock, G. & Dierich, M. P. HIV-2 transmembrane protein gp36 like HIV-1 gp41 binds to human lymphocytes and monocytes [1]. *AIDS*. **9**, 1193–1194 (1995).
103. Habte, H. H., Banerjee, S., Shi, H., Qin, Y. & Cho, M. W. Immunogenic properties of a trimeric gp41-based immunogen containing an exposed membrane-proximal external region. *Virology* **486**, 187–197 (2015).
104. Branson, B. M. The Future of HIV Testing. *JAIDS J. Acquir. Immune Defic. Syndr.* **55**, S102–S105 (2010).
105. Zhao, J., Chang, L. & Wang, L. Nucleic acid testing and molecular characterization of HIV infections. *European Journal of Clinical Microbiology and Infectious Diseases*. **38**, 829–842 (2019).
106. Ou, C. Y. *et al.* DNA amplification for direct detection of HIV-1 in DNA of peripheral blood mononuclear cells. *Science.* **239**, 295–297 (1988).
107. Mellors, J. W. *et al.* Prognosis in HIV-1 infection predicted by the quantity of virus in plasma. *Science.* **272**, 1167–1170 (1996).
108. Lepri, A. C. *et al.* The relative prognostic value of plasma HIV RNA levels and CD4 lymphocyte counts in advanced HIV infection. *AIDS* **12**, (1998).
109. Kumar Barik, S. *et al.* An Overview of Enzyme Immunoassay: The Test Generation Assay in HIV/AIDS Testing. *J. AIDS Clin. Res.* **09**, (2018).
110. Alexander, T. S. Human Immunodeficiency Virus Diagnostic Testing: 30 Years of Evolution. *Clin. Vaccine Immunol.* **23**, 249–253 (2016).
111. Mühlbacher, A. *et al.* Performance evaluation of a new fourth-generation HIV combination antigen-antibody assay. *Med. Microbiol. Immunol.* **202**, 77–86 (2013).
112. Branson, B. M. *et al.* Laboratory testing for the diagnosis of HIV infection : updated recommendations - Guidelines and Recommendations. *Centers Dis. Control Prev.* (2014)
113. Nkwo, P., PMTCT, N. & FMOH. National Guidelines for Prevention of Mother to Child Transmission of HIV in Nigeria. (2010).
114. Haney, K. *et al.* The Role of Affordable, Point-of-Care Technologies for Cancer Care in Low- and Middle-Income Countries: A Review and Commentary. *IEEE Journal of Translational Engineering in Health and Medicine*. **5** (2017).

115. World Health Organization. Fact sheet: Cardiovascular diseases (CVDs). https://www.who.int/news-room/fact-sheets/detail/cardiovascular-diseases-(cvds) (2017). Accessed 8.1.2021.
116. Aebischer Perone, S. et al. Non-communicable diseases in humanitarian settings: Ten essential questions Bayard Roberts, Kiran Jobunputra, Preeti Patel and Pablo Perel. Confl. Health 11, 1–11 (2017).
117. Shandilya, R. et al. Nanobiosensors: Point-of-care approaches for cancer diagnostics. Biosens. Bioelectron. 130, 147–165 (2019).
118. Dhawan, A. P. Collaborative Paradigm of Preventive, Personalized, and Precision Medicine with Point-of-Care Technologies. in IEEE Journal of Translational Engineering in Health and Medicine. 4 (2016).
119. Makki, N., Brennan, T. M. & Girotra, S. Acute coronary syndrome. Journal of Intensive Care Medicine. 30, 186–200 (2015).
120. Mueller, C. Biomarkers and acute coronary syndromes: An update. European Heart Journal. 35, 552–556 (2014).
121. Eisen, A., Giugliano, R. P. & Braunwald, E. Updates on acute coronary syndrome: A review. JAMA Cardiology. 1, 718–730 (2016).
122. Thygesen, K. et al. Recommendations for the use of cardiac troponin measurement in acute cardiac care. European Heart Journal. 31, 2197–2204 (2010).
123. Thygesen, K. et al. Fourth universal definition of myocardial infarction (2018). Eur. Heart J. 40, 237–269 (2019).
124. Farah, C. S. & Reinach, F. C. The troponin complex and regulation of muscle contraction. FASEB J. 9, 755–767 (1995).
125. Adams, J. E. et al. Cardiac troponin I: A marker with high specificity for cardiac injury. Circulation 88, 101–106 (1993).
126. Ooi, D. S., Isotalo, P. A. & Veinot, J. P. Correlation of antemortem serum creatine kinase, creatine kinase-MB, troponin I, and troponin T with cardiac pathology. Clin. Chem. 46, 338–344 (2000).
127. Mair, J. et al. How is cardiac troponin released from injured myocardium? European heart journal. Acute cardiovascular care. 7, 553–560 (2018).
128. Thygesen, K. et al. Third universal definition of myocardial infarction. Eur. Heart J. 33, 2551–2567 (2012).
129. Januzzi, J. L. et al. Recommendations for Institutions Transitioning to High-Sensitivity Troponin Testing: JACC Scientific Expert Panel. Journal of the American College of Cardiology. 73, 1059–1077 (2019).
130. Garg, P. et al. Cardiac biomarkers of acute coronary syndrome: from history to high-sensitivity cardiac troponin. Internal and Emergency Medicine. 12, 147–155 (2017).
131. Agnello, L. et al. Establishing the 99th percentile for high sensitivity cardiac troponin i in healthy blood donors from southern italy. Biochem. Medica 29, 402–406 (2019).
132. Loten, C., Attia, J., Hullick, C., Marley, J. & McElduff, P. Point of care troponin decreases time in the emergency department for patients with possible acute coronary syndrome: A randomised controlled trial. Emerg. Med. J. 27, 194–198 (2010).
133. Collinson, P. O. *et al.* A prospective randomized controlled trial of point-of-care testing on the coronary care unit. *Ann. Clin. Biochem.* **41**, 397–404 (2004).
134. Aldous, S. *et al.* Comparison of new point-of-care troponin assay with high sensitivity troponin in diagnosing myocardial infarction. *Int. J. Cardiol.* **177**, 182–186 (2014).
135. Bingisser, R. et al. Cardiac troponin: A critical review of the case for point-of-care testing in the ED. American Journal of Emergency Medicine. 30, 1639–1649 (2012).
136. Bock, J. L., Singer, A. J. & Thode, H. C. Comparison of Emergency Department Patient Classification by Point-of-Care and Central Laboratory Methods for Cardiac Troponin I. Am. J. Clin. Pathol. 130, 132–135 (2008).

137. Amundson, B. E. & Apple, F. S. Cardiac troponin assays: A review of quantitative point-of-care devices and their efficacy in the diagnosis of myocardial infarction. Clinical Chemistry and Laboratory Medicine. 53, 665–676 (2015).
138. Tiplady, S. Lateral Flow and Consumer Diagnostics. in The Immunoassay Handbook 533–536 (Elsevier Ltd, 2013).
139. Posthuma-Trumpie, G. A., Korf, J. & Van Amerongen, A. Lateral flow (immuno)assay: Its strengths, weaknesses, opportunities and threats. A literature survey. Anal. Bioanal. Chem. 393, 569–582 (2009).
140. O'Farrell, B. Evolution in Lateral Flow–Based Immunoassay Systems. in Lateral Flow Immunoassay 1–33 (Humana Press, 2009).
141. Chun, P. Colloidal Gold and Other Labels for Lateral Flow Immunoassays. in Lateral Flow Immunoassay 1–19 (Humana Press, 2009).
142. Mahmoudi, T., de la Guardia, M. & Baradaran, B. Lateral flow assays towards point-of-care cancer detection: A review of current progress and future trends. TrAC - Trends in Analytical Chemistry. 125, 115842 (2020).
143. Merck Millipore. Rapid Lateral Flow Test Strips - Considerations for Product Development. (2013).
144. Tisone, T. C. & O'Farrell, B. Manufacturing the Next Generation of Highly Sensitive and Reproducible Lateral Flow Immunoassay. (Humana Press, 2009).
145. Mansfield, M. A. Nitrocellulose Membranes for Lateral Flow Immunoassays: A Technical Treatise. in Lateral Flow Immunoassay 1–19 (Humana Press, 2009).
146. Low, S. C. et al. Electrophoretic interactions between nitrocellulose membranes and proteins: Biointerface analysis and protein adhesion properties. Colloids Surfaces B Biointerfaces 110, 248–253 (2013).
147. Brown, M. C. Antibodies: Key to a Robust Lateral Flow Immunoassay. in Lateral Flow Immunoassay 1–16 (Humana Press, 2009).
148. Washburn, E. W. The dynamics of capillary flow. Phys. Rev. 17, 273–283 (1921).
149. Gina E., F., Carly A., H., Shefali B., O. & Pauls, Y. The Evolution Of Nitrocellulose As A Material For Bioassays. MRS Bull. 38, 326–330 (2013).
150. Darcy, H. Les fontaines publiques de la ville de Dijon. (1856).
151. Wong, R. C. & Tse, H. Y. Quantitative, False Positive, and False Negative Issues for Lateral Flow Immunoassays as Exemplified by Onsite Drug Screens. in Lateral Flow Immunoassay 1–19 (Humana Press, 2009).
152. Gasperino, D., Baughman, T., Hsieh, H. V., Bell, D. & Weigl, B. H. Improving Lateral Flow Assay Performance Using Computational Modeling. Annu. Rev. Anal. Chem. 11, 219–244 (2018).
153. Katis, I. N., He, P. J. W., Eason, R. W. & Sones, C. L. Improved sensitivity and limit-of-detection of lateral flow devices using spatial constrictions of the flow-path. Biosens. Bioelectron. 113, 95–100 (2018).
154. Hecht, L., Van Rossum, D. & Dietzel, A. Femtosecond-laser-structured nitrocellulose membranes for multi-parameter Point-of-Care tests. Microelectron. Eng. 158, 52–58 (2016).
155. Rivas, L., Medina-Sánchez, M., De La Escosura-Muñiz, A. & Merkoçi, A. Improving sensitivity of gold nanoparticle-based lateral flow assays by using wax-printed pillars as delay barriers of microfluidics. Lab Chip 14, 4406–4414 (2014).
156. Quesada-González, D. *et al.* Signal enhancement on gold nanoparticle-based lateral flow tests using cellulose nanofibers. *Biosens. Bioelectron.* **141**, 111407 (2019).
157. de Puig, H., Bosch, I., Gehrke, L. & Hamad-Schifferli, K. Challenges of the Nano–Bio Interface in Lateral Flow and Dipstick Immunoassays. *Trends in Biotechnology*. **35**, 1169–1180 (2017).
158. Holstein, C. A. et al. Immobilizing affinity proteins to nitrocellulose: A toolbox for paper-based assay developers. Anal. Bioanal. Chem. 408, 1335–1346 (2016).
159. Omidfar, K., Khorsand, F. & Darziani Azizi, M. New analytical applications of gold nanoparticles as label in antibody based sensors. Biosensors and Bioelectronics. 43, 336–347 (2013).

160. Tang, D. et al. Magnetic nanogold microspheres-based lateral-flow immunodipstick for rapid detection of aflatoxin B2 in food. Biosens. Bioelectron. 25, 514–518 (2009).
161. Huang, X., Aguilar, Z. P., Xu, H., Lai, W. & Xiong, Y. Membrane-based lateral flow immunochromatographic strip with nanoparticles as reporters for detection: A review. Biosensors and Bioelectronics. 75, 166–180 (2015).
162. Grésenguet, G., Longo, J. de D., Tonen-Wolyec, S., Mboumba Bouassa, R.-S. & Belec, L. Acceptability and Usability Evaluation of Finger-Stick Whole Blood HIV Self-Test as An HIV Screening Tool Adapted to The General Public in The Central African Republic. Open AIDS J. 11, 101–118 (2017).
163. Li, J. et al. Gold immunochromatographic strips for enhanced detection of Avian influenza and Newcastle disease viruses. Anal. Chim. Acta 782, 54–58 (2013).
164. Chen, X. et al. Self-assembled colloidal gold superparticles to enhance the sensitivity of lateral flow immunoassays with sandwich format. Theranostics 10, 3737–3748 (2020).
165. Parpia, Z. A., Elghanian, R., Nabatiyan, A., Hardie, D. R. & Kelso, D. M. p24 antigen rapid test for diagnosis of acute pediatric HIV infection. J. Acquir. Immune Defic. Syndr. 55, 413–9 (2010).
166. Gordon, J. & Michel, G. Discerning Trends in Multiplex Immunoassay Technology with Potential for Resource-Limited Settings. Clin Chem. 58, 690-698 (2012)
167. Quesada-González, D. & Merkoçi, A. Nanoparticle-based lateral flow biosensors. Biosensors and Bioelectronics. 73, 47–63 (2015).
168. Li, C. et al. Development of an immunochromatographic assay for rapid and quantitative detection of clenbuterol in swine urine. Food Control 34, 725–732 (2013).
169. Wu, R. et al. Quantitative and rapid detection of C-reactive protein using quantum dot-based lateral flow test strip. Anal. Chim. Acta 1008, 1–7 (2018).
170. Deng, X. et al. Applying strand displacement amplification to quantum dots-based fluorescent lateral flow assay strips for HIV-DNA detection. Biosens. Bioelectron. 105, 211–217 (2018).
171. Yuan, J. & Wang, G. Lanthanide complex-based fluorescence label for time-resolved fluorescence bioassay. J. Fluoresc. 15, 559–568 (2005).
172. Näreoja, T., Vehniäinen, M., Lamminmäki, U., Hänninen, P. E. & Härmä, H. Study on nonspecificity of an immuoassay using Eu-doped polystyrene nanoparticle labels. J. Immunol. Methods 345, 80–89 (2009).
173. Järvenpää, M. L. et al. Rapid and sensitive cardiac troponin I immunoassay based on fluorescent europium(III)-chelate-dyed nanoparticles. Clin. Chim. Acta. 414, 70–75 (1970).
174. Liang, R.-L. et al. Europium (III) chelate microparticle-based lateral flow immunoassay strips for rapid and quantitative detection of antibody to hepatitis B core antigen. Sci. Rep. 7, 14093 (2017).
175. Härmä, H., Soukka, T. & Lövgren, T. Europium nanoparticles and time-resolved fluorescence for ultrasensitive detection of prostate-specific antigen. Clin. Chem. 47, 561–568 (2001).
176. Kekki, H. et al. Improved cancer specificity in PSA assay using Aleuria aurantia lectin coated Eu-nanoparticles for detection. Clin. Biochem. 50, 54–61 (2017).
177. Song, C. et al. Rapid and sensitive detection of β-agonists using a portable fluorescence biosensor based on fluorescent nanosilica and a lateral flow test strip. Biosens. Bioelectron. 50, 62–65 (2013).
178. Song, X. & Knotts, M. Time-resolved luminescent lateral flow assay technology. Anal. Chim. Acta 626, 186–192 (2008).
179. Xia, X. *et al.* A highly sensitive europium nanoparticle-based lateral flow immunoassay for detection of chloramphenicol residue. *Anal. Bioanal. Chem.* **405**, 7541–7544 (2013).
180. Haase, M. & Schäfer, H. Upconverting Nanoparticles. *Angew. Chemie Int. Ed.* **50**, 5808–5829 (2011).
181. Riuttamäki, T. & Soukka, T. Upconverting Phosphor Labels for Bioanalytical Assays BT - Advances in Chemical Bioanalysis. in Advances in Chemical Bioanalysis 155–204 (2013).
182. Ukonaho, T. et al. Comparison of infrared-excited up-converting phosphors and europium nanoparticles as labels in a two-site immunoassay. Anal. Chim. Acta 596, 106–115 (2007).

183. Corstjens, P. et al. Use of up-converting phosphor reporters in lateral-flow assays to detect specific nucleic acid sequences: A rapid, sensitive DNA test to identify human papillomavirus type 16 infection. in Clin. Chem. 47, 1885–1893 (2001).
184. Corstjens, P. L. A. M. et al. Up-converting phosphor technology-based lateral flow assay for detection of Schistosoma circulating anodic antigen in serum. J. Clin. Microbiol. 46, 171–6 (2008).
185. Corstjens, P. L. A. M. et al. A user-friendly, highly sensitive assay to detect the IFN-γ secretion by T cells. Clin. Biochem. 41, 440–444 (2008).
186. Mokkapati, V. K. et al. Evaluation of UPlink-RSV: Prototype rapid antigen test for detection of respiratory syncytial virus infection. in Annals of the New York Academy of Sciences. 1098, 476–485 (2007).
187. Juntunen, E. et al. Lateral flow immunoassay with upconverting nanoparticle-based detection for indirect measurement of interferon response by the level of MxA. J. Med. Virol. 89, 598–605 (2017).
188. Niedbala, R. S. et al. Detection of analytes by immunoassay using Up-Converting Phosphor Technology. Anal. Biochem. 293, 22–30 (2001).
189. Hampl, J. et al. Upconverting Phosphor Reporters in Immunochromatographic Assays. Anal. Biochem. 288, 176–187 (2001).
190. Corstjens, P. L. A. M. et al. Lateral flow assay for simultaneous detection of cellular- and humoral immune responses. Clin. Biochem. 44, 1241–1246 (2011).
191. Nilsson, O. et al. Antigenic determinants of prostate-specific antigen (PSA) and development of assays specific for different forms of PSA. Br. J. Cancer 75, 789–797 (1997).
192. Savukoski, T. et al. Epitope Specificity and IgG Subclass Distribution of Autoantibodies to Cardiac Troponin. Clin. Chem. 59, 512–518 (2013).
193. Talha, S. M. et al. A highly sensitive and specific time resolved fluorometric bridge assay for antibodies to HIV-1 and -2. J. Virol. Methods 173, 24–30 (2011).
194. Myyryläinen, T. et al. Simultaneous detection of Human Immunodeficiency Virus 1 and Hepatitis B virus infections using a dual-label time-resolved fluorometric assay. J. Nanobiotechnology 8, 27 (2010).
195. Talha, S. M. et al. Array-in-well platform-based multiplex assay for the simultaneous detection of anti-HIV- and treponemal-antibodies, and Hepatitis B surface antigen. J. Immunol. Methods 429, 21–27 (2016).
196. Talha, S. M. et al. All-in-one dry-reagent time-resolved immunofluorometric assay for the rapid detection of HIV-1 and -2 infections. J. Virol. Methods 226, 52–59 (2015).
197. Hyytiä, H. et al. Chimeric recombinant antibody fragments in cardiac troponin I immunoassay. Clin. Biochem. 48, 347–352 (2015).
198. Das, S. et al. Performance of an ultra-sensitive Plasmodium falciparum HRP2-based rapid diagnostic test with recombinant HRP2, culture parasites, and archived whole blood samples. Malar. J. 17, 118 (2018).
199. Allain, J.-P. & Opare-Sem, O. Screening and diagnosis of HBV in low-income and middle-income countries. Nat. Rev. Gastroenterol. Hepatol. 13, 643–653 (2016).
200. Casals, G., Filella, X. & Bedini, J. L. Evaluation of a new ultrasensitive assay for cardiac troponin I. Clin. Biochem. 40, 1406–1413 (2007).
201. Savukoski, T. *et al.* Troponin-Specific Autoantibody Interference in Different Cardiac Troponin I Assay Configurations. *Clin. Chem.* **58**, 1040–1048 (2012).
202. Mair, J., Apple, F. S., Thygesen, K. & Jaffe, A. S. Update on Quality Specifications for Cardiac Troponin Assays. in *Troponin: Informative Diagnostic Marker* (ed. Jin, J.-P.) (Nova Publishers, 2014).
203. Christenson, R. H. Toward Standardization of Cardiac Troponin I Measurements Part II: Assessing Commutability of Candidate Reference Materials and Harmonization of Cardiac Troponin I Assays. *Clin. Chem.* **52**, 1685–1692 (2006).

204. Tsai, J. S. C. *et al.* The Evolution of Cardiac Troponin Testing. in *Troponin: Informative Diagnostic Marker* (ed. Jin, J.-P.) (Nova Publishers, 2014).
205. Apple, F. S. Counterpoint: Standardization of Cardiac Troponin I Assays Will Not Occur in My Lifetime. *Clin. Chem.* **58**, 169–171 (2012).
206. Yang, X. *et al.* Development and Evaluation of Up-Converting Phosphor Technology-Based Lateral Flow Assay for Quantitative Detection of NT-proBNP in Blood. *PLoS One* **12**, e0171376 (2017).
207. You, M. *et al.* Household Fluorescent Lateral Flow Strip Platform for Sensitive and Quantitative Prognosis of Heart Failure Using Dual-Color Upconversion Nanoparticles. *ACS Nano* **11**, 6261–6270 (2017).
208. Land, K. J., Boeras, D. I., Chen, X. S., Ramsay, A. R. & Peeling, R. W. REASSURED diagnostics to inform disease control strategies, strengthen health systems and improve patient outcomes. *Nature Microbiology*. **4**, 46–54 (2019).

TURUN
YLIOPISTO
UNIVERSITY
OF TURKU

Painosalama Oy, Turku, Finland 2021

ISBN 978-951-29-8438-1 (PRINT)
ISBN 978-951-29-8439-8 (PDF)
ISSN 0082-7002 (Print)
ISSN 2343-3175 (Online)